KU LEUVEN

FACULTY OF SCIENCE

GHENT UNIVERSITY

FACULTY OF SCIENCES

Holocene Vegetation Reconstruction of the Zwarte Beek Catchment, Campine Area (Belgium)

A Pollen-based and Multivariate Statistical Approach

Femke AUGUSTIJNS

Supervisor: Prof. G. Verstraeten
KU Leuven

Co-supervisor: Dr. N. Broothaerts
KU Leuven

Mentor: R. Hoevers
KU Leuven

Thesis presented in fulfillment of the requirements for the degree of Master of Science in Geology (Ghent – Leuven)

Academic year 2018-2019

Acknowledgements

First of all I want to express my gratitude to my supervisors Renske Hoevers, Dr. Nils Broothaerts and Prof. Gert Verstraeten: your feedback on my work and patience in teaching me the basics of pollen analysis was indispensable for me and is very much appreciated. I want to thank as well Ward Swinnen for helping with the geomorphological transects and Katrien Wouters for the support with the fieldwork. I am grateful for the data that I was permitted to use from the research of Eveline Scherps, Laura Vervacke, Annelies Storme, Dr. Koen Deforce and Dr. Elena Marinova.

Special thanks goes to Dr. Elena Marinova for providing an intensive pollen training in her archaeobotanical laboratory and for encouraging me to pursue a future in the field of palaeobotany. I also want to thank my colleagues and friends Lijun Zhang, Laura Vervacke and Erika Vercammen: I am grateful that we decided to work as a team rather than competitors, always supporting one another.

To all the geologists that attended the research seminars, your questions and feedback were very helpful and motivating. Thank you as well to my lectors Prof. Patrick Degryse and Prof. Robert Speijer. I want to address gratitude to my fellow geology master students for accepting me and supporting me during the long days on campus. Special thanks goes to Pabitra Gurung and Axelle Van Campen for being my climbing mates and allowing me to refresh my mind at the wall. I also want to thank Thomas Gyselinck for transferring his passion and knowledge of plants to me, and Marie Gielen with whom I am able to share my fascination for the natural world with.

Finally, I want to thank my family: my parents for their limitless support and patience, especially in these stressful times, and my brother and sister for always being there when I needed it the most.

Summary

Pollen records from all over the globe have proved the dynamic nature of vegetation cover, resulting in dramatic changes in plant community composition and abundances over long time scales, including the current interglacial period. This interval, known as the Holocene epoch, is characterized by an additional factor influencing the established vegetation: apart from climatic and soil conditions, human impact also becomes a significant driver of vegetation changes. In Flanders these Holocene environmental changes are well clarified for the loamy region, but less high-resolution well-dated pollen records are available for the sandy region. Therefore, this study focuses on an over three meter long sediment core from the exceptionally thick peat deposits in the Zwarte Beek valley, situated in the Campine region.

Pollen analysis is chosen as a method to reconstruct the regional vegetation and human impact evolution from the studied peat sequence. In total, 31 levels of peat were studied by extracting and identifying their pollen content. This resulted in a high resolution pollen diagram which was further analysed using multivariate statistics: clustering techniques were used as the basis for the identification of biozones in the vegetation development. Ordination analysis, more specifically NMDS, was applied to detect the major patterns within the pollen data and used as validation of the obtained clusters.

Radiocarbon dating of four levels showed that the peat sequence spanned the interval from ca. 11.4 to 6.7 cal. kyr BP. A hiatus was detected based on the dating results and the presence of cereals, which indicated a significantly younger age above this level. Several causes were proposed including peat excavation, mineralisation by desiccation and halted peat growth during the Middle Holocene.

Integration of the pollen analysis with plant macrofossils, macro-charred particles and climatic data resulted in the subdivision of the Zwarte Beek vegetation development into six biozones: before 11.2 cal. kyr BP, an open landscape dominated by grasses, shrubs and pioneer trees was reconstructed. This was followed by the establishment of an open pine forest with frequent occurrence of fires. From 9.8 cal. kyr BP temperate trees were introduced in the region and a closed deciduous woodland was formed with hazel, oak and elm as the dominant tree types. At 8.5 cal. kyr BP, a major shift in the local wetland vegetation was observed: where the valley was originally covered with sedges in an open landscape, now a valley forest was formed. This alder carr dominated the local vegetation until 7.8 cal. kyr BP. From then, the valley was occupied by a mosaic of alder carr, sedges and peat mosses. During this phase the deciduous woodland of the regional vegetation became partially opened while heather and grasses expanded. Humans and fire were possibly involved in this vegetation alteration. The Middle

Holocene peat sequence continued until 6.7 cal. kyr BP, after which a hiatus was present until Medieval or recent times. The vegetation composition above this hiatus was strongly opened with abundant grasses and heather. Cereal pollen from buckwheat and rye were identified and peat mosses reached their maximum abundance.

The obtained vegetation evolution for the Zwarte Beek region was compared to previous research on this valley and to adjacent regions within sandy Flanders and the loamy region. This showed that the major Early and Middle Holocene vegetation stages were uniform across Flanders, however the timing of some transitions did differ significantly even over relatively short distances. Finally, a comparison to Eemian pollen diagrams was performed, thus showing the possibilities and limitations of using pollen records as analogues for contemporary vegetation changes.

List of abbreviations

Abbreviation	Meaning
AD	Anno domini
AP	Arboreal pollen
BC	Before Christ
BP	Before present (1950)
BR	Brussels
Cal	Calibrated
CHAR	Charcoal accumulation rate
CI	Confidence interval
Coniss	Constrained incremental sum of squares
GN	Grote Nete
HCA	Hierarchical cluster analysis
Kyr	Thousand years
Ma	Million years
NMDS	Non-metric multidimensional scaling
PAR	Pollen accumulation rate
Rpm	Rotations per minute
SB	Scheldt basin
ZB	Zwarte Beek
14C	Radiocarbon

List of plant names

Latin name	English name
Abies	Fir
Agrostis	Bentgrass
Alnus	Alder
Angelica Sylvestris	Wild angelica
Apiaceae	Umbellifer family
Asteraceae	Composite family
Betula pendula	Silver birch
Betula pubescens	Moor birch
Brassicaceae	Crucifer family
Callitriche	Water-starwort
Caltha palustris	Marsh-marigold
Campanula	Bellflower
Carex rostrata	Beaked sedge
Caryophillaceae	Carnation family
Cerealia	Cereals
Chenopodiaceae	Amaranth family
Chenopodium	Goosefoot
Cirsium palustre	Marsh thistle
Corylus	Hazel
Cyperaceae	Sedge family
Equisetum	Horsetail
Ericaceae	Heather family
Eriophorum angustifolium	Common cottongrass

Erodium	Storkbill
Eryngium	Amethyst sea holly
Fagopyrum	Buckwheat
Fagus	Beech
Filipendula ulmaria	Meadowsweet
Frangula alnus	Alder buckthorn
Fraxinus	Ash
Galeopsis tetrahit	Common hemp-nettle
Galium	Bedstraw
Hedera	Ivy
Juncus acutiflorus	Sharp-flowered rush
Juniperus	Juniper
Lactuceae	Cichorioid daisies
Larix	Larch
Lemna	Duckweed
Lotus pedunculatus	Marsh bird's-foot trefoil
Lycopodium	Creeping cedar
Lycopus europaeus	Gypsywort
Lysimachia vulgaris	Yellow loosestrife
Lythrum salicaria	Purple loosestrife
Mentha	Mint
Menyanthes trifoliata	Bogbean
Myriophyllum	Watermilfoil
Nuphar	Pond-lily
Nymphaea	Waterlily
Persicaria	Knotweed

Phragmites	Reed
Pinus	Pine
Plantago lanceolata	Ribwort plantain
Poaceae	Grass family
Polypodium	Rockcap fern
Populus	Poplar
Potamogeton	Pondweed
Potentilla	Cinquefoil
Quercus	Oak
Ranunculus	Buttercup
Rubus	Bramble
Rumex acetosa	Common sorrel
Salix	Willow
Saxifraga granulata	Meadow saxifrage
Scirpus sylvaticus	Wood club-rush
Secale cereale	Rye
Sphagnum	Peat moss
Succisa pratensis	Devil’s-bit
Thalictrum	Meadow-rue
Tilia	Lime
Typha	Bulrush
Ulmus	Elm
Viola palustris	Marsh violet
Viscum	Mistletoe

Table of contents

Acknowledgements IV

Summary V

List of abbreviations VII

List of plant names VIII

1. Introduction 1

1.1. Quaternary Research 1

1.2. The Interglacial vegetation pattern 1

1.3. Holocene geoecological changes 2

a. Loamy region 3

b. Sandy region 3

1.4. Reconstructing human activities in the sandy region 4

1.5. Pollen as a proxy 6

1.6. Peat as an archive 7

1.7. Peat as an actor 8

1.8. Analogs for the Holocene Interglacial 9

1.9. Research objectives 10

2. Study Area 12

2.1. Situation 12

2.2. The valley of the Zwarte Beek 14

2.3. Land cover and Soil 15

2.4. Geology 16

2.5. Hydrology 19

2.6. Vegetation 21

2.7. Human activities 22

3. Material and methods 25

3.1. Fieldwork 25
3.2. Training Germany 26
3.3. Laboratory work 26
3.4. Microscopic analysis 28
3.5. Data Analysis 28
a. Age-Depth model 28
b. Pollen diagrams 29
c. Statistical analysis: Clustering 29
d. Statistical analysis: Ordination 30
3.6. Data compilation 31
4. Results 32
4.1. Geomorphology 32
4.2. Age-Depth model 33
4.3. Pollen diagrams 35
4.4. Hierarchical cluster analysis 37
4.5. Vegetation zones 39
a. Regional vegetation zones 39
b. Local vegetation zones 41
4.6. Non-metric multidimensional scaling 42
a. Regional NMDS analysis 42
b. Local NMDS analysis 51
4.7. Additional records and final zonation 57
5. Discussion 64
5.1. Age-depth model 64
5.2. Comparison of pollen data with additional records 66
a. Plant macrofossils 66

b. Macro charcoal....67
5.3. Vegetation development in and around the valley of the Zwarte Beek....67
a. Zone ZB 1 (11.4-11.2 cal. kyr BP)....67
b. Zone ZB 2 (11.2-9.8 cal. kyr BP)....67
c. Zone ZB 3 (9.8-8.5 cal. kyr BP)....68
d. Zone ZB 4 (8.5-7.8 cal. kyr BP)....69
e. Zone ZB 5 (7.8-6.7 cal. kyr BP + hiatus)....70
f. Zone ZB 6 (hiatus-top)....70
5.4. Spatial comparison....71
a. Previous research Zwarte Beek....71
b. Sandy region....76
c. Loamy region....79
5.5. Temporal comparison: The Eemian....80
5.6. Final remarks....81
6. Conclusion....84
References....86
Appendix....95
Appendix A....95
Appendix B....98
Appendix C....99
Appendix D....102
Appendix E....103

1. Introduction

1.1. Quaternary Research

The Quaternary is the geological period spanning the last 2.588 million years (Cohen et al. 2013). It is preceded by a 50 Ma long period of gradual cooling and characterized by a high degree of instability in the Earth's climate. The Quaternary period is part of the Late Cenozoic Ice Age starting 33.9 Ma ago at the onset of the Oligocene. This Ice Age is one of the five major cold intervals in Earth's history, which is dominated by much warmer circumstances (greenhouse periods) than the contemporary icehouse climate.

The first and longest part of the Quaternary period is the Pleistocene epoch, characterized by strong climatic warming and cooling with simultaneous contractions and expansions of ice sheets (Holden 2017). This pattern of alternating glacial and interglacial periods starts at the onset of the Pleistocene and is the result of several driving forces, both internal (interactions between the Earth's spheres) and external (e.g. distance to the sun). The second and final Quaternary epoch is known as the Holocene and covers the last 11700 years of Earth's history. It is an interglacial interval and temperatures are thus relatively warm.

Insights into environmental changes throughout the Quaternary period are useful to increase understanding of the present-day climate system (atmosphere), the living world (biosphere) and the Earth's surface (i.a. hydrosphere) and subsurface (lithosphere) and how all these spheres influence each other. This insight can help us to understand the state of the Earth today and model possible future changes. In this way the Quaternary geological period forms a valuable research topic, bridging the gap between deep, geological time and the current global change.

1.2. The Interglacial vegetation pattern

Related to the rapid climatic changes during the succession of Pleistocene glacials and interglacials, strong changes in vegetation composition and structure occured in the terrestrial realm. The observed patterns for temperate regions during the Quaternary interglacials were summarized as a five-stage cycle by Iversen (Iversen 1958): first, the glacial steppe-tundra vegetation of the cold and dry Cryocratic phase is replaced by open pioneer forests (birch, pine) with fertile soil during the Protocratic phase. Towards the climatic optimum, a deciduous forest with many different taxa (hazel, elm, oak, etc.) is established (Mesocratic phase). In the Oligocratic phase, this climax forest degrades into an acidic ecosystem with leached soils underneath a vegetation dominated by beech, conifer trees or heather. During the Telocratic phase, the climate detoriates and the vegetation gradually evolves back into its glacial state.

For the Holocene interglacial, the temporal framework for describing and correlating postglacial paleoecological changes is delivered by the Blytt-Sernander scheme (Table 1.1). It consists of five Holocene phases which can be recognized in postglacial peat profiles worldwide, representing distinct climatic intervals (Rydin & Jeglum 2013): the Preoboreal with initial postglacial warming, the Boreal dry and warm phase, the wet Atlantic climatic optimum, the dry Subboreal and finally the cool and wet Subatlantic. The scheme was extended to the Late

Glacial by addition of three stadials (Oldest, Older and Younger Dryas) and two intervening interstadials (Bolling and Allerod).

Table 1.1: The classical subdivision of the Late Glacial and Holocene epoch for northwest Europe (Anderson et al. 2013, Mangerud 1974). Initially radiocarbon ages (14C) were used to define the boundaries.

Chronozone	14C kyr BP	Calibrated kyr BP
Subatlantic	2.5 – 0.0	2.6 – 0.0
Subboreal	5.0 – 2.5	5.7 – 2.6
Atlantic	8.0 – 5.0	8.8 – 5.7
Boreal	9.0 – 8.0	10.2 – 8.8
Preboreal	10.0 – 9.0	11.6 – 10.2
Younger Dryas	11.0 – 11.6	12.9 – 11.6
Allerod	11.7 – 11.0	13.6 – 12.9
Older Dryas	12.0 – 11.7	14.0 – 13.6

The described changes within an Iversen cycle are the result of several driving forces and feedbacks: most important are climatic changes with varying temperatures and humidity, and internal forces caused by the evolving vegetation itself (soil formation, shade, dispersion and competition capacity). However, this pattern driven by climatic and internal vegetational changes is disturbed during the current interglacial: a new factor -human impact- becomes significant in shaping ecosystems (Gibling 2018). In river systems, for example, disturbances of the pristine situation are caused by human activities including deforestations, cropping activities in the catchment, river damming and embarkments (e.g. Hudson et al. 2008, Kondolf 1997, Vanacker et al. 2014).

1.3. Holocene geoecological changes

River systems and floodplains in particular play an important role in sediment storage. This alluvial sediment provides a valuable archive of the past changes in geomorphological processes and vegetation developments in the river catchment. Throughout the Holocene epoch, floodplains underwent severe changes, including vegetational changes and changes in river geomorphology (e.g. Houben et al. 2013). Previous research showed that these changes cannot be generalised, as shown by the significant differences in Holocene floodplain developments in different environments across Europe (Verstraeten et al. 2017), as well as within Belgium (Notebaert et al. 2011a). Therefore, the available studies are incapable of fully capturing and understanding the variability of the indicated environmental changes and their responses in river systems throughout the Holocene.

a. Loamy region

In Flanders, the Dijle catchment has been the subject of intensive investigation (e.g. Broothaerts et al. 2013, Broothaerts et al. 2014a, Notebaert et al. 2011b). During the Early and Middle Holocene, marshy peat accumulating environments with alder carr vegetation and a multi-channel river system dominated the valleys. The Middle Holocene deciduous forests in the Dijle catchment were dominated by oak, hazel and lime. Human activities were limited to local deforestations until the onset of the Bronze Age (3.9 cal. kyr BP), when the opening of the vegetation started -indicated by an increase in grass and herb pollen- and anthropogenic indicator pollen appeared. The rise of agriculture and clear cutting of the forests caused a change in the floodplain system by increasing sediment input from the hillslopes. As a result, the present-day meandering river system with an open floodplain vegetation and clastic deposits was established. This increasing trend of human impact accelerated in the Iron Age and Roman period and was only interrupted during the Migration Period (1.75-1.6 cal. kyr BP). The highest degree of disturbance was found for the Medieval to modern period (1.6-0.5 cal. kyr BP).

Therefore, for loamy Flanders the relation between human impact and floodplain changes is mostly clarified. However, it is not clear how universal these changes are for floodplains during the Holocene period, and, more specifically, if they apply as well to more sandy regions where the human impact history is expected to be less intense due to the poor sandy soils.

b. Sandy region

In the Belgian cover sand region, the Scheldt estuary is probably the most intensely studied area. It has a unique Holocene development because it was prone to sea level rise and anthropogenic interventions, including reclamation of land and successive inundations in the Middle Ages (Deforce 2011). Peat growth started most commonly in the Atlantic due to the rising sea level and was covered by marine sediments from the Middle Ages (Deforce 2011, Gelorini et al. 2006, Janssens & Ferguson 1985). The first possible evidence of small-scale human impact was observed starting from 7.0 cal. kyr BP with Cerealia-type pollen suggesting local crop cultivation (Storme et al. 2017). In the Late Holocene, a simultaneous decrease of elm and lime trees along with increasing values of anthropogenic indicators was recorded around 4.0 cal. kyr. BP, representing the onset of regional human landscape alterations. It was interpreted as final Neolithic-Bronze Age human occupations sites in a partially opened landscape.

The vegetation history of the eastern border of the cover sand area was studied on several Meuse terraces in the southeast part of the Netherlands (Zuidhoff & Bos 2017). The Middle Holocene closed vegetation cover became gradually more open from the Bronze Age, with real opening by human forest clearings only happening from the Roman Period for high topographies and from the Middle Ages for the lower grounds. Compared to the loess region, the human impact history in this area is thus relatively short.

In the Campine area, the forest started to open from the Subboreal period with indications of grazing appearing from the Iron age (2.8 cal. kyr BP) and cereals starting from the Subatlantic period (Verbruggen et al. 2019, Gelorini et al. 2008). Beerten et al. (2014b) reconstructed an open heather landscape for the last millennium on the Campine plateau, and reforestation in recent times (ca. 100 cal. years BP).

Despite the high number of paleoecological studies describing Holocene changes in river valleys, many uncertainties remain. In many cases the relative contributions of humans versus climate to these postglacial geo-ecological changes remain unclarified. This is especially the case for sandy Flanders, where detailed holistic studies on floodplain changes are missing. The density of vegetation reconstructions in this cover sand region is limited due to the low preservation potential of plant remains in sandy soils. We therefore depend on sparse lake and peat records -often limited to some thousand years- to reveal the vegetation history of these regions (Verbruggen et al. 2019).

The Zwarte Beek river catchment is selected as study site in this thesis, to help filling this knowledge gap for sandy Flanders and the Campine area in particular. It is considered as an interesting study site for several reasons. The first and decisive criterium is its locality in sandy Flanders, contrasting with the well-studied Dijle river situated in loamy Flanders. As explained above, sandy Flanders is dominated by a low soil fertility making the region less suitable for agriculture: for this, a different land use history and floodplain development is expected compared to the fertile loamy Flanders where intensive long-term human impacts were observed (Broothaerts et al. 2014a). A second reason is the presence of fen areas, resulting in good conditions for preservation of microfossils, with locally exceptionally thick peat accumulations up to six meters (Maes et al. 2018). Also important is natural biodiversity of the study area: the Zwarte Beek valley forms a major nature reserve and is part of the Habitats Directive, due to the presence of numerous endangered species and a large variability in habitats including heathland and fen areas (ANB 2018). Finally, human activities such as drainage, channeling and bank reinforcement have endangered the valuable valley system and its biodiversity in the past (Rogiers et al. 2011). Several measures are now being introduced to restore the natural hydrology, including re-meandering of the Zwarte Beek river, requiring a good knowledge of the pristine situation.

1.4. Reconstructing human activities in the sandy region

Apart from the Holocene vegetation development in the sandy region, several authors have also contributed to a reconstruction of human settlements in this area. The first traces were encountered in the Late Glacial: during the Allerod period, the nomadic Federmessergroupen arrived in the Campine region (Derese et al. 2012). Occupation sites were found close to water and situated on dry elevated ridges. Climatic detoriation and increased wind activity during the Younger Dryas resulted in the local disappearing of the Federmesser nomads. At some localities in the Campine region, Ahrensburgian sites were discovered (e.g. Zonhoven Molenheide, Vermeersch 2011), but in general the occupation density during this cold stadial was low. The climatic improvements from the onset of the Holocene onwards were accompanied by the appearance of new settlements: Early Mesolithic groups arrived, showing strong similarities in subsistence and site preferences to the Paleolithic Federmesser groups (Derese et al. 2012).

Between the Early and Late Mesolithic, a change in site location was observed in sandy Flanders (Vanacker et al. 2001): when late glacial lakes disappeared and the upland became less suitable for collecting of resources due to increasing vegetation cover, settlements moved closer to river valleys. The increased interest in river valleys could be linked to the transition

from discontinuous river discharge regimes (Younger Dryas and Preboreal) towards more permanent discharges from the Mid-Boreal due to increased humidity.

The Mesolithic to Neolithic transition for the Scheldt-Meuse-Rhine region was a long-term gradual process dated between ca. 7.25 and 5.45 cal. kyr BP (5.3-3.5 cal. kyr BC, Meylemans et al. 2018). On the loess plateau, the first farmers were the LBK (Linear Bandkeramiker) groups appearing from 7.25 cal. kyr BP: this loamy area was the first region in West Europe to undergo neolithization (Vanmontfort 2008). Clarifying the influence of these groups on the hunter-gatherers in the cover sand areas remains a challenge. Cereals dated up to ca. 6.75 cal. kyr BP (4.8 cal. kyr BC, Meylemans et al. 2018) were found in the Scheldt valley: they are the oldest direct evidence of plant domestication for sandy NW Europe. This could indicate interaction of the local late Mesolithic Swifterbant culture with southern Blicquy and later Rossen farmers from the loess area, possibly by herders in a context of transhumance. This influence of surrounding Neolithic groups is confirmed by the abundant finds of exotic ceramics in sandy Flanders and this stage could thus represent the onset of farmer-forager interaction and associated gradual neolithization of the sandy region. From ca. 6.25 cal. kyr BP (4.3 cal. kyr BC) the main Neolithic influence became the Michelsberg culture, with the potential start of local farming in the sandy region (Meylemans et al. 2018). The transmission of Michelsberg elements is found for lithics, ceramics and cereals (*Triticum turgidum*) and this culture was most likely the driver of the northwards spread of agropastorialism to the coversand region. Intensification of this interaction resulted in a final replacement of the Mesolithic Swifterbant by Neolithic Michelsberg culture around 5.95 cal. kyr BP (4.0 cal. kyr BC, Crombé et al. 2009).

Opening of the forest in the Campine cover sand area was reported from the Subboreal period and was probably linked to human deforestations (Verbruggen et al. 2019). In the Subatlantic period these forest clearings intensified for agricultural purposes. Other human disturbances increased as well, including manuring to improve the fertility of the sandy soils from the Middle Ages (resulting in truncated soils on non-arable fields), and heath-to-conifer conversions and drainage of wetlands from the late 19th century due to agricultural intensification (Vanacker 2001).

Despite the existence of numerous studies trying to reconstruct human activities in sandy Flanders, high-resolution continuous records of human impact over time are lacking. However, this is required to directly link possible driving forces (including human impact) to vegetation developments and changes of floodplain geomorphology. Reconstructions of human occupations and their activities often rely on archaeological findings in the proximity of the study site. Artefacts include mainly pottery and lithic remains and can be derived from surface sites or corings and excavations (e.g. Crombé et al. 2009). In many cases, a detailed and representative reconstruction is held back by an insufficient number of artefacts and lack of absolute dating options, resulting in a coarse temporal framework delivered by typo- and technological dating (Sergant et al. 2009). An alternative approach to study the history of human activities around a study site, for instance the valley of the Zwarte Beek, uses plant remains derived from sediment cores (e.g. Verbruggen et al. 2019). In this way an indirect but continuous reconstruction of human impact can be obtained, embedded in a well-established temporal framework by radiocarbon dating on organic remains. Possible strategies to convert plant fossil data (pollen or plant macroremains) to information on human presence and disturbances include the detection of anthropogenic indicator species (Behre 1981). Certain taxa (e.g. Cerealia) can prove the occurrence of agricultural practices in the vicinity of the study

site, while the ratio of tree to herb taxa (AP/NAP) can indicate human deforestations. Elevated fire activity can be linked to human presence, derived from counting of charred particles (Mooney & Tinner 2011). Finally, statistical approaches can be applied to these paleoecological records to objectively quantify human impact (Broothaerts et al. 2014a).

1.5. Pollen as a proxy

In this thesis, pollen will be used as main information source to reconstruct vegetation changes and human activities in the study region (Zwarte Beek catchment). The studied pollen are (sub)fossil grains derived from plants living in ancient times. Pollen are the result of a meiotic cell division and represent the male gametophytic part of a plants life cycle (Moore & Webb 1991). Their size is on average between 20 and 40 µm, facilitating the necessary dispersion to their final target, the female stigma. This is different for spores which do not have to merge with an egg cell to allow germination. Due to the very limited chance that a pollen grain will ever arrive at the stigma, the production of pollen grains is enormous with, for example, typically higher numbers in case of wind dispersion compared to insect transport.

The first spores ('cryptospores') in the geological record are found in Mid-Ordovician deposits (Armstrong & Brasier 2013). The first pollen ('prepollen') only appear in the Late Devonian and are produced by seed ferns, a group of progymnosperms. Angiosperms or flowering plants are found in the fossil record since the Early Cretaceous. The contemporary success of this group is partly attributed to a new pollen morphology which arose (tricolpate pollen), and can be seen as the arrival of modern pollen grains. In the Mid-Tertiary, simultaneous to the climatic deterioration resulting in the onset of the current Late Cenozoic Ice Age, the rise of the two most successful present-day plant families occurred: Poaceae or the family of grasses and Asteraceae, including for instance daisies, dandelions and thistles.

Pollen analysis is considered as the most valuable tool for vegetation reconstructions during the Quaternary period and provided insight in the climatic patterns during the glacial-interglacial cycles (Seppä 2013). In more recent times, they were used to reveal the arrival of agriculture and impact of man on vegetation in general. On very short time scales, they can be used to detect vegetational succession patterns after small scale single events (storm, fire, forest clearings). Many other applications exist such as the study of past ranges of species, plant evolution and taxonomy. The variety of applications in Quaternary and older research is mainly due to the resistant nature of the exine, the pollens outer wall (Moore & Webb 1991). This material does decay much slower than other organic materials and only requires conditions with limited activity of micro-organisms (e.g. anoxic, very dry/wet, saline) to be preserved.

The identification of plant taxa based on pollen analysis relies on the large morphological variation of the pollen wall structures. In this way, pollen records can be obtained and used as proxy in paleo-environmental research, allowing to reconstruct vegetation developments and disturbances of plant communities by human activities. Pollen represent the regional vegetation composition, due to transport of the small pollen grains over large distances: for most mires a pollen source area of a few 100 km^2 is applicable (Seppä 2013). The major advantages of using pollen as proxy of past vegetation are their abundant presence in

sediment archives and their good preservation potential, resulting in continuous proxy records and the possibility of statistical analyses.

However, identification of the pollen grains is mostly limited to supra-species level and insect-pollinating plant are often lacking in pollen spectra due to low production rates. Though pollen records can clearly indicate shifts in the vegetation composition, it is often impossible to attribute these changes to their specific cause (e.g. climatic vs. human impact as driving force, Oldfield & Dearing 2003). The provided information on the local vegetation composition is also limited. To overcome these limitations and increase the insight in the past vegetation composition it is recommended to use complementary proxies (Parducci et al. 2015). Plant macrofossils and ancient DNA analysis for instance allow to identify underrepresented taxa in pollen records, to reveal the local vegetation history and to increase the taxonomic resolution.

The main challenge in palynological research is reconstructing the vegetation composition and structure from a pollen spectrum (Seppä 2013). Equifinality can occur, meaning that different plant communities can be indistinguishable in pollen counts. In addition, a series of factors leads to a mismatch between the 'living' plant abundance and the pollen plant abundance in sediment archives: pollen grains of different taxa can be produced in varying quantities, transported over varying distances and preserved with varying success. This is revealed by the comparison of modern pollen accumulation rates and their producing plant communities. The simplest correction method for these biases uses present-day information to assign a factor to each taxon, which should be multiplied with the pollen counts to obtain an estimate of the corresponding vegetation cover. This traditional method was improved by addition of a background pollen value in the ERV method (extended R-value). For studies covering more than 1000 years this method is not considered to be reliable, since the assumptions of constant pollen production rates and background pollen will be violated. To obtain a quantitative reconstruction of both regional and local vegetation composition, correction models are now available. The Landscape Reconstruction Algorithm for instance uses the REVEALS model for quantification of regional vegetation from large lakes and combines this information with cores from small sites on which the LOVE model is applied to reconstruct the local vegetation (Sugita 2007a & 2007b).

1.6. Peat as an archive

Pollen and other microfossils are best preserved in anaerobic conditions, such as in floodplain deposits and especially in peat accumulations. Peat is defined as a type of sediment consisting of minimal 30% organic matter (Joosten & Clarke 2002). It accumulates in mires which are typically waterlogged due to a high water table, creating the necessary anaerobic conditions to limit microbial breakdown of organic matter as soon as it passes below the groundwater surface (Bell & Walker 2005). This results in excellent preservation of fossil material in archives of a layered fashion, ideal for terrestrial paleoenvironmental research (Moore & Webb 1991). Apart from information on past vegetation, they can reflect human activities by e.g. Hg, Si, Pb and Ti concentrations or by the presence of minerogenic sediment due to increased erosion rates.

Pollen in a peat archive can be derived from several sources (Moore & Webb 1991): Above-canopy winds transport tree pollen over long distances before deposition at open spaces in

the forest (canopy component). Below-canopy winds in a forest can transport pollen from trees, shrubs and other forest plants to the site of deposition (trunk space component). Pollen can leave the atmosphere when water vapour condenses on their surface and pulls them down, taking several other pollen grains with them on their way to the Earth's surface (rain component). Streams can deliver pollen from the upstream catchment, fallen directly into the water or as a result of reworking of ancient deposits (inwashed component). The distance of dispersion can also be limited, when pollen from the wetland vegetation fall directly on the mire surface (local component).

There are several ways of classifying peatlands, but the most well-known uses the discrimination between bogs and fens (Joosten & Clarke 2002). The first are raised structures in the landscape while the latter are found in depressions. Peat extraction at bogs results in land suitable for agriculture, which is not the case for fens which turn into open water. This classical descriptive classification is now largely replaced by ombrotrophic versus minerotrophic mires (Bragg & Lindsay 2003). The first are entirely fed by rainwater while the latter depend on groundwater inflow. Minerotrophic mires can display a large variability in characteristics depending on the hydrological structure and composition of the inflowing water. Ombrotrophic bogs are generally acidic systems poor in nutrients, and important archives for climate reconstructions since they reflect the atmospheric composition. A more extensive classification based on the hydrological condition of peatlands discriminates between terrestrialisation mires (including schwingmoor and immersion mires), water rise mires and flood mires, percolation mires, surface flow mires and acrotelm mires.

1.7. Peat as an actor

Peatland ecosystems occur all over the globe, covering in total 3% of the terrestrial surface. They represent a major reservoir of organic soil carbon, storing a third of the Earth's stocks by the accumulation of organic matter (Joosten & Clarke 2002). In this way they form a carbon reservoir equally big in size as the atmospheric reservoir and exceeding the storage in the world's forests. Apart from the carbon storage ecosystem service, peatlands function as important hotspots of biodiversity and ensure the well-functioning of the hydrological system. They play an important role in flood attenuation, drought mitigation and purification of water (Bragg & Lindsay 2003). Finally they provide unique paleoenvironmental archives, valuable for the knowledge on the pristine ecosystem situations and the development of the present-day situation.

According to the International Peatland Society, peatlands can both act as CO_2, CH_4, O_3 and N_2O sinks and sources. In general, they function as net CO_2 sinks and CH_4 sources and very limited N_2O sources. Wetlands, including peatlands, form the largest natural global CH_4 source, with an average emission of 185 $TgCH_4$/yr or 30% of the global emission according to the Global Carbon Project. Combining all the greenhouse gass effects results in a negative radiative forcing for undisturbed peatland systems, mitigating global warming. The effects on climate change on these fluxes are highly variable depending on the specific geographical, hydrological and ecological characteristics. The role of peat as carbon sink is expected to decrease in the coming decades due to enhanced drying and burning of these ecosystems (Strack, 2008). Due to drainage of peatlands for forestry and agriculture in the past, the world's

cover of peatlands has already decreased severely, with estimates running upto 20% since 1800 AD (Joosten & Clarke 2002). In Europe, peat accumulation has stopped in 50-60% of the original peat systems. The drainage of peatlands results in lowering of the water table and thus increases the zone where oxidation of the stored organic matter can take place (acrotelm, Figure 1.1). In this way, the stored carbon is partly released into the atmosphere and a shift from carbon sinks to carbon sources can occur. This can enhance the greenhouse warming of the atmosphere, with similar effects being observed for the greenhouse gas N_2O: Nitrogen mineralization slows down in wetter soils, so lowering of the water table results in an increased N_2O flux to the atmosphere (Sleutel et al. 2008).

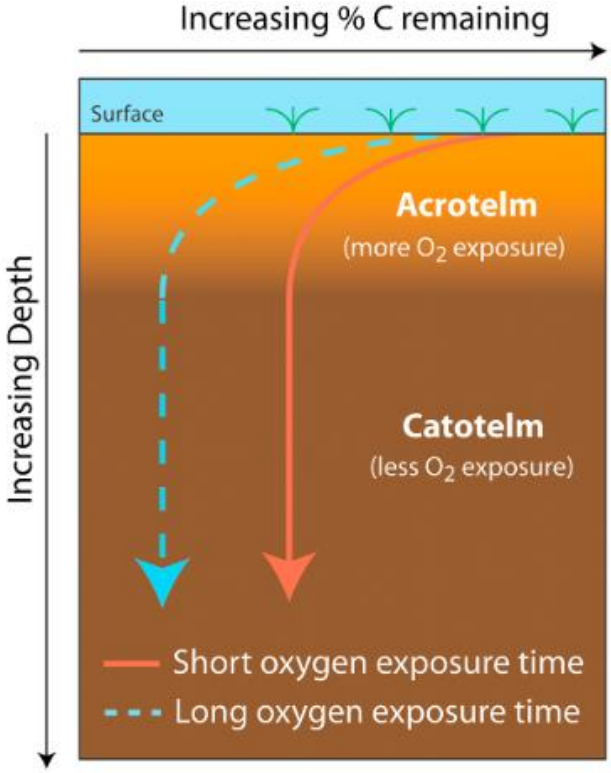

Figure 1.1: Diagram of the acrotelm and catotelm zone in a peat accumulating environment. The red line represents rapid accumulation of organic matter resulting in rapid burial. The organic matter thus enters the catotelm more quickly and is less strongly decomposed compared to a situation with slow organic matter accumulation, which is shown by the dashed blue line (Philben et al. 2014).

Peatlands are threatened by more human activities than drainage and desiccation alone. Sometimes, peat is removed directly by humans: peat extraction has been carried out for several purposes including the use of peat as fuel for heating and as fertilizers (Strack 2008). Alluvial mining in peatlands was also performed in the past, to gain for example iron ores, and resulted in a severe disruption of the peat accumulating environments.

1.8. Analogues for the Holocene Interglacial

Possible strategies to unravel human disturbance of the natural vegetation development include the comparison to undisturbed ecosystems. But, despite absence of local human impact, interferences of large scale human impacts during recent times can never be excluded (Goudie 2018). Therefore comparison to past analogues can be preferred: In paleoclimatic and

paleoecological research, past states of the Earth's systems are used as a reference to compare recent, current or future climatic and environmental changes. When it comes to modelling future warming, the Mid-Pliocene (3 Ma) and Early Eocene (50 Ma) offer the best analogue systems (Burke et al. 2018). These warm periods in the Earth's history are characterized by respectively similar and higher carbon dioxide concentrations than today and temperatures consistent to the RCP 8.5 emission scenario (2.6-4.8°C warming by 2100) for the coming decades resp. centuries.

However, when looking for a reference system for past Holocene environmental changes, the above mentioned analogues are not suitable: extinction and speciation over millions of years result in a significant difference in species composition, and the typical climatic and vegetational dynamics of the Quaternary (de)glaciations are missing. Therefore comparison to past Pleistocene interglacials is preferred. The most recent candidate for this is the Eemian or last interglacial period (129-116 ka), having the advantage of a rather similar ecosystem composition, plate tectonic settings, carbon dioxide level and temperature evolution as the current Holocene interglacial (Guiot et al. 1989).

For several locations in Europe long core records are available spanning several interglacials, with most cores reaching into the Eemian (e.g. Guiot et al. 1989, Magri 2010, Woillard 1978). In long pollen records the interglacials are reflected by forested intervals with northwards species migrations. Comparison of the vegetation dynamics during the current Holocene and the undisturbed Last Interglacial can reveal differences pointing towards human alterations of the expected vegetation development.

1.9. Research objectives

In this thesis, the Late Quaternary vegetation development in the surroundings of the Zwarte Beek will be studied. Previous research on the peat deposits in the Zwarte Beek valley has been carried out by Allemeersch (2010). Vegetation reconstructions were made for the Early Holocene, where peat forming alder carr and sedge vegetations were dominant. The top of the investigated peat sequence was dated at ca. 6.7 cal. kyr BP and Allemeersch was not able to assign the (natural/anthropogenic) cause for this stop in organic matter accumulation. The truncated sequence thus prevented the reconstruction of the entire Holocene vegetation and human impact history. However, based on available pollen and macroremain data for the Early Holocene and comparison to the modern vegetation in the valley, it was hypothesized that the vegetation would have remained stable throughout most of the Holocene without significant human alterations, consisting of an alder carr and sedge vegetation persisting until present.

To clarify the complete Holocene vegetation development and human impact history for the Zwarte Beek area, another peat core from the Zwarte Beek valley will be studied in this thesis. In this way we aim to gain insight in the relation between the possible driving forces (climatic vs. anthropogenic) and the observed changes in the valley environment (including floodplain morphology, vegetation composition and structure). The geomorphological component is studied by coring transects, while the vegetation and land use changes are reconstructed by pollen analysis in this thesis and complemented by data on macroremains in a parallel thesis (Laura Vervacke). The specific research objectives of this thesis are summarized below.

1) Provide knowledge on the regional vegetation development and possible anthropogenic disturbances in the area of the Zwarte Beek by creating a high resolution pollen diagram for the selected peat sequence.

2) Combine this information with other proxies (especially plant macroremains) and datasets (e.g. Allemeersch 2010 and geomorphological data by coring transects made in this project) to establish a multi-proxy vegetation reconstruction of the local geoecology and its development under changing climatic conditions and human impact throughout the Holocene period.

3) Comparison to Eemian vegetation patterns in northwestern Europe to gain insight into climatic versus human drivers of vegetation change during the current Holocene interglacial.

In a next step this study can contribute to the installation of sustainable management in the Zwarte Beek valley, its surroundings and similar valley systems. More specifically, the aimed increased understanding of the interaction between ecology, geomorphology and hydrology can be used to optimize desired ecosystem services using a set of models for the future development of the complete valley system. These models will be developed in the context of the ongoing Future Floodplains Project, targeting several river catchments in Flanders (https://www.futurefloodplains.be). The Zwarte Beek is one of the seven study areas in this project for which the long-term evolution of ecosystems is investigated as well as their corresponding ecosystem services.

2. Study Area

2.1. Situation

The study area is the catchment of the Zwarte Beek. It has a surface area of 160 km^2 for the total catchment and 70 km^2 for the part upstream of the Albert Channel. The Zwarte Beek is situated in the eastern part of the Belgian sand belt (Figure 2.1), with its source area on the Campine Plateau (Figure 2.2 & 2.4). The river with its NEE-SWW orientation leaves this plateau at the southwestern border and descends from 70 mTAW to 50 mTAW at the study site to 30 mTAW at the Albert Channel. The Zwarte Beek is a tributary of the Demer of which the confluence is found in Diest.

Within the Demer catchment, the adjacent subcatchment to the north of the Zwarte Beek belongs to the Winterbeek and to the south to the Mangelbeek (Figure 2.3). The Nete catchment is found northwards of the Demer catchment, to the east we encounter the Meuse catchment.

The study area is situated in the Campine archeo-region. Here the density of palynological research is low compared to the intensively studied western sandy region (Deforce 2008). Within the Campine region, past pollen research mainly focused on the northern and western parts while the available studies for the eastern part -where the Zwarte Beek is situated- is rather sparse.

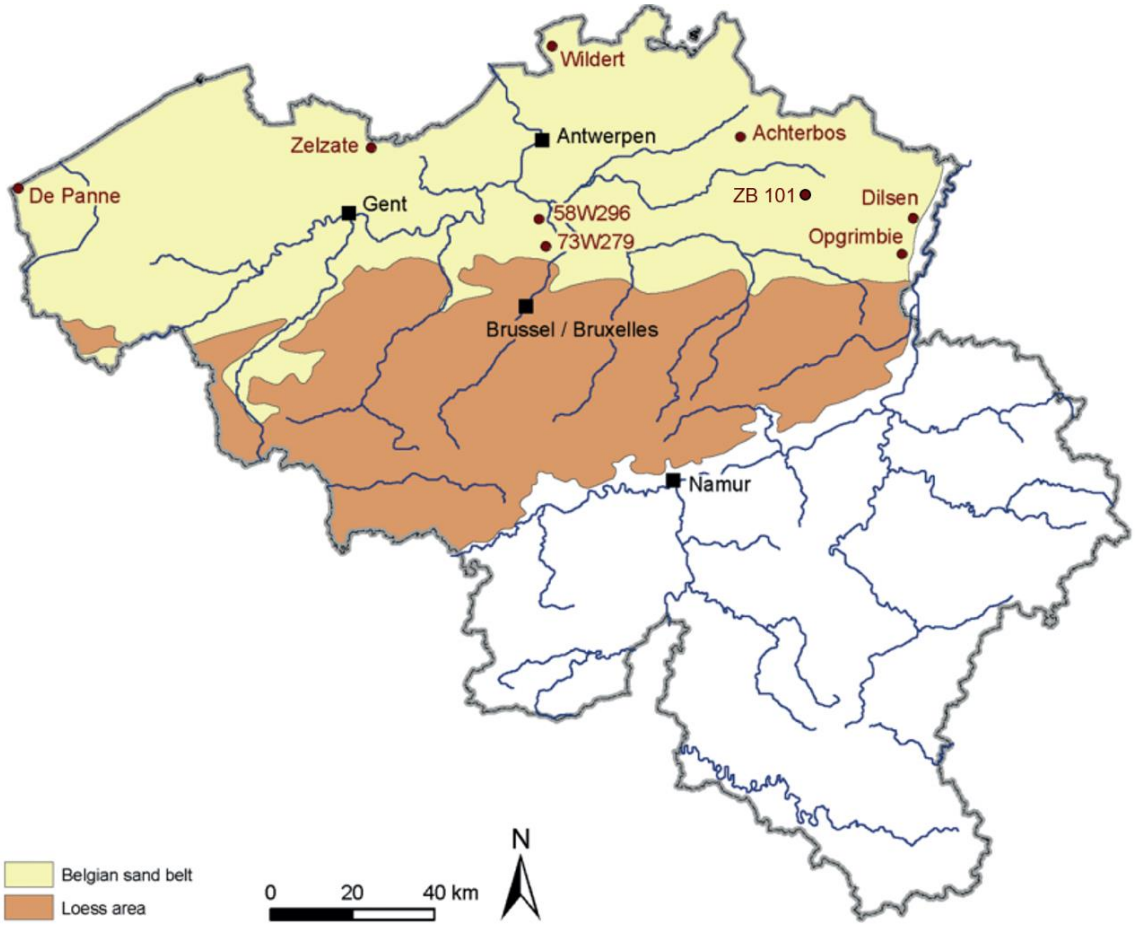

Figure 2.1: Belgian sand belt ('sandy region') and loess area ('loamy region') with stratotype localities and peat core location indicated (Beerten et al. 2017).

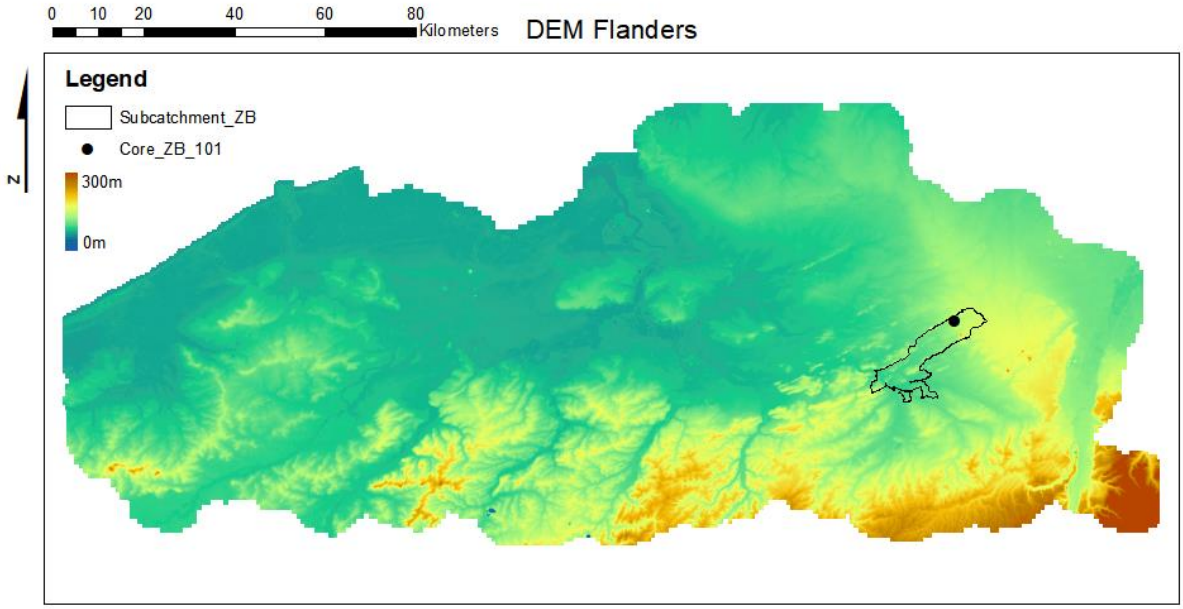

Figure 2.2: Digital Elevation Model (DEM) of Flanders. The location of the Zwarte Beek catchment at the western border of the Campine plateau is indicated (LiDAR-based DEM Flanders, Informatie Vlaanderen 2015).

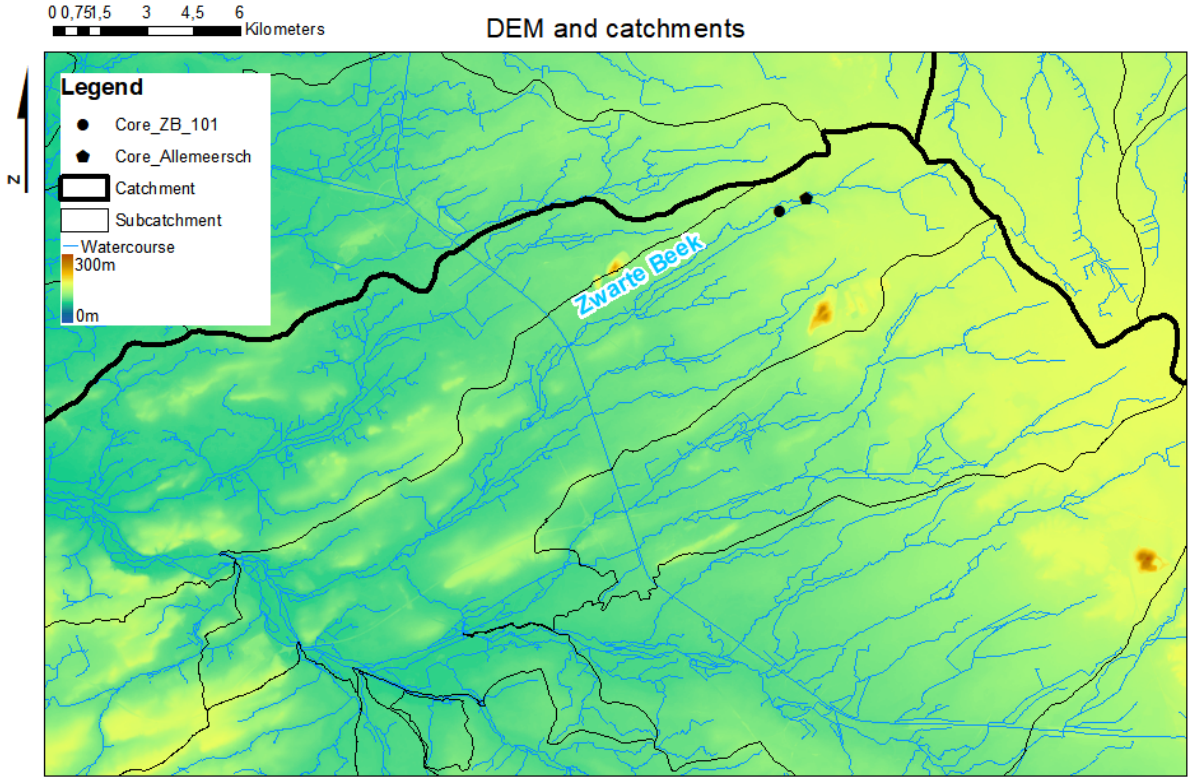

Figure 2.3: Map of the Zwarte Beek subcatchment within the Demer catchment. Clockwise the Meuse, Demer and Nete catchment are displayed (Informatie Vlaanderen 2015, VMM 2016).

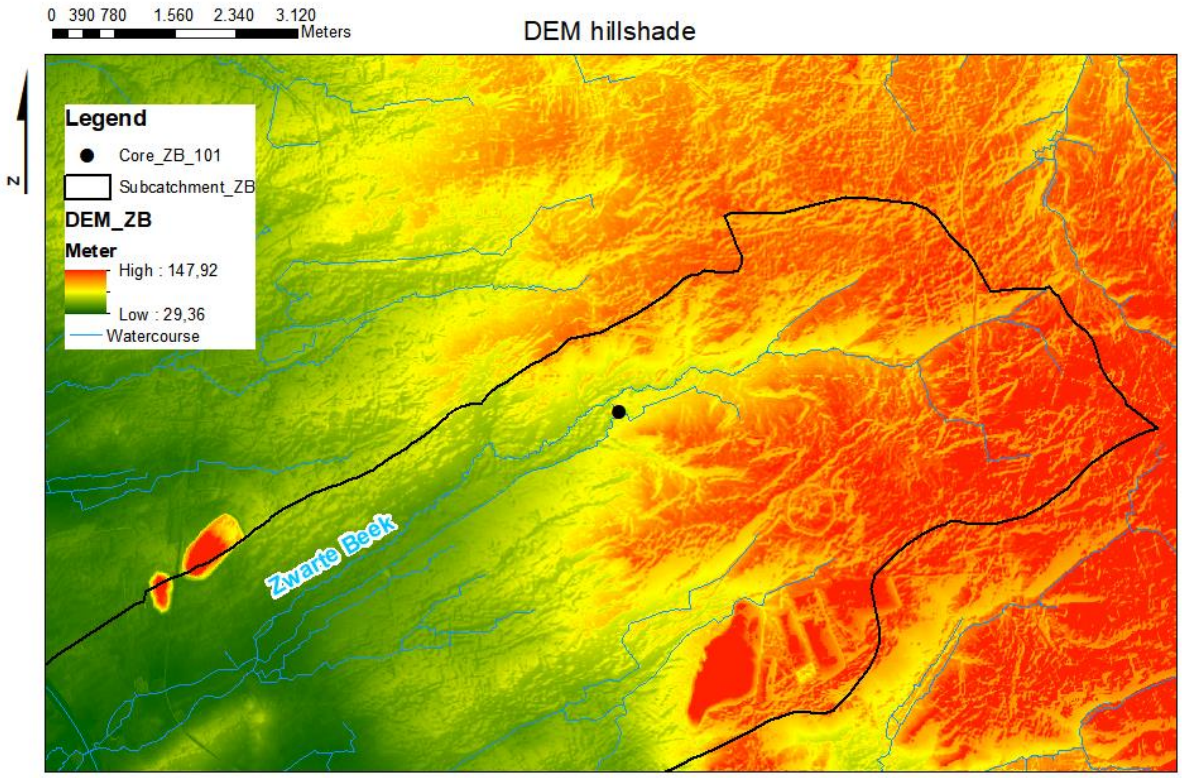

Figure 2.4: Detailed elevation map of the upstream part of the Zwarte Beek catchment. In the east the elevated topography of the Campine Plateau is visible. The southwestern peaks in the landscape are mine terrils (Informatie Vlaanderen 2015, VMM 2016).

2.2. The valley of the Zwarte Beek

The valley of the Zwarte Beek forms the largest fen complex of Flanders: De Becker (2009) reported a continuous peat body of 188 ha starting from 300 m width going to 600 m width downstream based on 660 corings along several transects. The valley itself is occupied by peat underlain by sand, the slopes -steeper in the north than the south- have sandy soils (De Becker & Huybrechts, 2000). Except from the coarse sand under the peat, finer sands were found at some locations in the valley: these were interpreted as river dunes and are on some locations not completely covered by peat.

The Zwarte Beek runs to the north of the peat body while the man-made Oude Beek (Figure 3.1) flows through the middle of it for most of its length. Corings by De Becker (2009) suggest the existence of a paleo-valley at the current position of the Oude Beek, which was active in the glacial period with steep slopes and a width of 80 m. In this incision the thickest peat accumulations are found with peat up to 6 meter thick (Maes et al. 2018). This is also the location where the peat growth started and from where the entire valley was colonized by peat deposits.

The abiotic conditions in the Zwarte Beek catchment are very diverse including sandy plateaus, steep slopes and wet valleys, resulting in a high biotic diversity with many vegetation types (heather, sedges, grasslands, dunes) and opportunities for several rare animal and plant species. Therefore, the potential for nature conservation and restoration in the Zwarte Beek valley is high (Maes et al., 2018).

2.3. Land cover and Soil

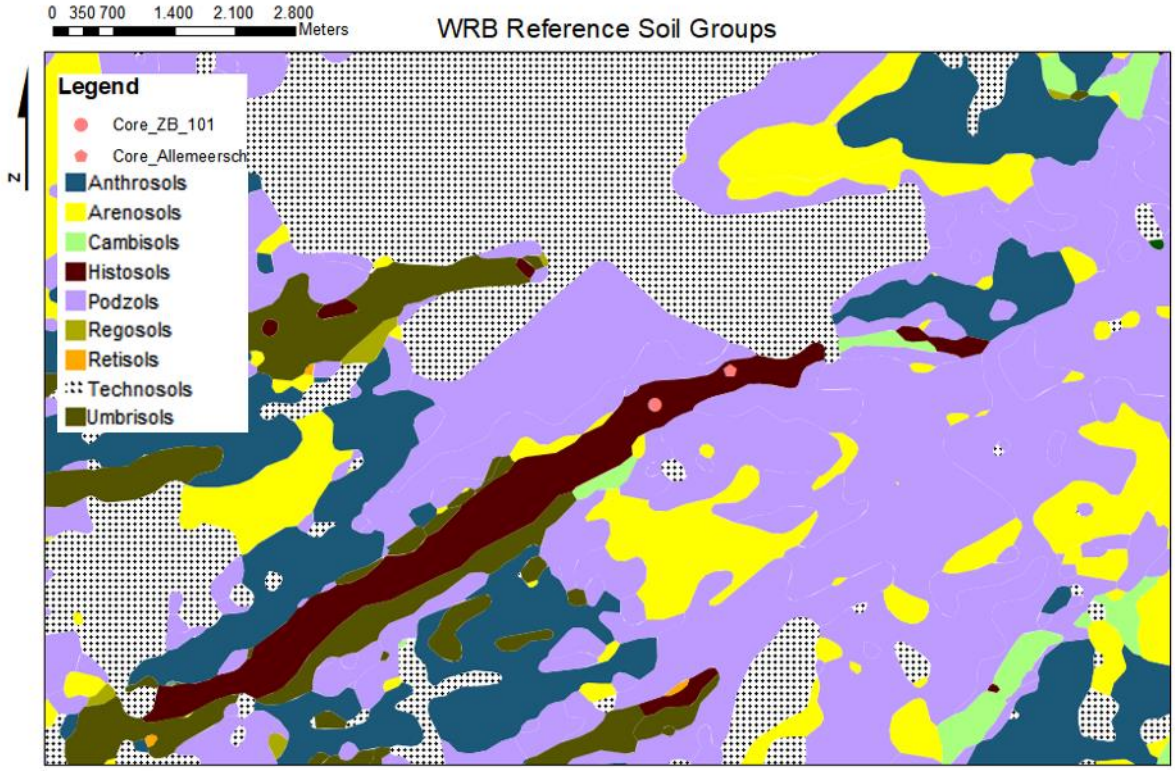

Figure 2.5: Map showing the soil types according to the WRB (World Reference Base) classification (DOV 2015). The Zwarte Beek catchment upstream of the Albert Channel is displayed.

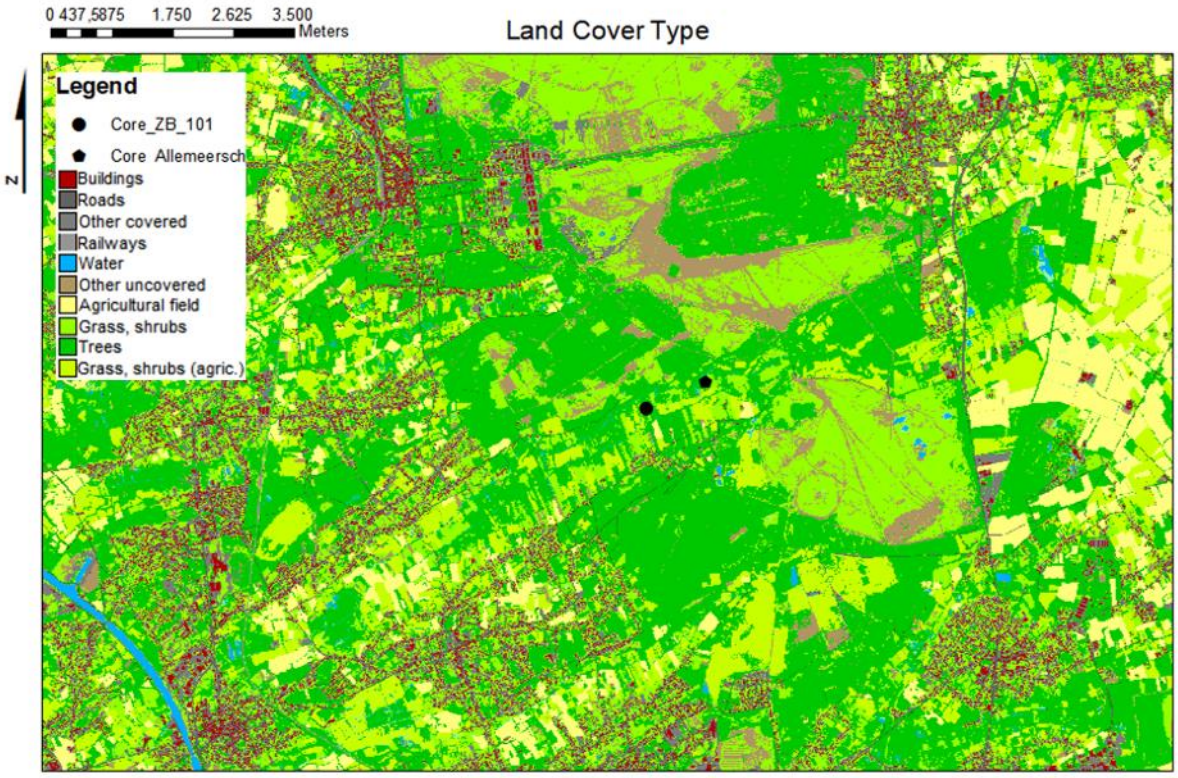

Figure 2.6: Landcover types in the Zwarte Beek catchment and its surroundings for the study area upstream of the Albert Channel (Informatie Vlaanderen 2012).

The soil types in the Zwarte Beek valley are dominated by histosols in the centre and umbrisols at the borders (Figure 2.5). The slopes and the plateau are dominated by podzols, followed by arenosols. Anthrosols are encountered mostly in the low lying areas but also on the plateau. Histosols are typically rich in organic material and correspond mostly to lowland fens or rain fed raised bogs (IUSS, 2015). Umbrisol are also rich in organic matter and are characterized by a darkly coloured topsoil. The sandy podzols can be recognized by the bleached eluvial horizon on top of an organic or ironoxide rich illuvial horizon. The associated vegetation is heathland and coniferous forest. The other dominant type of sandy soils in the study area are the arenosols which lack extensive profile development. The anthrosols finally are the result of intensive agriculture and often contain darkly coloured mineral horizons rich in soil organic carbon (plaggic horizons).

The current land cover in the valley itself is mainly occupied by grassland and shrubs not used for agriculture (Figure 2.6). A limited amount of arable fields is present and forest patches occur. The slopes of the plateau are strongly dominated by woodland. On the plateau, the military domains are covered by shrublands while to the east forest becomes dominant again in alternation with arable fields. When approaching the Albert Channel the surface covered by residual area, in and around the valley, increases.

2.4. Geology

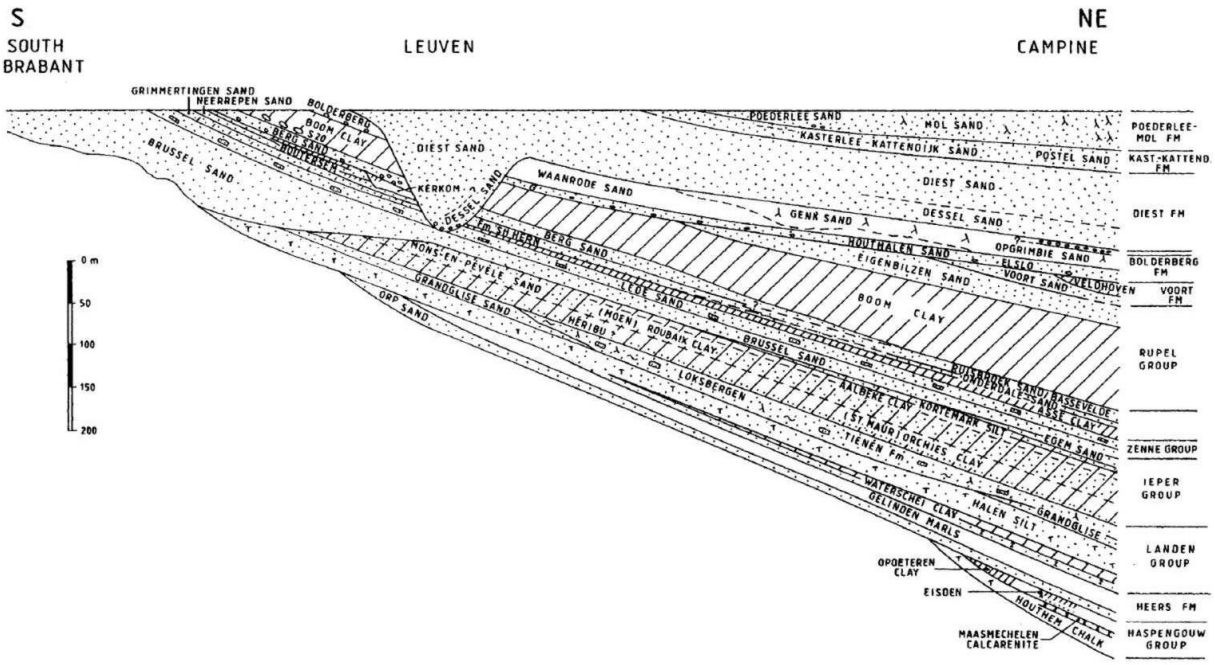

Figure 2.7: Generalized geological cross section through the subsurface between the south of Brabant and the Campine area (Vandenberghe et al. 1998).

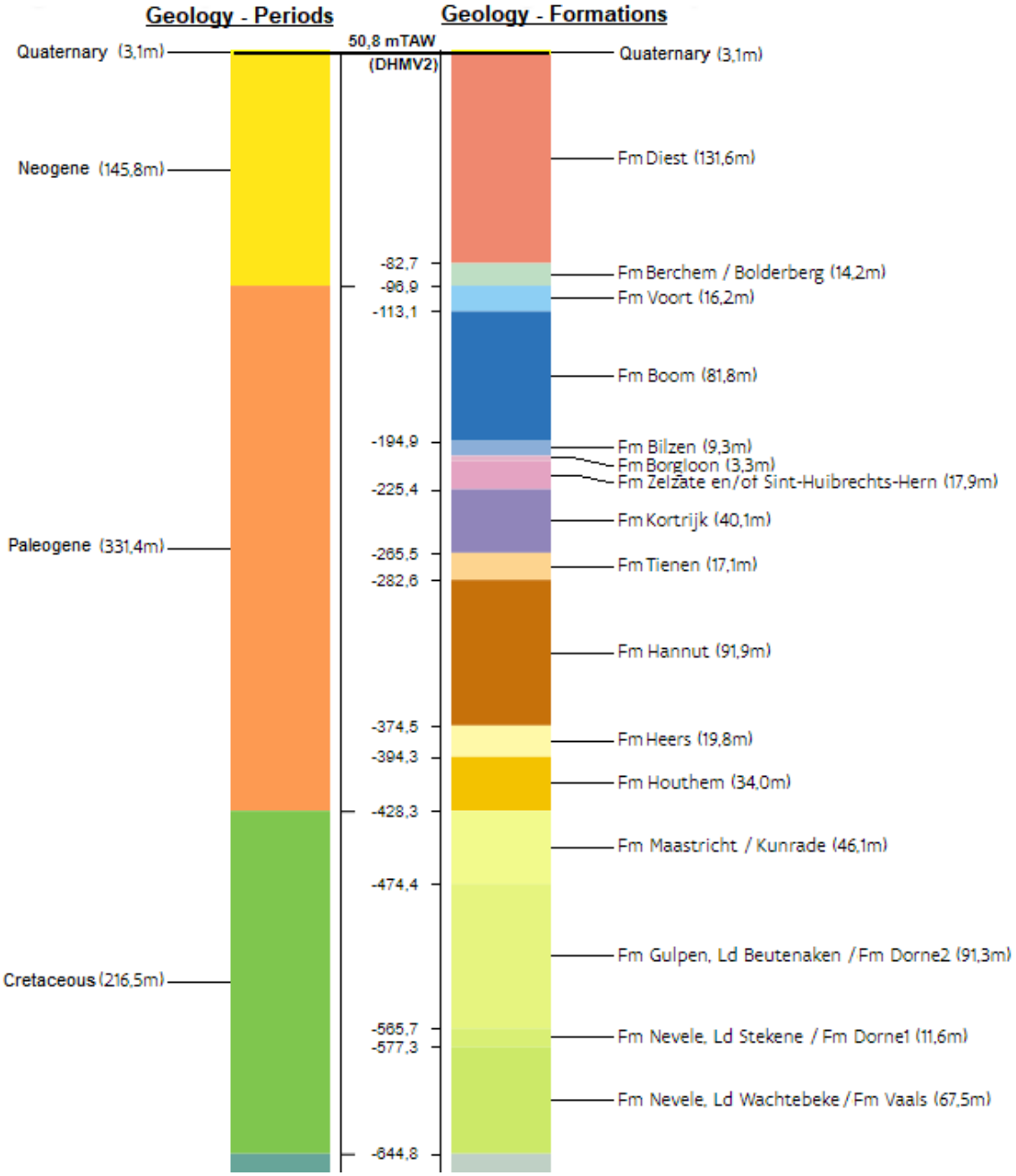

Figure 2.8: The results of a virtual drilling at the location of the selected peat sequence is displayed. The left column shows the estimated thickness of the geological systems, the right column the corresponding formations (DOV, 2018).

In Figure 2.7 the geological structures in the broad surroundings of the study area are displayed. The deep subsurface at the location of the Zwarte Beek valley is shown in Figure 2.8. Below the Quaternary and Tertiary formations, over 200 meters of Cretaceous deposits are found: The represented formations are from old to young the Nevele, Gulpen and Maastricht formation. The Nevele formation consists of fine grained grey chalk containing glauconite (Dusar & Lagrou, 2007). The Gulpen Formation contains silex banks and consists of white yellowish chalks. The Maastricht Formation at last is composed of yellowish chalks and hardgrounds.

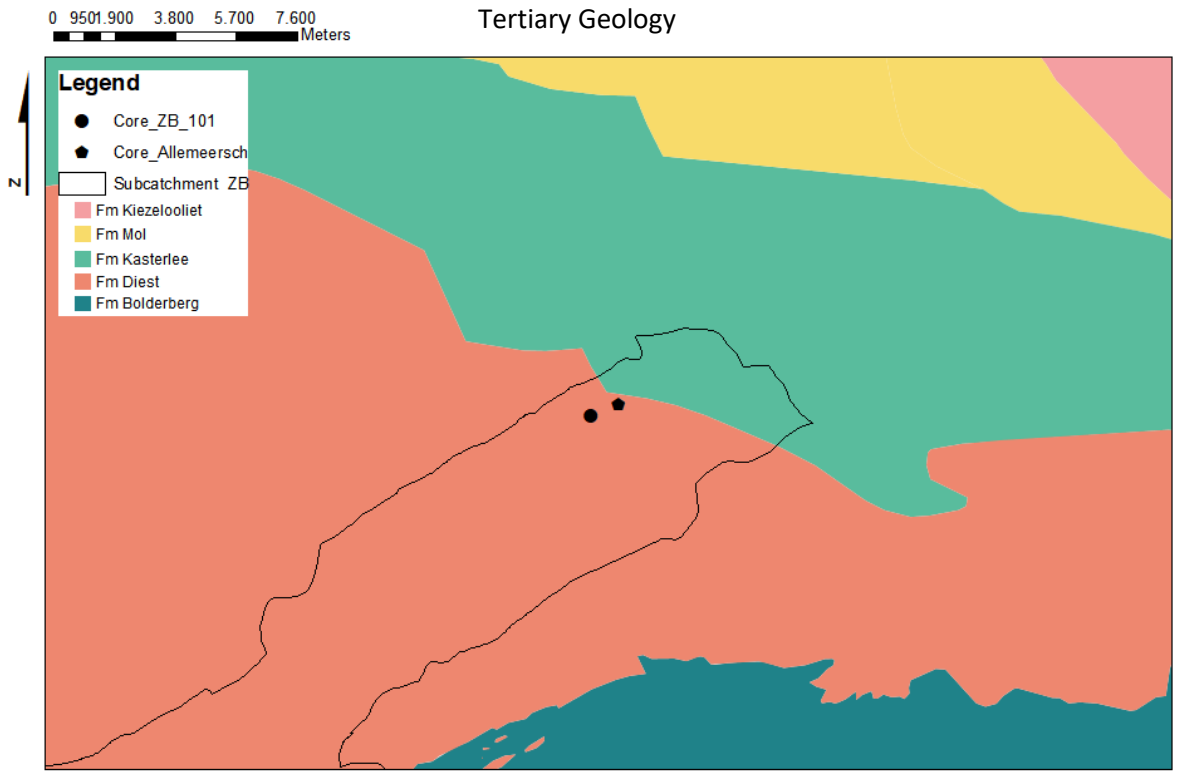

Figure 2.9: Tertiary geological map of the Zwarte Beek area (DOV 2001).

According to the virtual coring (Figure 2.8), approximately 330 meters of Paleogene deposits are present. The thickest formations are the Fm Hannut, consisting of marine clays to sands, and the Formation of Boom: The latter is composed of alternating silts and clays containing septaria concretions (limestone nodules). The formation is rich in glauconite and pyrite (Vandenberghe, 1978).

The Neogene is almost exclusively represented by the Diest Formation (130m) at the location of the coring. This formation is described as coarse glauconiferous sand with occurrence of silex pebbles. It overlays the Bolderberg formation composed of green fine sands. The map in Figure 2.9 shows that the Diest Fm is the upper tertiary formation at the study site. To the north this formation is overlain by the Kasterlee formation, composed of fine glauconiferous micaceous sands.

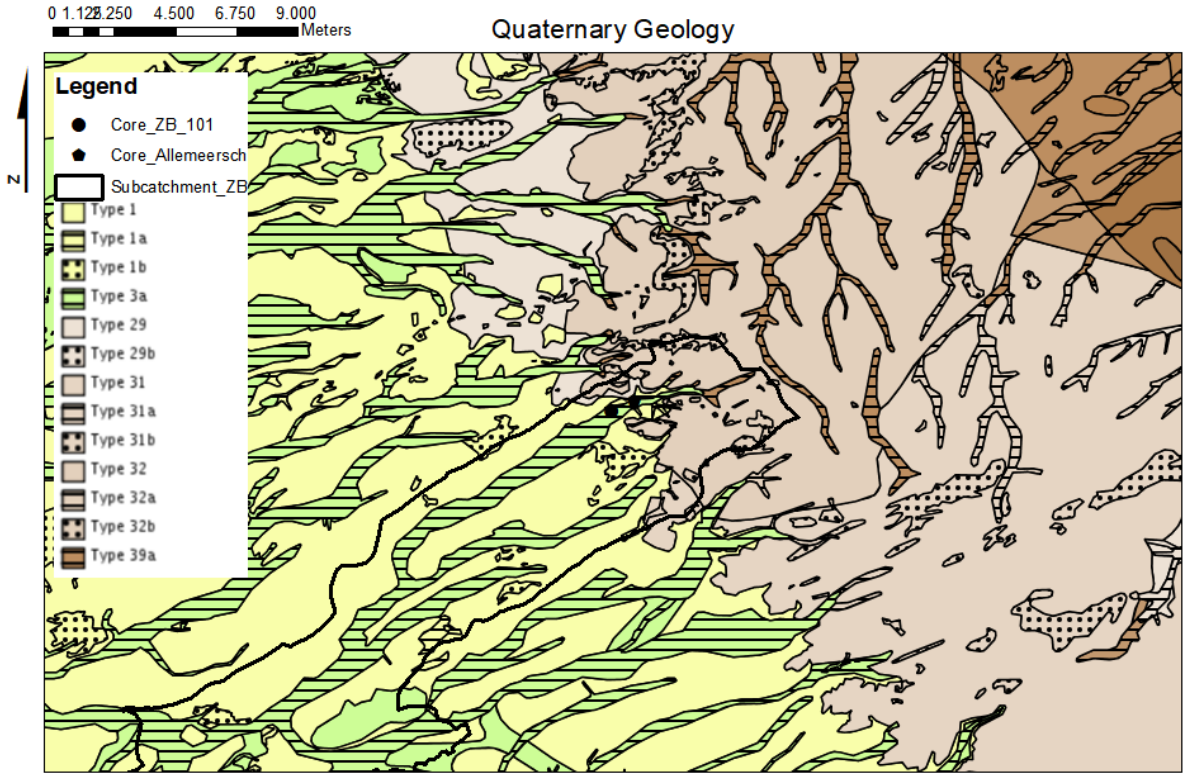

Figure 2.10: Quaternary geological map of the Zwarte Beek area. Stripes indicate postglacial fluviatile deposits, while dots indicate postglacial eolian deposits (DOV 2005).

In Figure 2.10 the Quaternary deposits in the surroundings of the study area are shown. The entire region is dominated by Late Weichselian cover sands: the yellow area (type 1) represents eolian Weichselian deposits, green (type 3) are eolian Weichselian deposits on top of fluvial (Scheldt) Weichselian deposits. Brown colours indicate the presence of Meuse and/or Rhine deposits, covered with eolian Weichselian/Saalian sands: Type 29 contains Mid-Late Pleistocene Meuse/Rhine deposits, type 31 Early-Mid Pleistocene Meuse deposits, type 32 and 39 Early Pleistocene on Rhine deposits.

The brownly coloured northeastern part on the Quaternary geological map (Figure 2.10) has an elevated topography and is known as the Campine Plateau. It is the result of differential erosion: the present-day plateau is composed of coarse sands and gravels deposited by the Pleistocene Rhine and Meuse braided rivers, resulting in a highly permeable erosion resistant unit (Gullentops et al. 2001).

2.5. Hydrology

The hydrogeological situation at the location of the study site is displayed in Figures 2.11 & 2.12. A continuous aquifer is found over the first 225 meter (Campine aquifer). Then, the Boom aquitard with a thickness of 50 meters is encountered. This layer with low permeability is underlain by a small aquifer (water-bearing permeable layer) of Oligocene age (33 meter) followed by an aquitard of 1 meter (Ieperian). Next, 133 meters of aquifer of Paleocene age are followed by the thick Cretaceous aquifer of approximately 260 meter thickness.

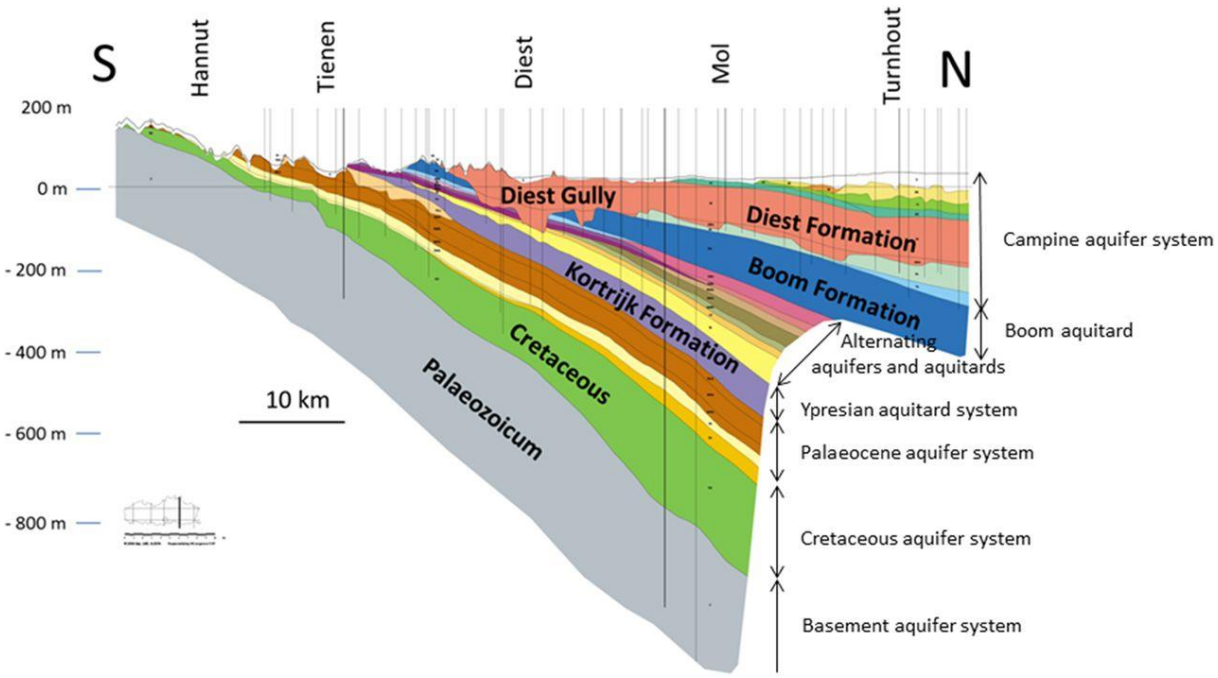

Figure 2.11: Hydrological structure of the Campine area along a N-S transect (Beerten et al. 2014a).

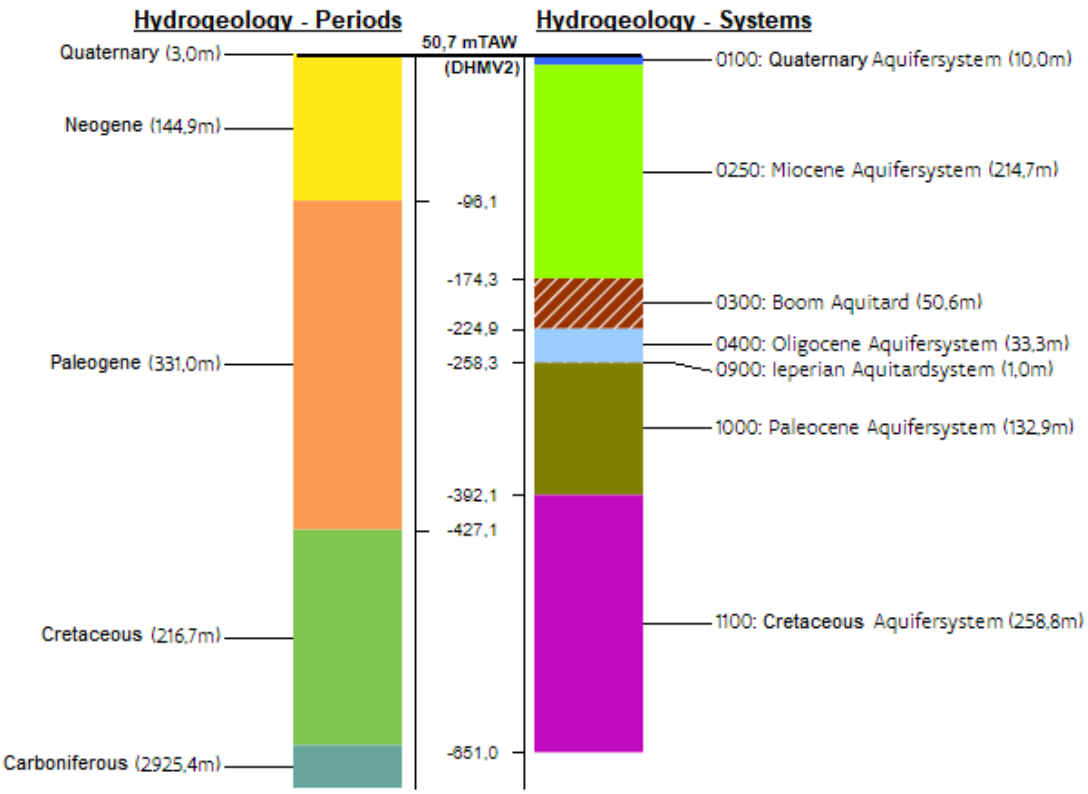

Figure 2.12: A virtual drilling at the location of the selected peat sequence is displayed. The right column shows the hydrogeological units (DOV, 2018).

Groundwater infiltrates on the highly permeable Campine plateau, flows through the Diest formation parallel with the Zwarte Beek and feeds the valley (De Becker & Huybrechts, 2000). The valley is characterized by a high water table, reaching up to the surface or maximal 1.5 m

below it. A strong iron rich seepage of 35 mm/day was observed (Maes et al. 2018). The source area of the Zwarte Beek is situated in intensive agricultural land on the plateau. This results in severe eutrophication of the incoming surface and groundwater of the Zwarte Beek valley. However, the influence of the surface water on the valley is limited to occasional flooding of the Zwarte Beek in a zone of tens of meters around the channel. Bio et al. (2002) characterized the groundwater chemistry: the pH ranged between 5.5 and 6.5, concentrations of SO_4, NO_3, NH_4, Cl, K, Mg and Ca were relatively low compared to other valley systems, while Fe values were intermediate and PO_4 was high.

2.6. Vegetation

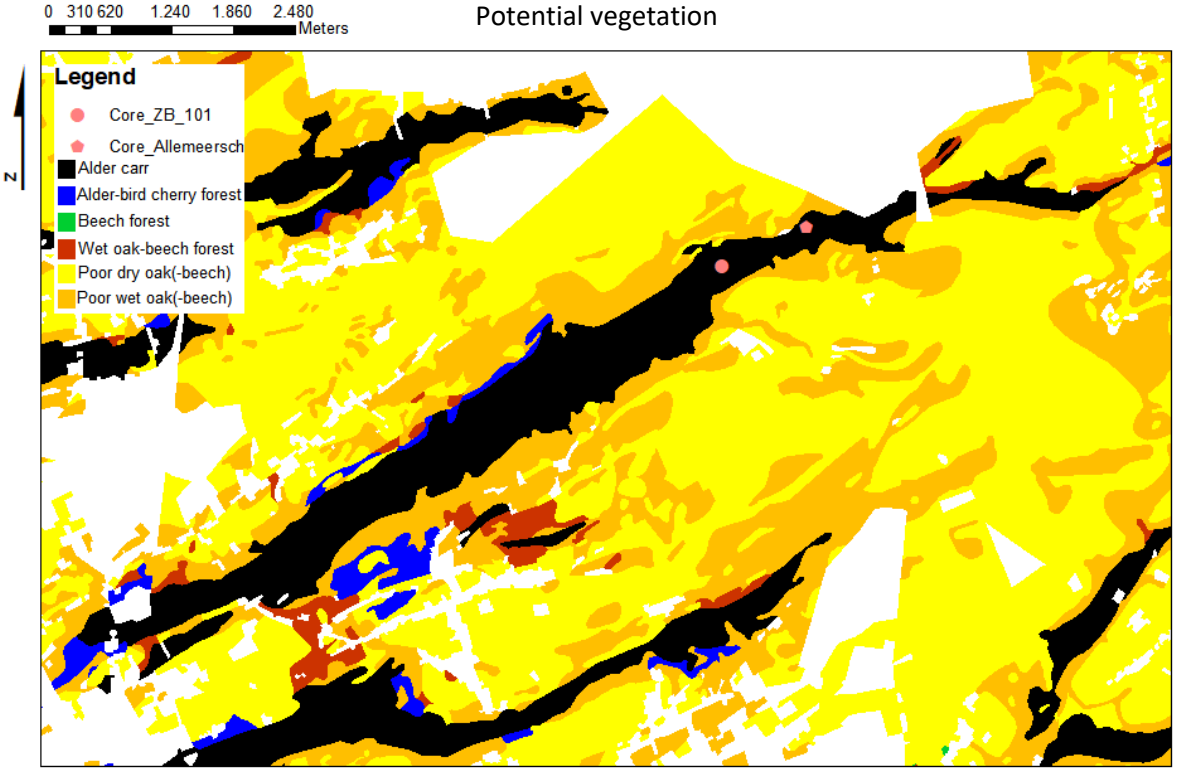

Figure 2.13: Map of the potential vegetation in the Zwarte Beek catchment (Informatie Vlaanderen 2015).

The potential vegetation is defined as the vegetation which is expected to be present at a location in absence of any human interference in past or present times. It is assesses based on a combination of the soil map with historical data and vegetation surveys. In the valley of the Zwarte Beek, alder carrs are indicated as the potential natural vegetation type (Figure 2.13). In the surrounding areas, oak-beech forests would dominate in absence of human disturbances, with a wet-to-dry gradient from the valley border to the plateau. Open vegetation types such as heather are absent.

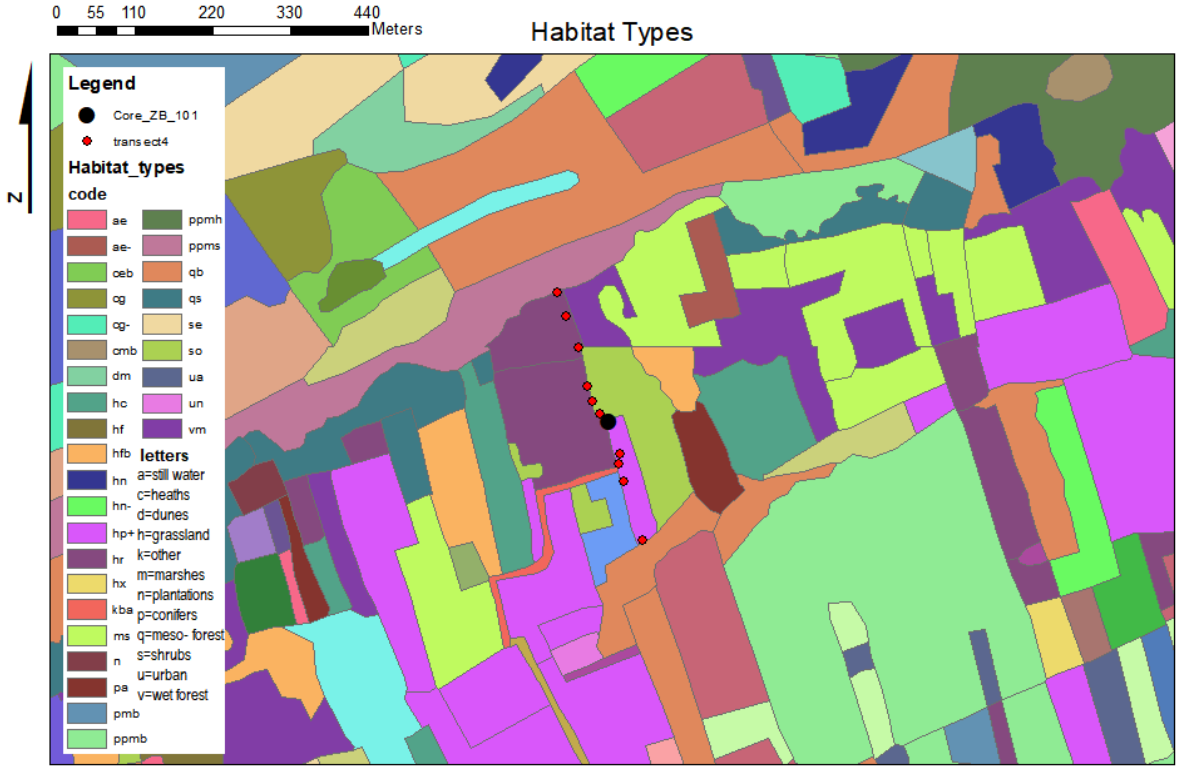

Figure 2.14: The map shows the habitat types according to the Biological Valuation Map (INBO 2018). The meaning of the first letter of the habitat codes is provided in the legend.

In the valley today a large variety of habitat types is observed (Figure 2.14). Examples are acidic fen areas, alder carrs, species rich cultivated grasslands, encroached grasslands, pine plants, acidic oak forests and willow stands. The slopes are occupied by oak birch forests and pine plants. On a larger scale conifer plants and dry shrub heath are dominant. Degraded types of heathland and residual areas are present in large proportions as well.

ANB and Natuurpunt are responsible for the management of the valley system. It is part of the largest Natura 2000 site in Flanders, covering an area of 83 km^2 ('Valley and spring area of the Zwarte Beek, Bolisserbeek and Dommel with heathland and fen areas', INBO 2015). According to the vegetation recording uploaded on the website waarnemingen.be, 529 plant species occur in the 4x4 kilometre box of the study site (at 9-12-2018). Some typical species are *Angelica Sylvestris*, *Cirsium palustre*, *Filipendula ulmaria*, *Galeopsis tetrahit*, *Juncus acutiflorus*, *Lotus uliginosus*, *Lycopus europaeus*, *Lythrum salicaria* and *Scirpus sylvaticus* (Bio et al. 2002). Several rare species find a suitable habitat in the Zwarte Beek valley (e.g. *Menyanthes trifoliata*, *Carex rostrata*, *Eriophorum angustifolium*, *Viola palustris*).

2.7. Human activities

Allemeersch (2010) studied the long-term evolution of the Zwarte Beek valley. He reconstructed an open vegetation during the Late Glacial followed by an increased forest cover from the Preboreal onwards. For the local vegetation he observed a with a pine- birch fen followed by a sedge fen gradually evolving to an alder carr. In this peat sequence no material

younger than 6.7 cal. kyr BP was present and therefore Allemeersch was not able to reconstruct the complete Holocene human impact history. He did found a remarkable similarity between the Early Holocene and modern vegetation composition in the valley, suggesting a vegetation history without severe alterations by human activities.

Verdurmen & Tys (2007) give an overview of archeological findings in the surroundings of the study area (Figure 2.15). Apart from some Stone Age artefacts from the militairy domain to the north, the most important archeological site in the proximity of the Zwarte Beek is Spiekelspade (1200 AD), which consisted of a group of farms. For this site, peat mining was recorded, as well as other land use activities and alterations including alder coppice, ditches, orchards, hayland and fishponds.

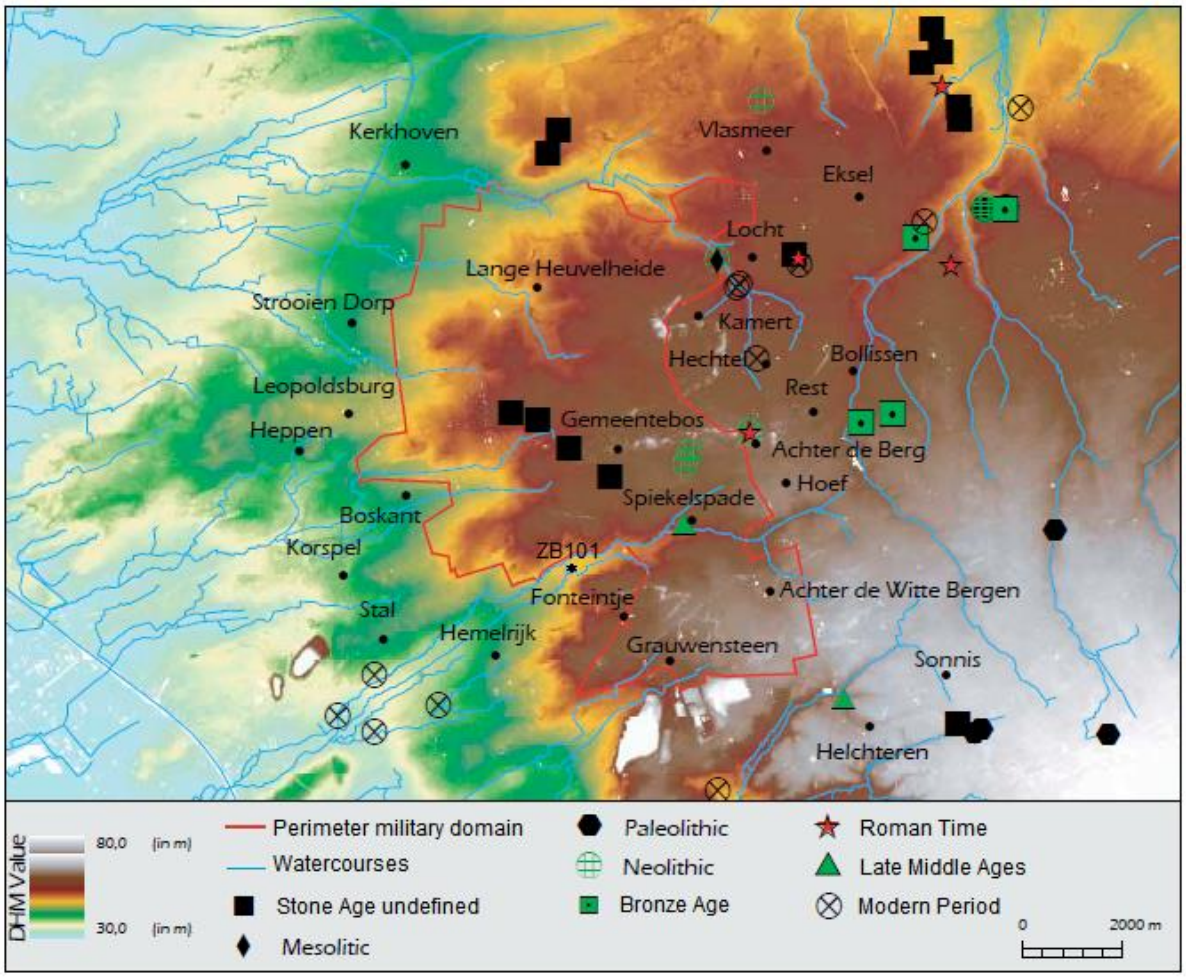

Figure 2.15: Overview of archeological evidence in the surroundings of the study site (Verdurmen & Tys 2007). The study site (ZB-101) is indicated by the black star.

Maes et al. (2018) give an overview of the human impact history for the past centuries in and around the Zwarte Beek valley: a semi-natural heather landscape was in use as extensive agriculture up to 1900 AD (Burny, 1999). The landdunes that can be observed today in these areas are interpreted as the result of the intensive use of the heather landscapes. The contemporary deciduous valley forests on the slopes were among the very rare forested areas in the period before 1850 AD. Forest cover increased with the introduction of conifer forests starting from 1775 AD on the plateau. These plantations strongly expanded from the arrival of

coal mining in the Beringen area (1920 AD) at the expense of heather. The heather further declined due to the conversion to industrial agriculture zones from 1935 AD. Residential areas and fishing ponds were introduced in the valley. De Becker and Huybrechts (2000) report the use as grassland (with dam construction to improve hayfields) and mining of peat and iron as dominant land use types before 1950 AD. Afterwards, this decreased while drainage activities increased for agricultural purposes. The Oude Beek (already present on Ferraris maps, Allemeersch 2010) for instance was deepended as a drainage channel. Together with smaller ditches a whole drainage network was created forming a main cause of peat degradation: Drainage results in a lowered water table, allowing mineralization of the stored organic matter (Maes et al. 2018). However, problems of subsidence and accessibility persisted, leading to spontaneous forestation to alder carrs and increased installation of plantations such as poplar plants over time.

According to Rogiers et al. (2011), human activities in the valley of the Zwarte Beek caused some severe disruptions of the natural hydrology: A drainage system and a weir were installed in the valley and the course of the river was altered, putting pressure on the wetland biotopes. In the recent past, some restoration measures were introduced in the valley with the aim of reinstalling the pristine hydrological conditions. The effect was evaluated using groundwater modelling: this showed that the structure of the natural hydrology was indeed locally restored but the effect on the water table was poor, which is crucial to protect the wetland system.

3. Material and methods

3.1. Fieldwork

In the summer of 2018 the fieldwork in the valley of the Zwarte Beek was performed. During the first two days coring transects were created (Figure 3.1, Appendix B.2). Several corings were made following a line perpendicular to the river valley, with 11 corings for transect 1 spanning 380 m and 12 for transect 2 spanning 600 m. A handhold GPS was used to capture the location of all points along the transects. When a coring was performed, the upper part of the soil was collected with an Edelman core. The remaining depth was cored using a narrow gouge auger. Several segments (max. 1 m) were collected until deeper perforation into the subsurface was not possible. The collected segments were lined up along a ruler for a detailed description of the texture, colour and organic content (Appendix A.1 for transect 1 and A.2 for transect 2). The information of all corings along one transect was combined into a geomorphological transect and used for the reconstruction of the thickness of the peat layer and other sediments throughout the Zwarte Beek valley.

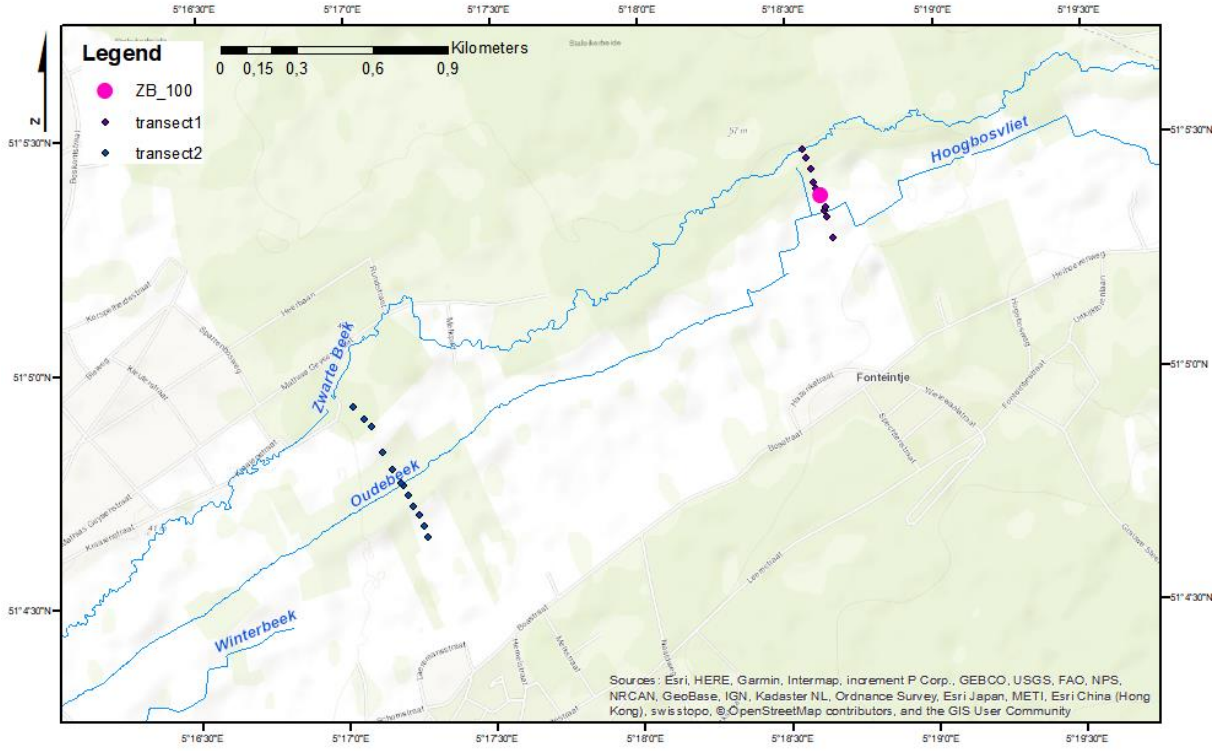

Figure 3.1: Map of the Zwarte Beek valley with the two transects displayed together with the location of the final peat core.

Based on the created transects, the location of the final core was chosen according to the location with the thickest undisturbed peat accumulation: this was point 4 along transect 1 (5° 18' 41.7" E, 51° 5' 20.2" N). During the last day of the fieldwork the final sediment sequence was collected at this location using a broad guts core (6 cm). Two identical corings (ZB-100 and ZB-101) were performed with a spacing of 20 centimetres to ensure enough material for all analyses and to complement the other core in case of gaps and disturbances. The peat was cored to its bottom, indicated by the transition to sand deposits. The exact length and

intactness of all collected segments was noted (Appendix A.3 for ZB-100 and Appendix A.4 for ZB-101) and the material was transferred to tubes and packed in foil to prevent contamination. These tubes were transferred to the KU Leuven cooling space and stored until the start of the laboratory processing.

3.2. Training Germany

During the final week of August we were invited by Dr. Elena Marinova for a research stay at the archaeobotanical lab of the State Office for Cultural Heritage Baden-Wuerttemberg in the city of Gaienhofen, Germany. In the first part of our stay we learned the basics of microscopy in palynological research, including the use of phase contrast and image analysis software. Typical Holocene pollen species of north-west Europe were studied from pre-existing slides with the aid of several determination keys (Beug 2004, Faegri & Iversen 1989, Punt & Blackmore 2003) and the help of our supervisor Dr. Elena Marinova. Detailed drawings were made to record all necessary details for identification of pollen grains during the analysis of our own samples back in Belgium. During the last days of the research stay we created a reference collection of pollen slides for the KU Leuven. In addition, we were taught the lab procedure for pollen slide preparation starting from modern plant samples derived from freshly collected plants and herbarium specimens.

3.3. Laboratory work

In October core ZB-101 was subsampled by cutting the core into slices of 1 centimetre thick over its entire length. The outer boundary of the slices was removed to prevent contamination from the borehole walls, using a freshly cleaned knife. The remaining material was transferred to labelled plastic bags and stored in the fridge. All work was done on a surface covered with foil to prevent contamination.

Processing of peat samples started during the last week of October. Approximately every 8 cm a sample was taken, except for severely disturbed parts (Appendix A.5). In the upper part of the core additional intermediate samples were investigated to obtain a higher resolution for the important vegetation transitions situated in these parts. In total 31 levels of peat were investigated

The peat samples (representing 1 cm of depth) were subsampled to a volume of 1 cm^3. For the pollen extraction, the procedure described by Faegri & Iversen (1989) was used as displayed in Figure 3.2. Potassium hydroxide (10%, 20 ml) was added while heating the solution to achieve disaggregation of the samples, as well as a *Lycopodium* tablet. The addition of a known quantity of exotic *Lycopodium* pollen allows to calculate the absolute accumulation of pollen grains in the analysed peat samples. Subsequently the samples were sieved at a 200 µm mesh size filter and centrifuged (1 min, 2000 rpm) and decanted to remove the KOH. Next, water washing was applied twice: 2 ml water is added, the tube is put for 10 seconds on the vortex and the tube is filled with water until 12 ml, before centrifugation is applied.

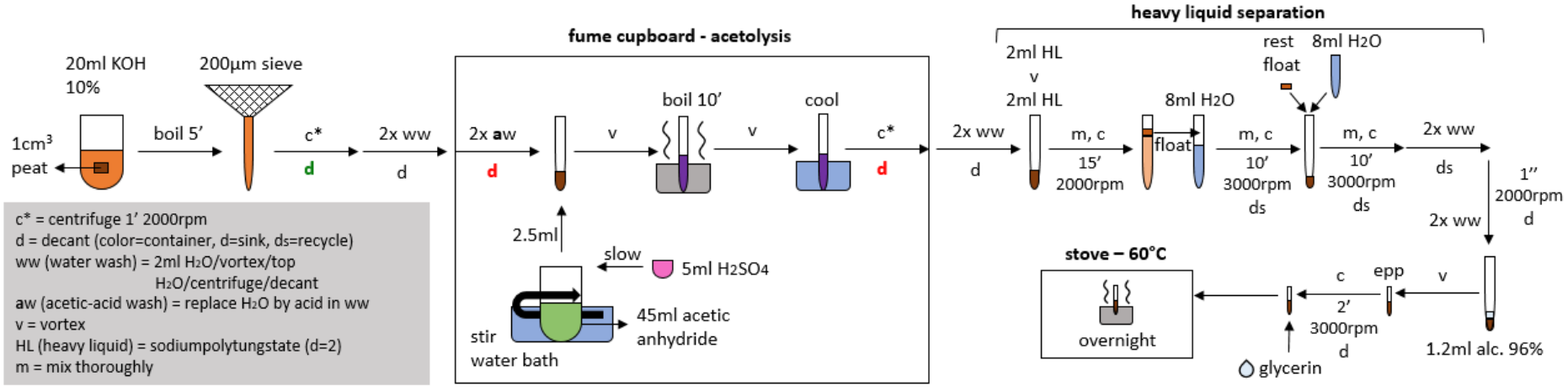

Figure 3.2: Schematic overview of the laboratory procedure for pollen extraction of peat samples (after Faegri & Iversen 1989).

A mixture of H_2SO_4 (5 ml) and acetic anhydrite (45 ml) was created while stirring and cooling in a water bath to perform the acetolysis. First the samples were washed with acetic acid to remove all water: 2 ml acetic acid is added, the sample is vortexed, 4 ml acetic acid is added and centrifugation is performed. Then 2.5 ml of the acid mixture was added and the samples were mixed and heated to speed up the reaction leading to breakdown of all organic matter other than the pollen itself. After cooling, centrifugation was performed and the samples were water washed twice to remove all remaining acids.

Heavy liquid separation was performed to separate the pollen from the remaining sediment in the samples. For this 2 ml of sodiumpolytungstate (2 kg/l) was added and after vortexing again 2 ml were added. After centrifugation (15 min, 2000 rpm), the float was transferred to new tubes and the heavy liquid was saved. Next, 8 ml of water was mixed through the samples before centrifugation at 3000 rpm for 10 min. This step was repeated and followed by three water washes.

To allow the transfer of the extracted pollen to Eppendorf tubes, 1.2 ml methanol (96%) was added to the centrifuge tubes. A volume of glycerine equal to the residue was added. Finally the tubes were put in a stove at 60°C overnight. The next day the slides could be made: One droplet of sample material was added to a glass plate, while heating on a hotplate. A small amount of glycerine jelly was mixed through it if the pollen were too dense. The samples were closed by melting of parafine on a hotplate around the sample spot before coverage with a cover slide.

3.4. Microscopic analysis

The microscopic study of the pollen slides started in November. The identification of pollen taxa and other material on the slides was done using the determination keys of Moore & Webb (1991) and Beug (2004), together with the self-made reference collection and the aid of our supervisors. Using a 400x magnification the slides were scanned from the left lower corner in horizontal rows to the right upper corner (Appendix D.2). This was done until a minimal count of 200 pollen was reached, requiring the preparation of additional slides when pollen were sparse. The remaining part of the slide was scanned to look for additional species. Apart from pollen, spores of ferns, mosses and fungi were counted as well as charred particles.

3.5. Data Analysis

a. Age-Depth model

Seeds were selected from four levels (303, 183, 127 and 32 cm) in the core and send to the Koninklijk Instituut voor het Kunstpatrimonium (Royal Institute for Cultural Heritage) lab for AMS (Accelerator Mass Spectrometry) radiocarbon dating. An Age-Depth model was created using the ‘clam’ package and function clam() in R (Blaauw 2010). As input values the uncalibrated radiocarbon ages and associated errors, as provided by the AMS analysis, were used. The IntCal13.14C calibration curve was selected to convert radiocarbon ages to calendar ages. A linear extrapolation function was chosen to construct the final age-depth model since the use of smooth splines resulted in unrealistic outputs.

b. Pollen diagrams

The processing of the pollen data started with the conversion of the absolute number (counted pollen grains per taxon per depth level) to relative percentages of a taxon per depth level. This was done in Excel using the pollen sum as denominator: The pollen sum $\sum P$ is defined as the sum of all regional pollen of a single investigated level, with wetland plants, water plants and spores excluded. For all counts (x) the relative abundance was then calculated by $x/\sum P$, which results in a maximum of 100% for regional pollen, but possible higher values for the groups not included in the pollen sum. For the graphical display of the relative abundances, the software C2 was used (Juggins 2007). In the final pollen diagrams a time axis was added next to the depth axis, based on the output of the Age-Depth model.

The pollen taxa were divided into six groups (trees and shrubs, upland herbs, wetland plants, aquatic plants, climbers and epiphytes, spore plants) based on their physiognomy and ecology as described in Heukels' Flora (Van der Meijden 2005). For these groups the pollen sum was used to calculate the total group percentage on each level. The same approach was used to calculate the percentage of anthropogenic indicator species: Behre 1981 and Bakels 2009 were used to identify the taxa indicating human activities. Chenopodiaceae, Cerealia, *Secale cereale*, *Plantago lanceolata*, *Rumex acetosa* and *Fagopyrum* were considered to be anthropogenic indicators while Asteroideae, Brassicaceae, Apiaceae, Caryophyllaceae, Ericaceae, *Cirsium*, *Rumex sp*., *Ranunculus*, *Eryngium*, *Galium*, *Campanula*, *Persicaria* and *Succisa pratensis* were described as possible anthropogenic indicators.

The pollen accumulation rate (PAR) of each investigated level was calculated based on the number of encountered *Lycopodium* grains in the pollen slides. The following formula was used: $PC = \frac{L_t \cdot PS}{Lc}$ with L_t the total amount of *Lycopodium* grains in a tablet (9666), PS the pollen sum and L_c the counted number of *Lycopodium* grains. This gives the pollen concentration (PC, pollen/cm³) and is multiplied by the sedimentation rate (cm/yr) to obtain the PAR in $\frac{pollen}{cm^2 \cdot year}$ (Seppä et al. 2009). The same formula can be used to calculate the charcoal accumulation rate (CHAR) when PS in replaced by the absolute number of counted charcoals.

c. Statistical analysis: Clustering

For the cluster analysis, Bray-Curtis dissimilarities were used because abundance vegetation data is represented in the pollen data matrix and this measure is the most appropriate for the investigated data type (Wildi 2017). A hierarchical cluster analysis (HCA) was performed using Flexible Beta as linkage method, with β=-0.25 since this results in space conserving dendrograms (Aho et al. 2008). Input data included the vegetation matrix of all pollen occurring in more than two samples. Non-pollen taxa which were included are *Sphagnum*, *Equisetum* and monolete ferns. *Secale cereale* only occurs in two samples but was retained due to its significance as anthropogenic indicator. This resulted in a total of 41 taxa included in the clustering analysis: 29 taxa were used for the regional clustering and 12 for the local analysis. In R the package 'cluster' with function agnes() was used. A cluster analysis results in a dendrogram which orders the samples according to their similarity in pollen spectrum. To obtain vegetation zones from such a dendrogram, it can be cut at a certain height (h) corresponding to the dissimilarity between the created groups (Wildi 2017).

An alternative cluster analysis was performed by using a constraint clustering method. The output of the clustering alghorithm was constrained by the variable depth, in order to create clusters between adjacent samples in the core only. In R, function chclust() from the package 'rioja' was used with Coniss (constrained incremental sum of squares, Grimm 1987) as clustering method. The results of this cluster analysis were used to divide the pollen diagrams into local (LPAZ) and regional (RPAZ) vegetation zones and the resulting clusters were also plotted on the ordination diagrams to help their interpretation.

d. Statistical analysis: Ordination

An ordination analysis was performed on the pollen data: the goal of this analysis is to detect major patterns in the pollen data. Similar to the cluster analysis, the ordination analysis was applied to 29 regional pollen taxa and 12 local taxa separately. After calculation of the Bray-curtis dissimilarities, NMDS (non-metric multidimensional scaling) was chosen as ordination method since this technique yields the best results for vegetation data (i.e. the high-dimensional data are displayed with a few ordination axes with minimal loss of information, Zuur et al. 2007). In R, the package 'vegan' was used to perform the analysis (Dixon 2003). A scree plot was created representing the stress analysis to choose the optimal number of ordination axes with 0.1 being used as threshold for a 'good' ordination (Zuur et al. 2007).

For the regional NMDS analysis, three axes were investigated based on the scree plot values. The interpretation of the third axis was not straightforward but was linked to a certain extent with external variables (e.g. corrosion and charcoal). The NMDS analysis was also performed for two axes only, but this resulted in a biplot very similar to the biplot of axes 1 and 2 in the 3D analysis: therefore the use of three axes was not considered disadvantageous for further interpretation of the vegetation data and the third axis was retained for completeness. For the local analysis two ordination axes were used since a detailed interpretation of the multivariate data was not eligible due to the low number of included taxa. This resulted in a stress value of above 0.1, but below 0.2 corresponding to the class 'acceptable' (Zuur et al. 2007).

To help the interpretation of the ordination axes, additional external variables were plotted on top of the ordination diagrams. The closedness of the vegetation (AP%), abundance of charcoal and corroded pollen were taken from our own sample analyses. In addition, pollen-based local climatic data from Mauri et al. 2015 were analysed, with a temporal resolution of 500 years and spatial resolution of 1°. These consist of the mean annual air temperature (MAT, °C) and mean monthly precipitation (MMP, mm/month), both expressed as anomalies from the year 1850. Lastly, community weighted mean Ellenberg values (MEV) were used as an approximation of changing environmental conditions over time. The corresponding values for light, pH, moisture and nutrients (L, R, F, N) per plant type were taken from Hill et al. 1999. The following formula was used to calculate the mean value for each of the four variables per investigated depth: $MEV_j = \frac{\sum_i c_{ij} \cdot E_i}{T_j}$ with i representing the investigated pollen taxon and j the investigated depth. C represents the pollen abundance, E the Ellenberg value and T the sum of the pollen counts at a certain depth. For the regional analysis 21 pollen taxa were used to calculate the L, R, F and N MEV while Poaceae, Asteroideae, Brassicaceae, Cerealia, Apiaceae, Caryophillacea and Lactuceae were left out of the analysis since these groups are too big to calculate a representative Ellenberg value from the species values in the list of Hall et al. (1999). For the local MEV values, all pollen taxa were retained in the analysis. The function envfit() in R from the package 'vegan' was used to calculate the normalized values of

the arrow tips of all variables and their correlation coefficient with the ordination configuration as well as the associated p-value. Plot() was used to add them as arrows to the ordination biplots and ordisurf() was used to show the variables as contour lines in case a non-linear trend inhibited the representation of the variable by an arrow.

In a final step, a NMDS analysis was performed on all the pollen data, combining the input data from the local and regional analyses. The analysis was performed for two ordination axes and was mainly used as visualization tool for the final clustering of the vegetation development of the Zwarte Beek. No detailed interpretation of the ordination configuration was made because it represents a mixed signal of two largely independent vegetation evolutions, since environmental conditions between the local valley and the regional uplands are expected to be the result of different processes (e.g. local hydrology vs. climatic control).

3.6. Data compilation

A combined diagram was made for the local vegetation development of the Zwarte Beek valley, including data on plant macrofossils (Master Thesis Laura Vervacke), wetland and aquatic pollen. The vegetation data was integrated with the local fire history, based on the results of an analysis of macro charred particles (Bachelor Thesis Eveline Scherps). Both additional proxy records were derived from analysis of the same peat core (ZB-101) on which the pollen analysis was performed. The local pollen-based climate reconstructions from Mauri et al. 2015 were also correlated to the obtained results. Based on an integration of the multiple proxies and statistical analyses of the pollen records (clustering and ordination), a final zonation of the development of the Zwarte Beek landscape was established. The results were compared to the independent vegetation reconstruction for the Zwarte Beek area by Allemeersch (2010) and other records from the surrounding regions. Data were also collected on the Eemian environmental changes of western Europe to allow a qualitative comparison of the reported patterns during both interglacials.

Maps of the study area were created using Arcmap 10.4.1. All layers were derived from Geopunt, except for the gps-files of the Zwarte Beek transect and core locations. The geomorphological transect (by Ward Swinnen) and other figures were created using Inkscape.

4. Results

4.1. Geomorphology

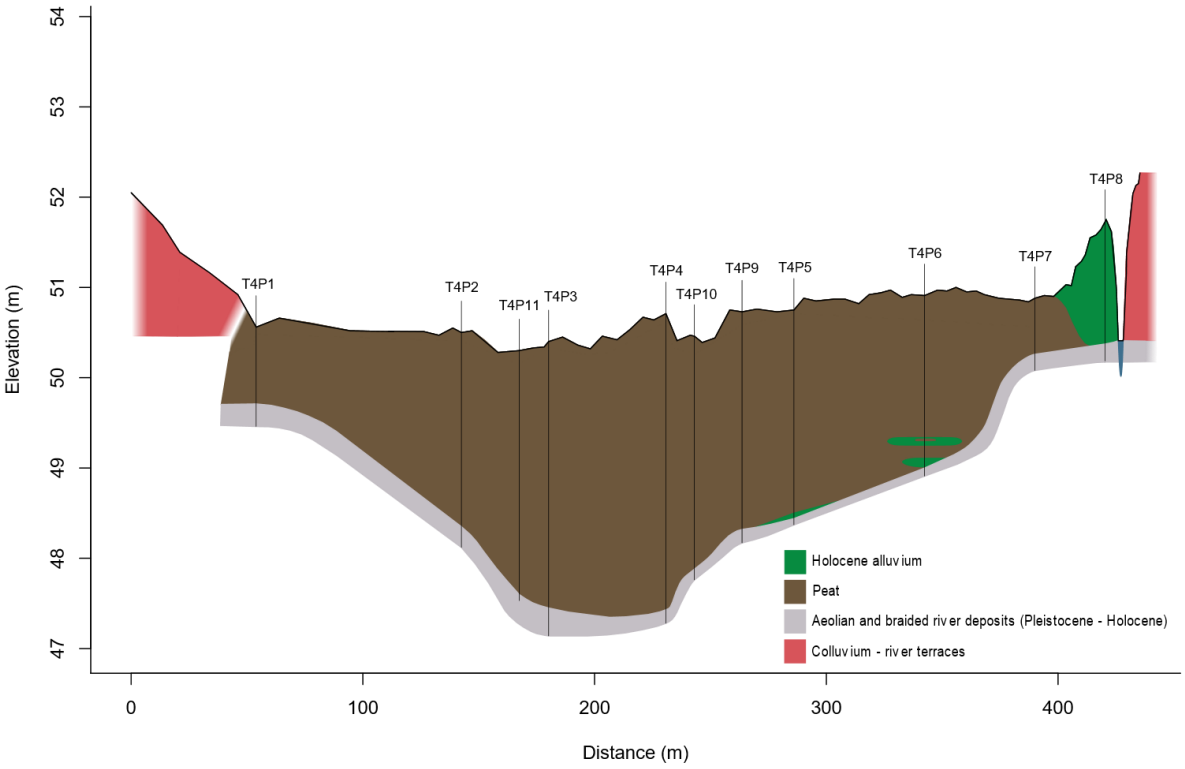

Figure 4.1: Transect 1 based on the corings made during the fieldwork. Point T4P4 indicates the location of the selected core for further analysis (See Appendix A.1 for description of the cores).

In Figure 4.1 the transect perpendicular to the Zwarte Beek valley is shown, from which the final peat core was taken. The transect indicates the existence of a narrow pre-Holocene valley, suggested by the position of the sand layer. This valley is almost entirely filled with peat reaching a maximum thickness of over three metres in the centre of the valley. The Zwarte Beek itself is situated in the very north of the valley, left of coring 8 on Figure 4.1. Close to this channel, fine sandy deposits were encountered interpreted as alluvial clastic deposits. Similar sediments were found in cores 5 and 6 and could indicate the former position of the Zwarte Beek channel in the valley. More downstream in the valley (Figure 4.2), open water gyttja deposits were encountered close to the location of the contemporary anthropogenic Oude Beek channel. The paleovalley is also observed on this transect, but seems to widen in downstream direction.

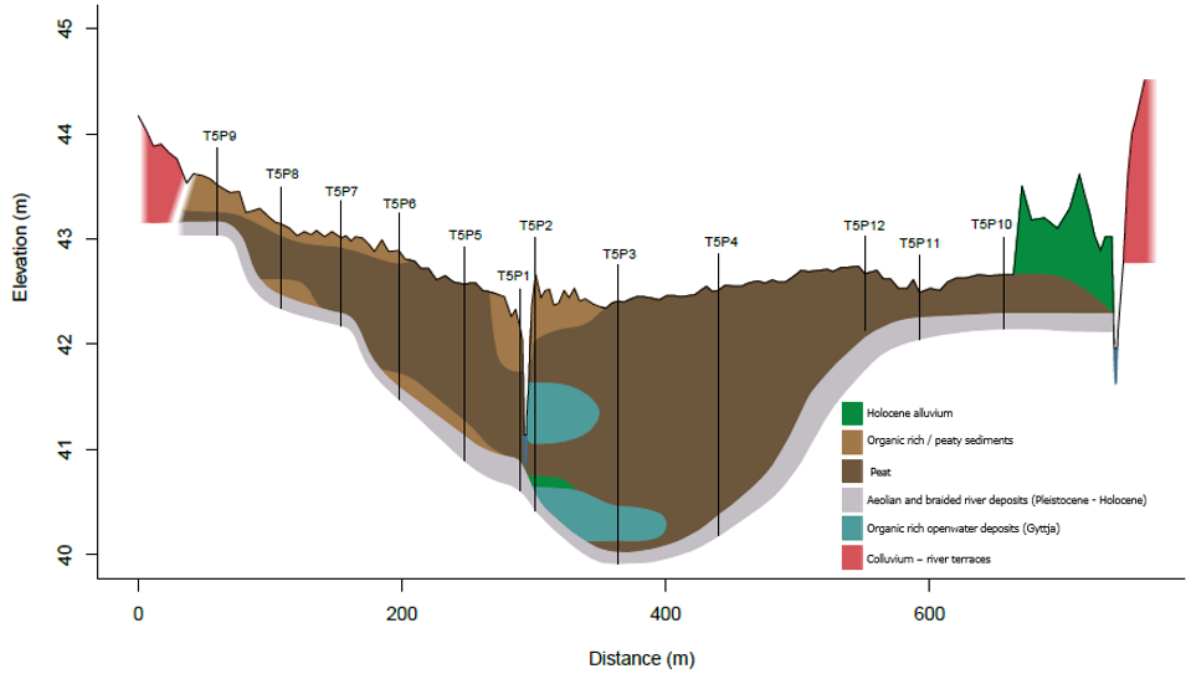

Figure 4.2: Transect 2 based on the corings made during the fieldwork, situated more downstream in the valley of the Zwarte Beek compared to transect 1 (See Appendix A.2 for description of the cores).

4.2. Age-Depth model

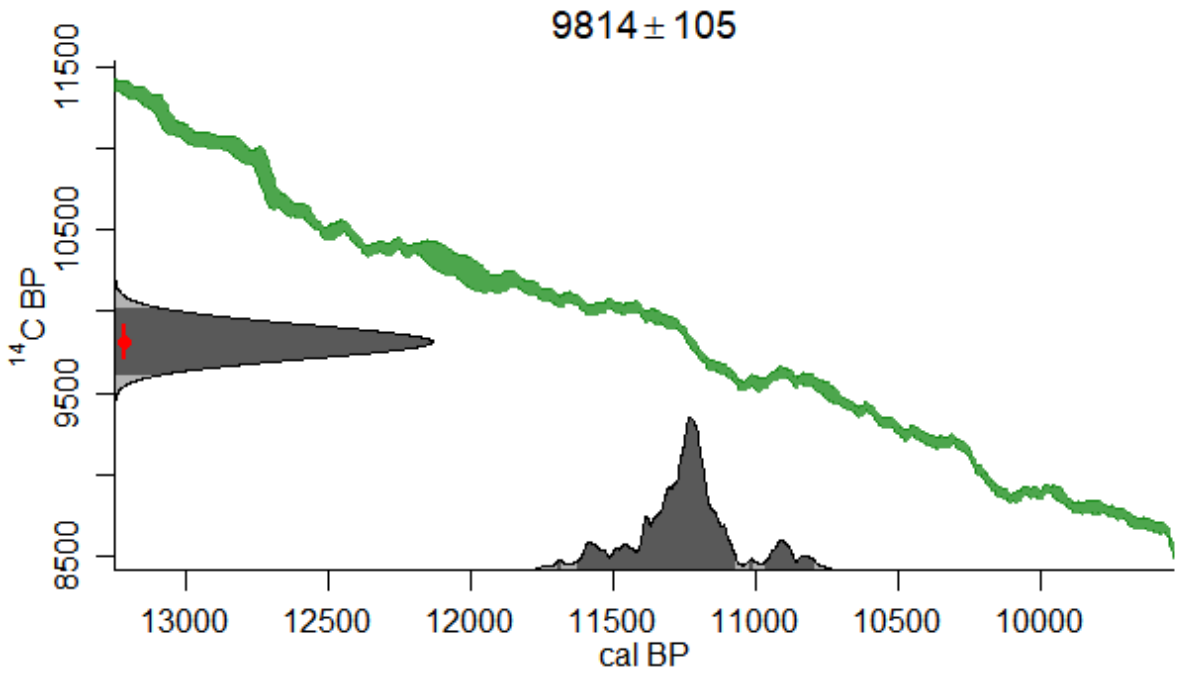

Figure 4.3: Example of the calibration of radiocarbon ages (y-axis) to calibrated ages (x-axis) for depth 303 cm. The green line represents the calibration curve.

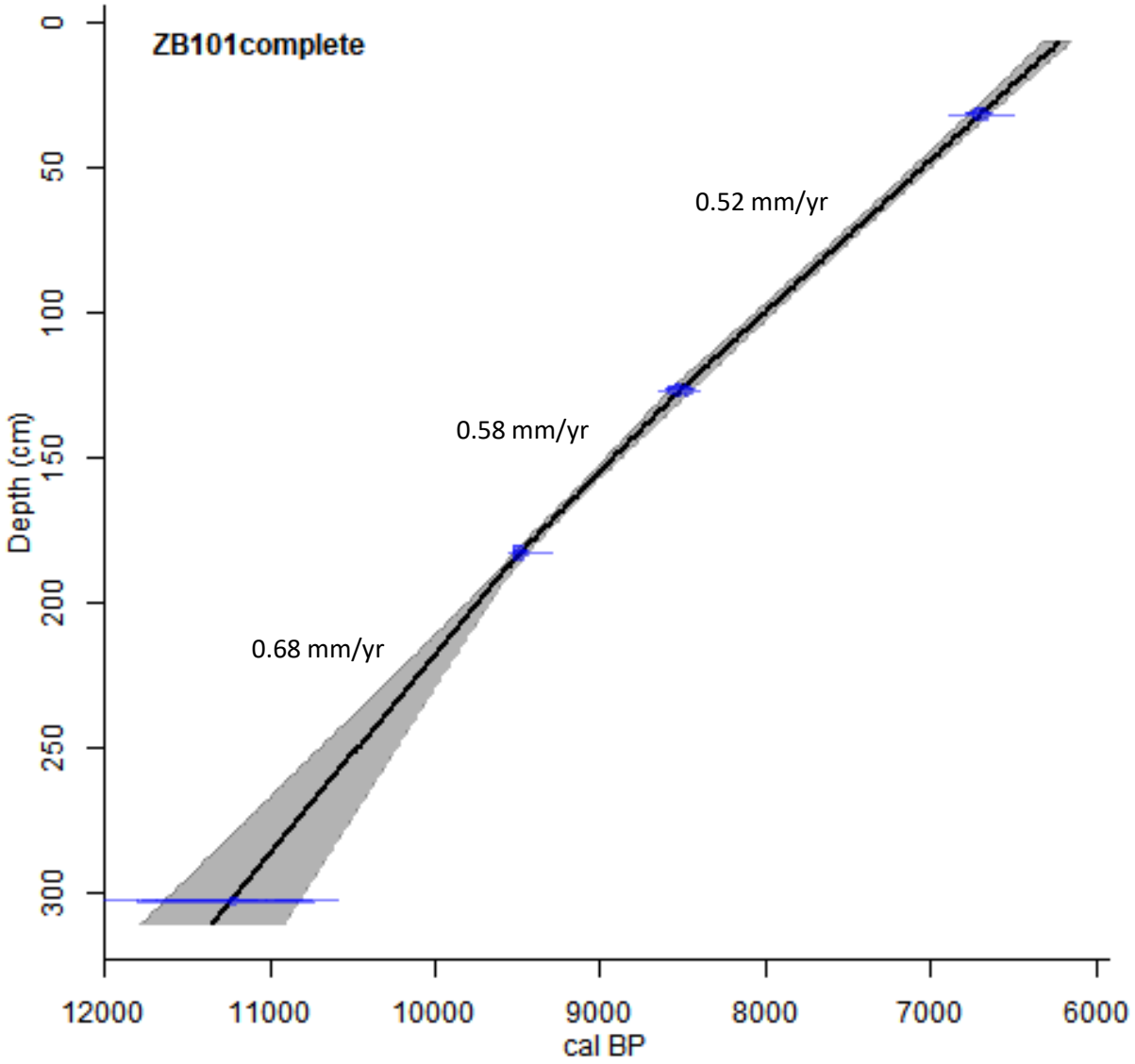

Figure 4.4: Age-Depth model for the ZB-101 peat core, using linear interpolation for the depth interval 311 – 7 cm over which the pollen samples were taken. In this model no hiatus is included: alternative models are presented in the discussion (Figure 5.1).

In Table 4.1 the results of the radiocarbon dating of the four investigated levels in the peat core are displayed. Figure 4.3 illustrates the use of the calibration curve. The resulting calibrated ages are combined into an age-depth model represented in Figure 4.4. The lower age of the core (311 cm) is estimated as 10915-11782 cal. years BP (95% confidence interval) while the top (7 cm) has an approximate age of 6148-6316 cal. years BP. The average peat accumulation rate for the entire peat core is approximately 0.60 mm/year when interpolating between the dated levels 303 and 32 cm. Below 183 cm, the accumulation rate is calculated as 0.68 mm/year, between 183 and 127cm 0.58 mm/year and above 127cm 0.52 mm/year.

Table 4.1: Overview of the obtained radiocarbon ages by AMS and the corresponding calibrated ages.

Sample code	Lab code	Depth (cm)	Material	14C age (yrs BP, error)	Cal. age (yrs BP, 95 % CI)	Best estimate (cal yrBP)
ZB-T4P4-101-32	RICH-26911	32	*Betula* fruits	5879±31	6643-6773	6702
ZB-T4P4-101-127	RICH-26652	127	Wood with bark	7745±33	8443-8587	8520
ZB-T4P4-101-183	RICH-26649	183	Wood with bark	8464±33	9441-9527	9489
ZB-T4P4-101-303	RICH-26708	303	*Carex* fruits	9814±105	10825-11640	11244

4.3. Pollen diagrams

In Appendix C (C.1, C.2 and C.3) the complete pollen diagram including all encountered groups can be found. Figure 4.5 shows an overview of the dominant pollen types in the investigated samples.

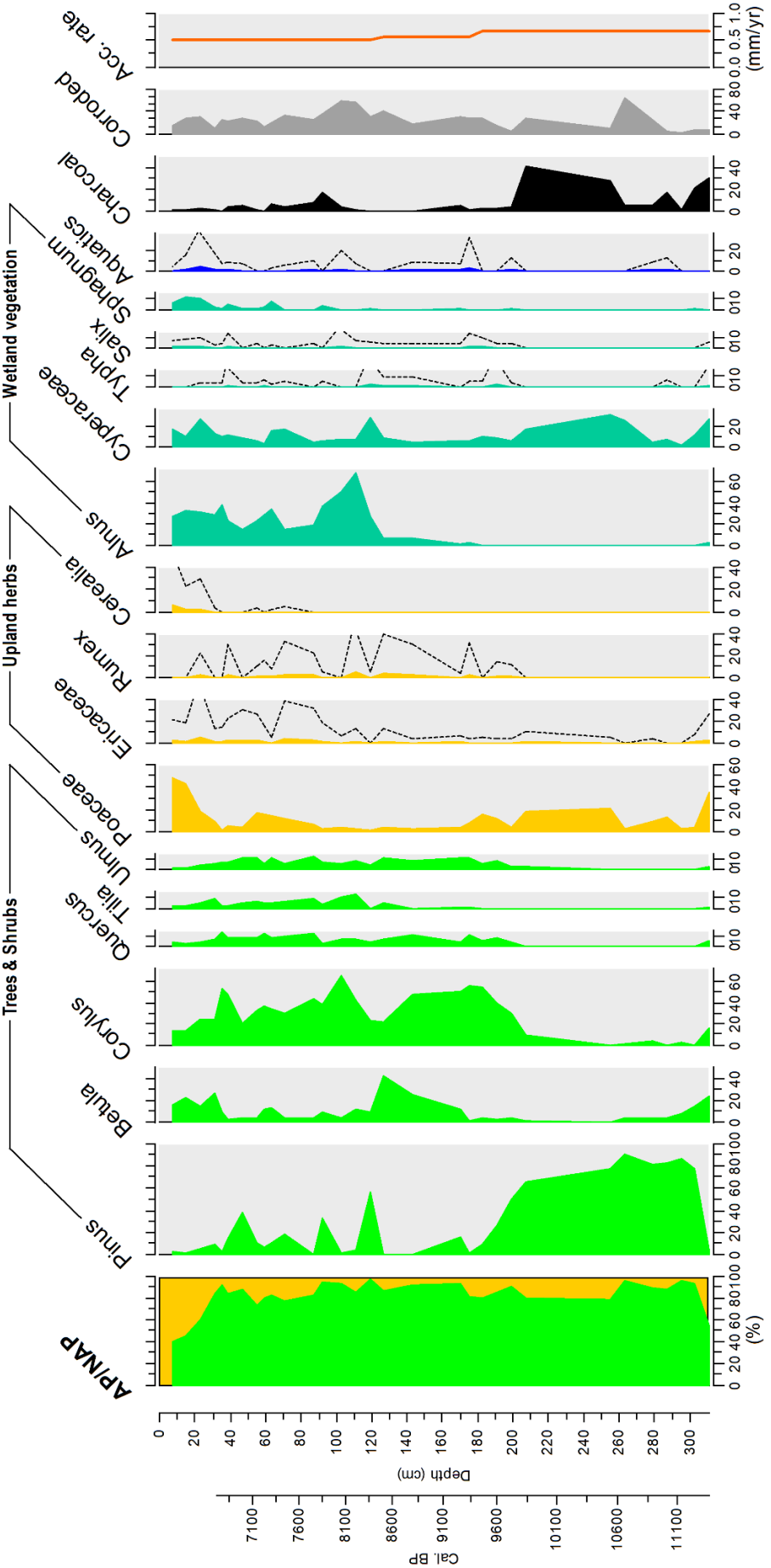

Figure 4.5: Overview pollen diagram of selected taxa (dotted lines show 10 times exaggeration). Percentages of corroded pollen, charcoal and peat accumulation rates are displayed on the right.

4.4. Hierarchical cluster analysis

The dissimilarity matrices on which the clustering is based are shown in Figure 4.6. The results of the Flexible-Beta hierarchical cluster analyses are displayed in Figures 4.7 & 4.8. Figures 4.9 & 4.10 show the output of the Coniss constrained cluster analyses.

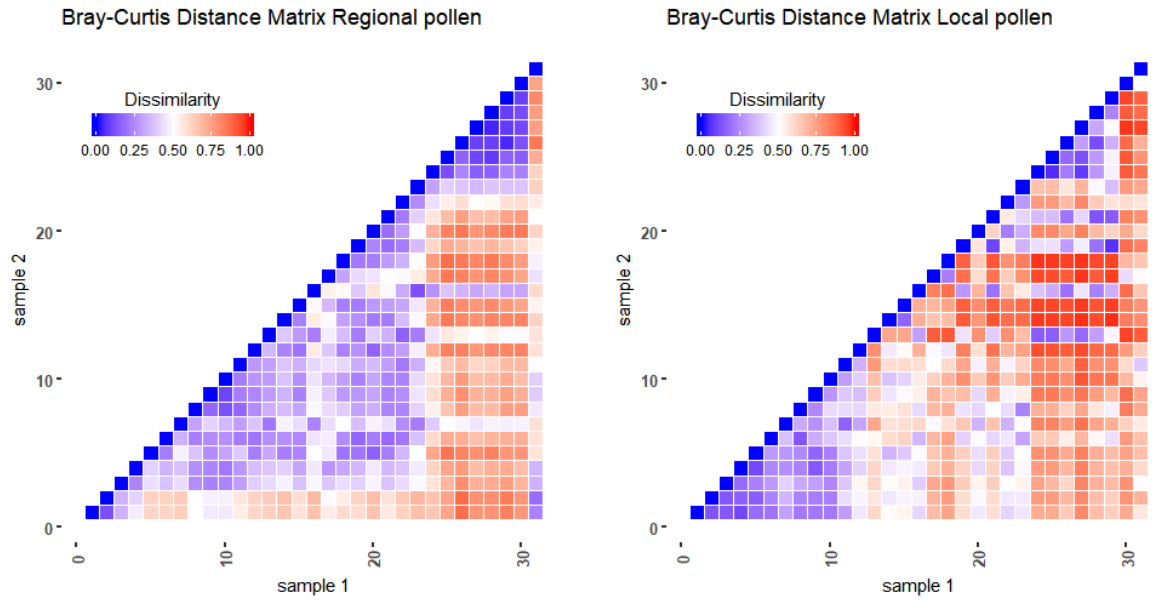

Figure 4.6: Bray-Curtis dissimilarity matrix for the regional pollen taxa (left) and local pollen taxa (right). The 31 samples are numbered from shallow to deep.

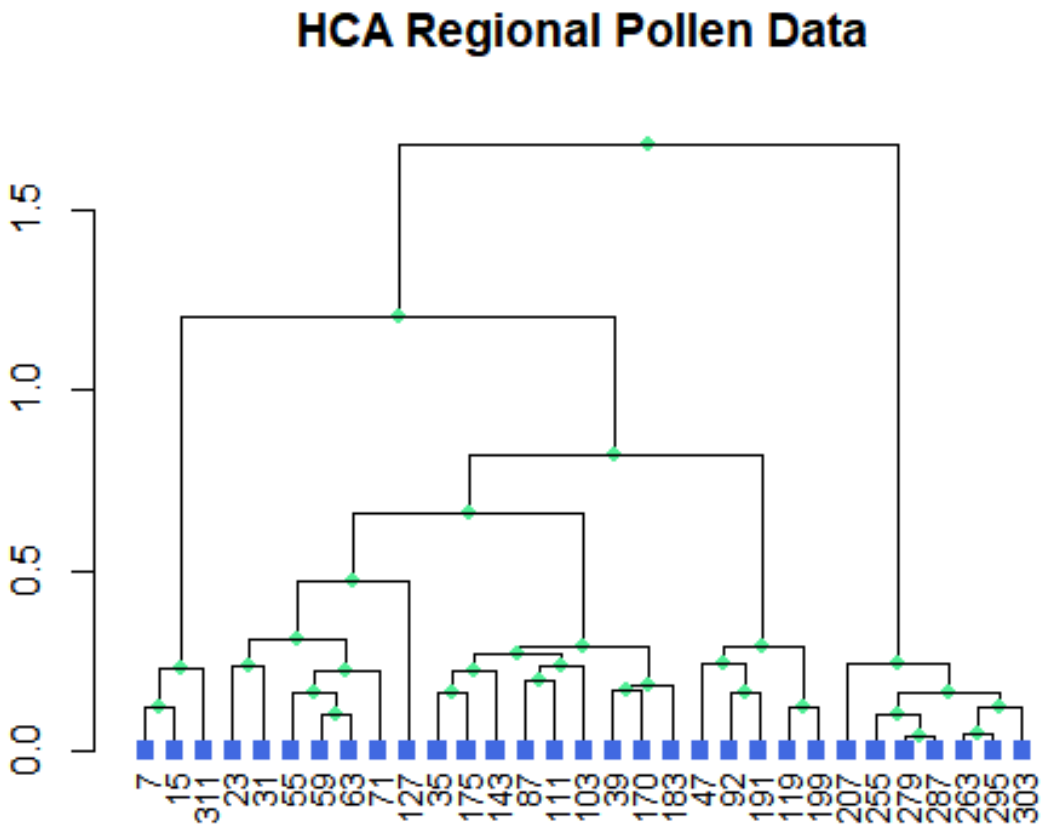

Figure 4.7: Dendrogram representing the result of the Flexible-Beta hierarchical cluster analysis of the regional plant taxa. Labels show the depth (cm) of the analysed samples.

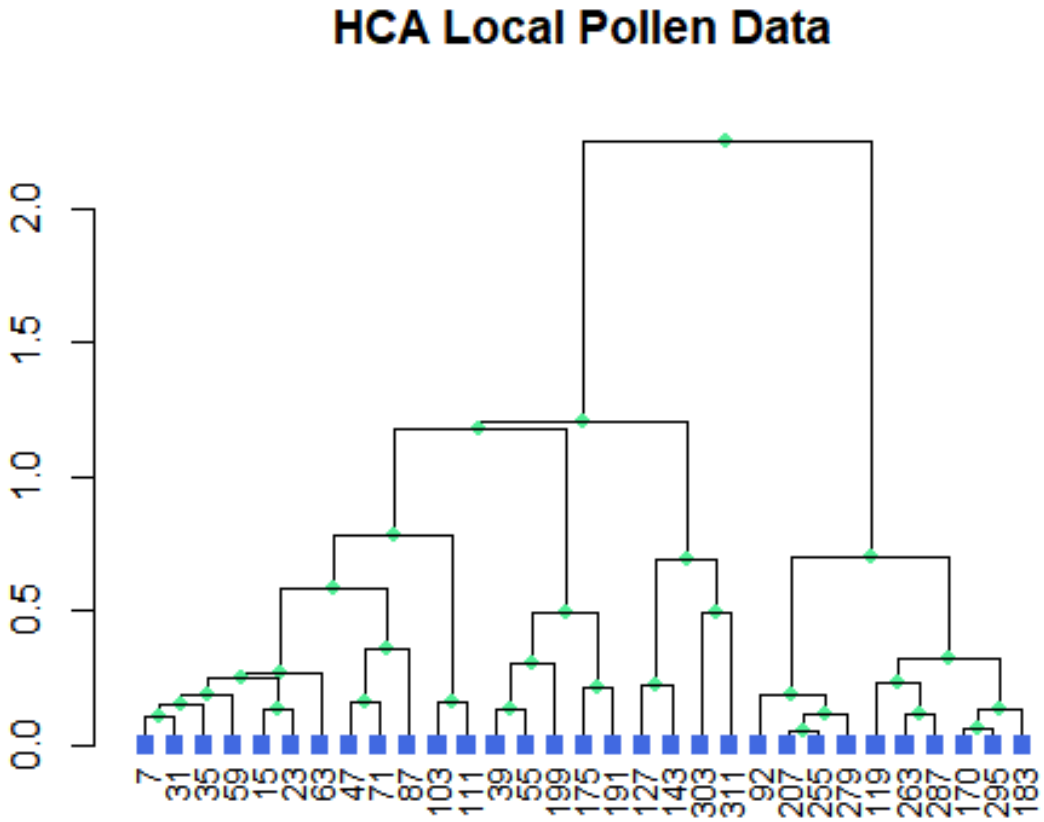

Figure 4.8: Dendrogram representing the result of the Flexible-Beta hierarchical cluster analysis of the local plant taxa. Labels show the depth (cm) of the analysed samples.

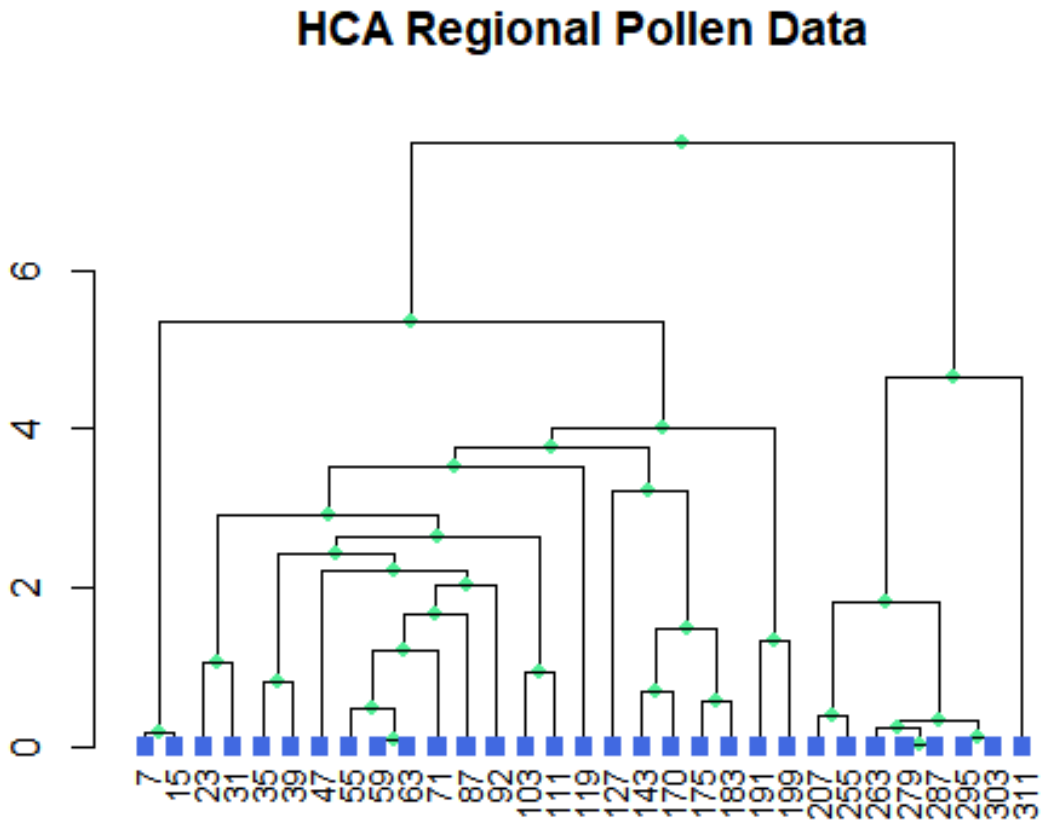

Figure 4.9: Dendrogram representing the result of the Coniss constrained cluster analysis of the regional plant taxa. Labels show the depth (cm) of the analysed samples.

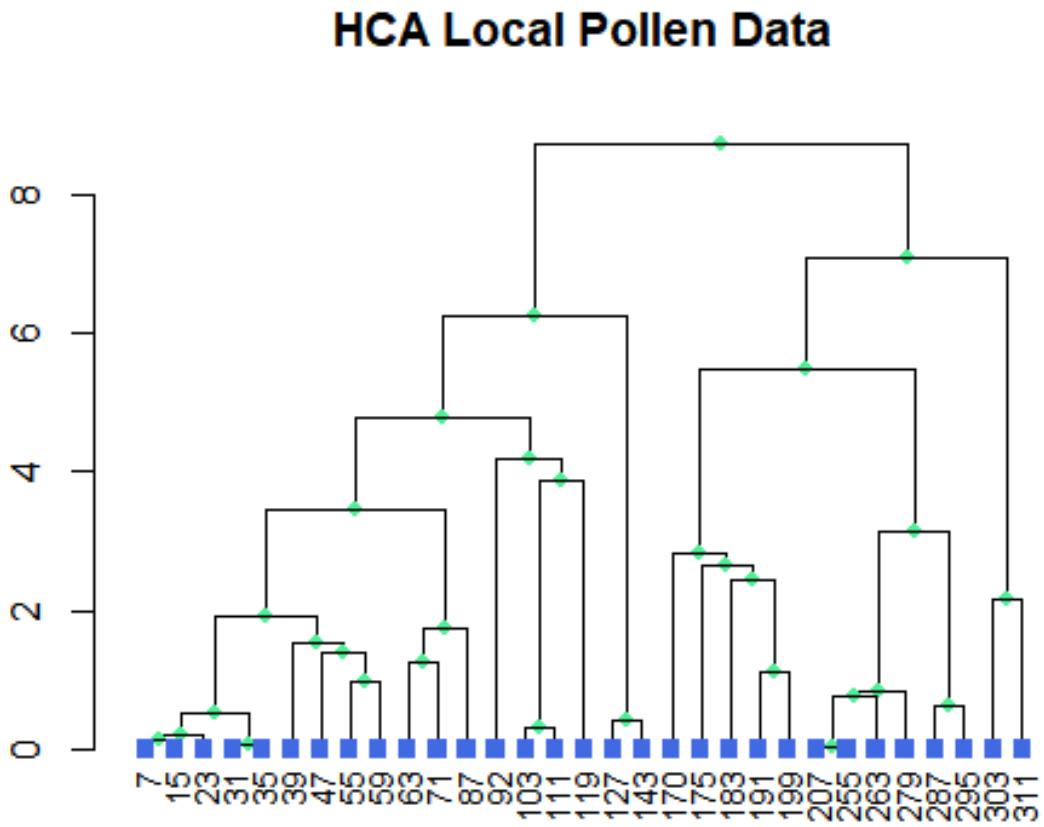

Figure 4.10: Dendrogram representing the result of the Coniss constrained cluster analysis of the local plant taxa. Labels show the depth (cm) of the analysed samples.

4.5. Vegetation zones

a. Regional vegetation zones

The subdivision into vegetation zones (Regional Pollen Accumulation Zones, RPAZ) is based on the Coniss constrained cluster analysis (Figure 4.9). The dendrogram was cut into 6 separate clusters as depicted in the regional pollen diagram (Figure 4.11).

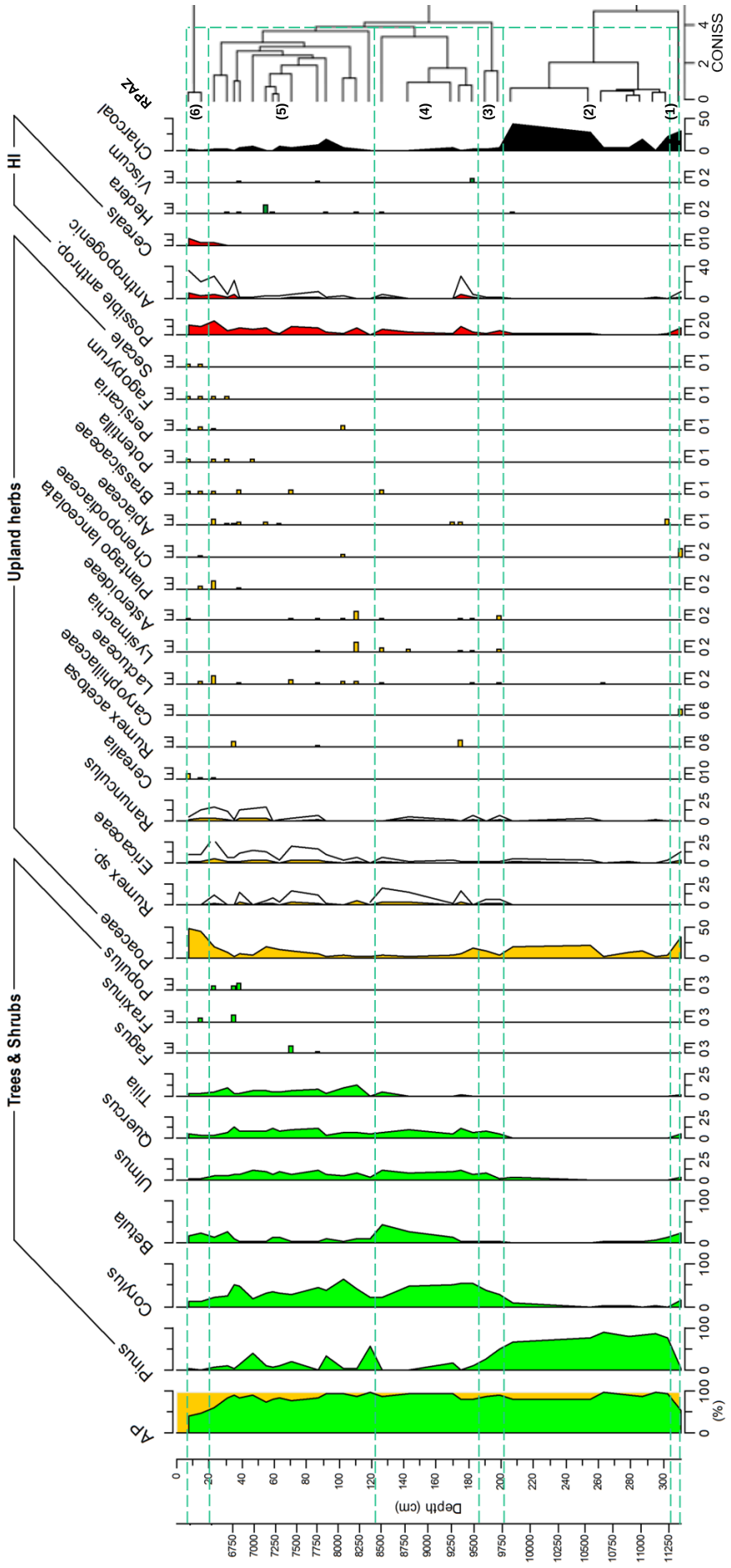

Figure 4.11: Pollen diagram of the 29 regional plant taxa included in the statistical analyses (black lines show 5 times exaggeration). Blue dashed lines show the Coniss clusters (RPAZ, indicated by the numbers on the right).

In RPAZ 1 Poaceae, *Betula* and *Corylus* are dominant (Figure 4.11). Pollen of upland herbs (Caryophillaceae, Chenopodiaceae, Ericaceae) are found in limited numbers. The percentage of arboreal pollen (AP) is approximately 50% and the charcoal abundance is high. RPAZ 2 is strongly dominated by *Pinus* pollen. Poaceae are found in intermediate abundances and the AP values are between 80 and 100%. Charcoal is rare in the first half of the zone but increases to high values in the second half. During RPAZ 3, pollen of *Pinus* decrease while *Corylus*, *Quercus* and *Ulmus* start to rise. The tree pollen are dominated by *Pinus* and *Corylus* and AP values are between 80 and 90%. Charcoal abundance is very low. In RPAZ 4 *Corylus* becomes the dominant pollen type while *Pinus* almost completely disappears. Intermediate values of *Quercus* and *Ulmus* persist throughout this zone. *Betula* starts to rise and reaches in maximum close to the end of this zone. *Rumex* percentages are slightly elevated and upland herbs in general are found more frequent during this zone. Charcoal abundance is low and AP values are between 80 and 95%. While *Corylus* remains the dominant pollen type in RPAZ 5, a return of elevated *Pinus* pollen is observed in this interval. Intermediate values for *Quercus*, *Ulmus* and *Betula* are found, as well as *Tilia*. A further increase of upland herbs is recorded with elevated values of Ericaceae throughout this zone and increases of Poaceae in the middle and end of the zone. AP values vary from 90 to 60% at the end of this interval and charcoal founds are slightly elevated. In RPAZ 6, pollen of Poaceae become dominant with rising values up to 50%. *Betula* and *Corylus* are the dominant tree pollen, but AP values decrease to 40%. Charcoal abundance is low. Anthropogenic indicator species show an elevated abundance in this zone and a limited number of cereal pollen (Cerealia, *Secale*, *Fagopyrum*) was found.

b. Local vegetation zones

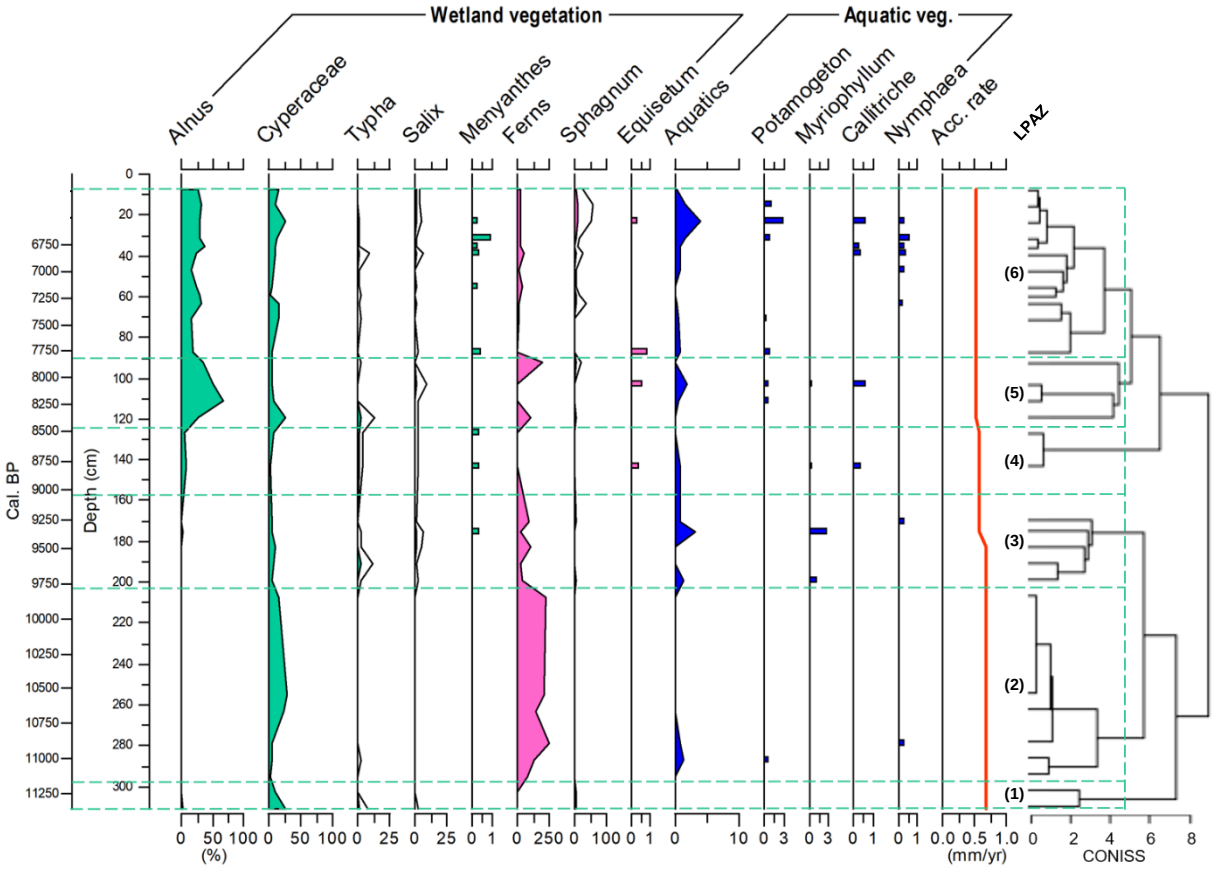

Figure 4.12: Pollen diagram of the 12 local plant taxa included in the statistical analyses (black lines show 5 times exaggeration). Blue dashed lines show the Coniss clusters (LPAZ, indicated by the numbers on the right).

The subdivision of the local vegetation (Local Pollen Accumulation Zones, LPAZ) is also based on the Coniss constrained cluster analysis (Figure 4.10). The dendrogram was cut into 6 separate clusters as depicted in the local pollen diagram (Figure 4.12). Local pollen taxa in LPAZ 1 are dominated by Cyperaceae. *Salix* and *Typha* occur in very low frequencies. Aquatic pollen are absent. Cyperaceae remain the dominant pollen type in LPAZ 2, and spores of ferns become very abundant. In the lower half of this some aquatic taxa are encountered (*Potamogeton*, Nymphaea). In LPAZ 3 Cyperaceae and ferns show a clear decrease, while aquatic pollen become more dominant. Also *Typha* and *Salix* show a slight increase in pollen abundance and *Menyanthes* is found for the first time. From LPAZ 4, fern spores further decrease while *Alnus* pollen rise slightly for the first time. Low values of Cyperaceae, *Typha*, *Salix* and aquatic taxa are found throughout this zone. LPAZ 5 is characterized by a strong dominance of *Alnus* pollen. Peaks occur for Cyperaceae and ferns and to a lower extend for *Typha*, *Salix* and aquatics. During LPAZ 6 *Alnus* pollen decrease but remain the dominant pollen type, followed by Cyperaceae. *Menyanthes* pollen become more frequent and a peak of aquatic taxa is found in the upper part of this zone. A rise of *Sphagnum* spores is observed throughout this zone, reaching its maximum close to the end of it.

4.6. Non-metric multidimensional scaling

a. Regional NMDS analysis

The scree-plot and shepherd diagram of the regional NMDS analysis are shown in Figure 4.13. In Figure 4.14 the output of the ordination is shown in three dimensions. The NMDS biplots for dimensions 1 and 2 are shown in Figure 4.15, for dimensions 1 and 3 in Figure 4.16. High scores on axis 1 are recorded for *Pinus* and low values for *Secale cereale*, *Fagopyrum*, *Plantago lanceolata*, Cerealia, *Potentilla*, *Persicaria*, Brassicaceae, *Populus* and Asteroideae. On axis 2, high values are found for *Secale cereale*, *Fagopyrum*, *Plantago lanceolata*, Cerealia, *Potentilla*, *Persicaria* and Brassicaceae while *Rumex* and *Lysimachia vulgaris* have low values. The 3th axis has high values for *Fagus* followed by *Persicaria*, Lactuceae, Asteroideae and *Lysimachia vulgaris*. Low values were found for Apiaceae, Caryophyllaceae and *Populus*.

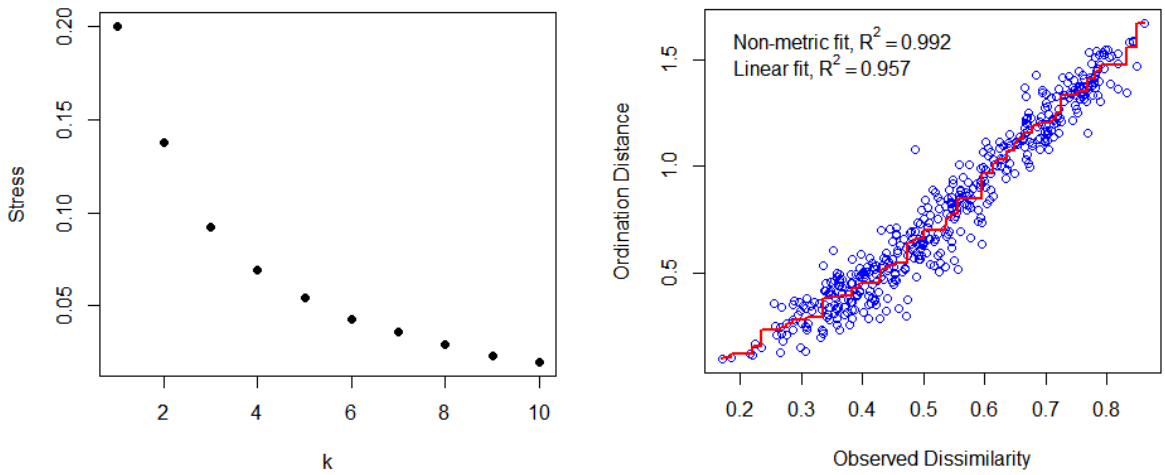

Figure 4.13: The scree-plot on the left shows the stress associated with a certain number of NMDS dimensions k for the regional pollen data. The shepherd diagram on the right shows the relation between the distance on the ordination plot and the dissimilarity in the Bray-Curtis matrix for k=3. The stress is defined as the deviations of the points from the monotonically increasing function.

Different vegetation types can be discriminated within the ordination space (Figure 4.15 & 4.16): High scores on axis 1 and intermediate values on axis 2 correspond to an Early Holocene boreal forest vegetation, as indicated by the position of *Pinus* in the ordination diagram. Low scores on both axis 1 and axis 2 and values close to zero on axis 3 indicate the presence of temperate deciduous woodland, based on the ordination scores of *Quercus*, *Ulmus*, *Tilia* and *Corylus*. Extreme values on axis 2 in combination with low values on axis 1 indicate a vegetation that is strongly altered by humans as indicated by the positions of *Secale cereale*, *Fagorypum*, Cerealia and *Plantago lanceolata*. The interpretation of the third ordination axis is less clear based on the pollen type scores.

On the biplot of axes 1 and 2 (Figure 4.15), the sample scores start in the middle with sample 311 cm, after which they move to the right (303 – 255 cm) of the diagram indicating the establishment of the boreal forest type vegetation. The following samples plot in the lower left corner of the diagram, indicating the dominance of a deciduous woodland vegetation for samples 199 – 35 cm. The last 4 and especially samples 15 and 7 cm plot in the upper left corner of the biplot, indicating the start of severe human alterations of the vegetation.

Figure 4.17 shows the evolution of the NMDS axes scores over time: axis 1 shows increased values from 11.2 to 9.9 cal. kyr BP interpreted as boreal forest vegetation, followed by a sharp decrease to low values showing the arrival and persistence of deciduous woodland for the rest of the record. Axis 2 has intermediate values before 10.0 cal. kyr BP, low values until 8.0 cal. kyr BP and gradually rising values afterwards reaching the highest values at the top of the record indicating human disturbance in this zone. On axis 3, the axis scores rise until 10.7 cal. kyr BP, followed by a period of high to very high values until 8.0 cal. kyr BP when the values start to decrease again.

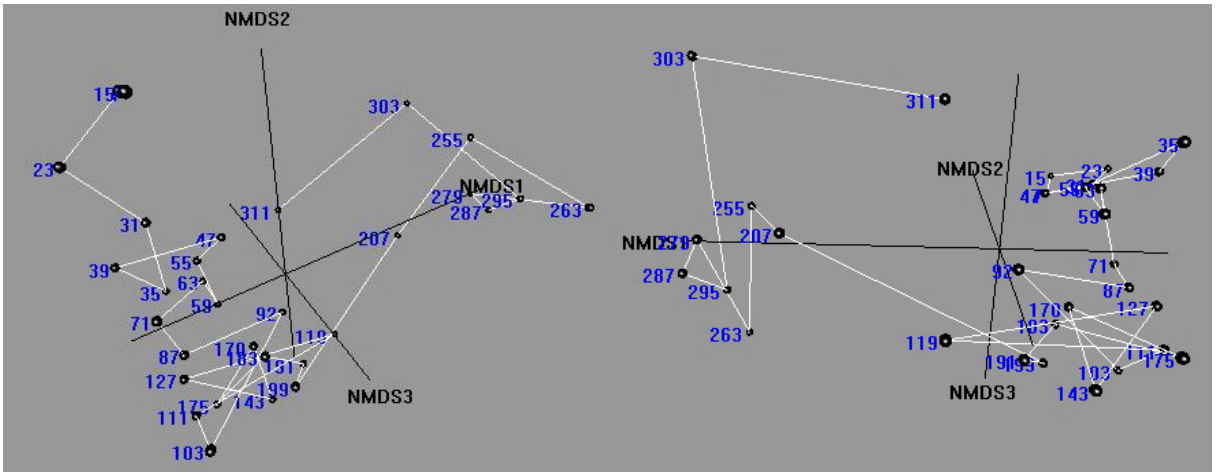

Figure 4.14: Triplots of the NMDS analysis of the regional pollen data, seen from two different angles. Positions of the investigated samples are displayed, for the position of the pollen types see Figures 4.15 and 4.16. The white line connects the samples according to their depth.

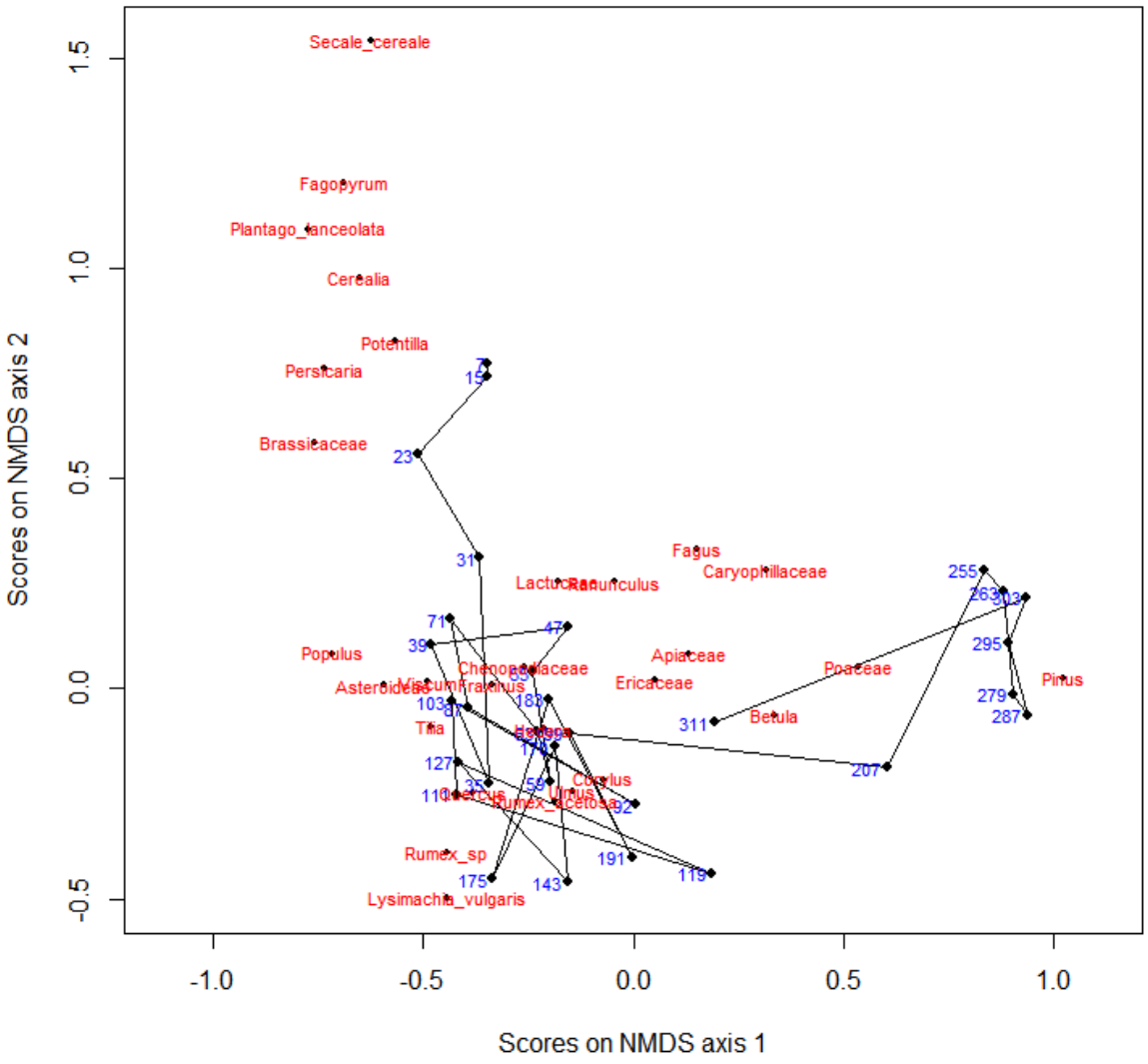

Figure 4.15: Biplot of axes 1 and 2 of the NMDS analysis of the regional pollen data. The position of the investigated samples is indicated (blue labels) as well as the different pollen types (red labels). The black line connects the samples according to their depth.

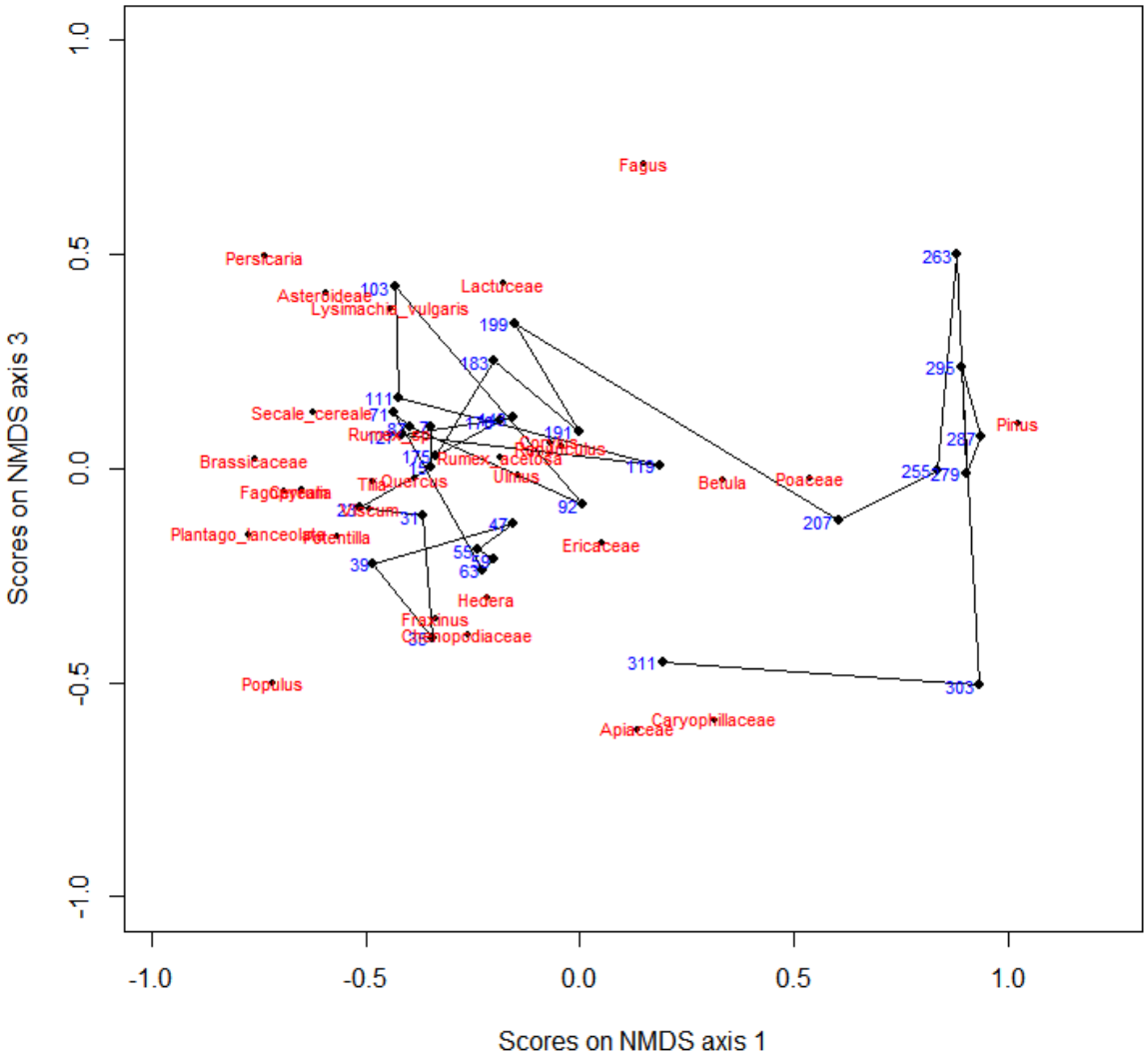

Figure 4.16: Biplot of axes 1 and 3 of the NMDS analysis of the regional pollen data. The position of the investigated samples is indicated (blue labels) as well as the different pollen types (red labels). The black line connects the samples according to their depth.

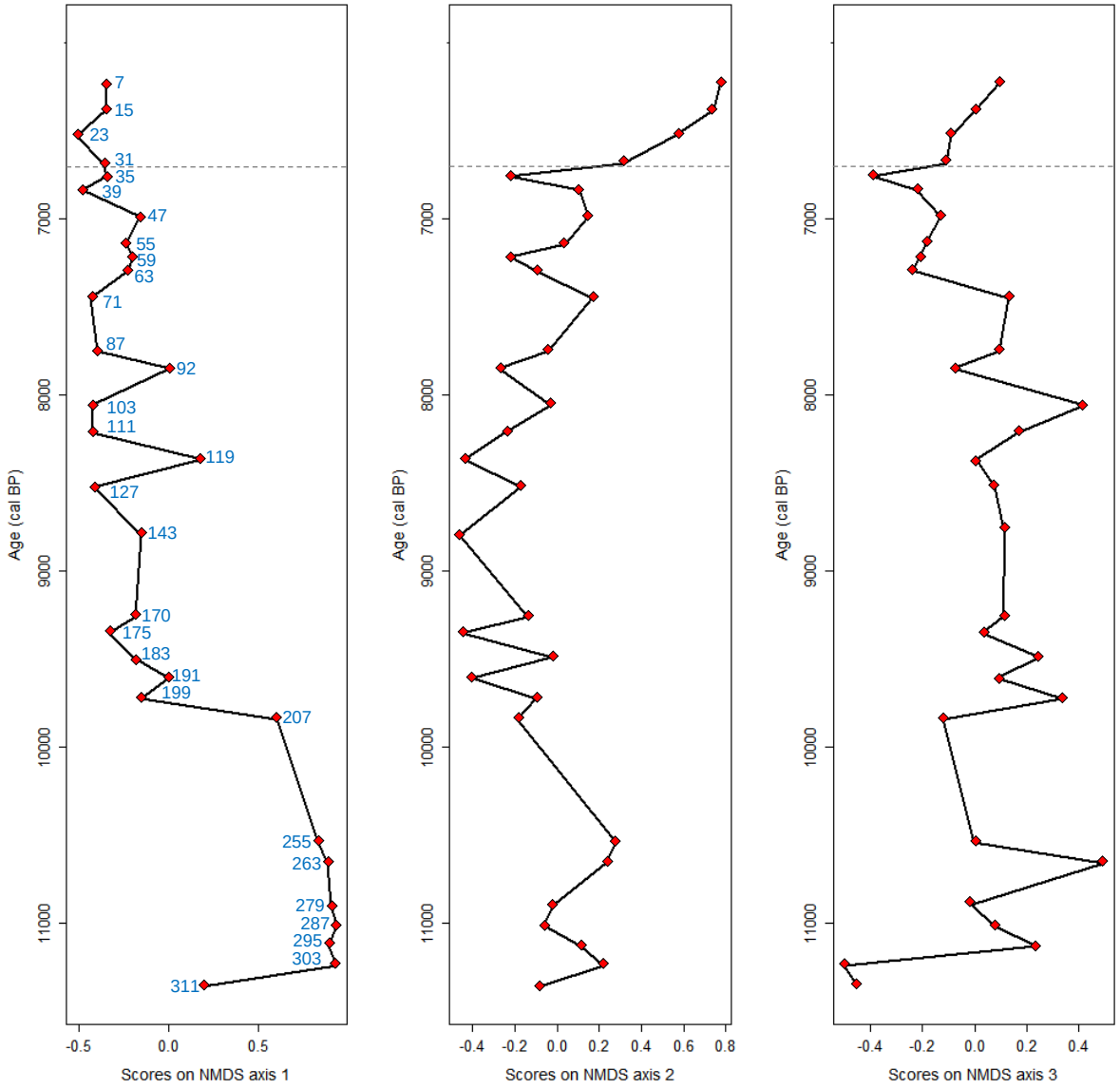

Figure 4.17: The graphs show the evolution of the axes scores of the regional NMDS analysis over time. Red points indicate the position of the investigated samples and their depth in cm (blue labels). The gray dashed line indicates the position of a possible hiatus.

In Figures 4.18 & 4.19, a selection of environmental variables is plotted on top of the biplots. The corresponding three dimensional triplot is shown in Figure 4.20. The normalized values for the positions of the arrow tips of the investigated variables are displayed in Table 4.2 together with the squared correlation coefficients (r^2) and the p-values. The variables are shown as surfaces (Figure 4.21) when the relation of the variable with the ordination configuration is clearly not linear. The analysis of environmental variables shows that high values for NMDS axis 1 may be interpreted as conditions of high light availability and moisture, while low values rather indicate high temperatures and precipitation (non-linear, Figure 4.21), high nutrient availability and basic pH conditions (Table 4.2). For NMDS axis 2, high values correlate with moist conditions, while low values indicate a high percentage of arboreal pollen (non-linear, Figure 4.21) and thus a more closed canopy. High values on NMDS axis 3 correlate to strong corrosion and low values to a high charcoal abundance (non-linear, Figure 4.21).

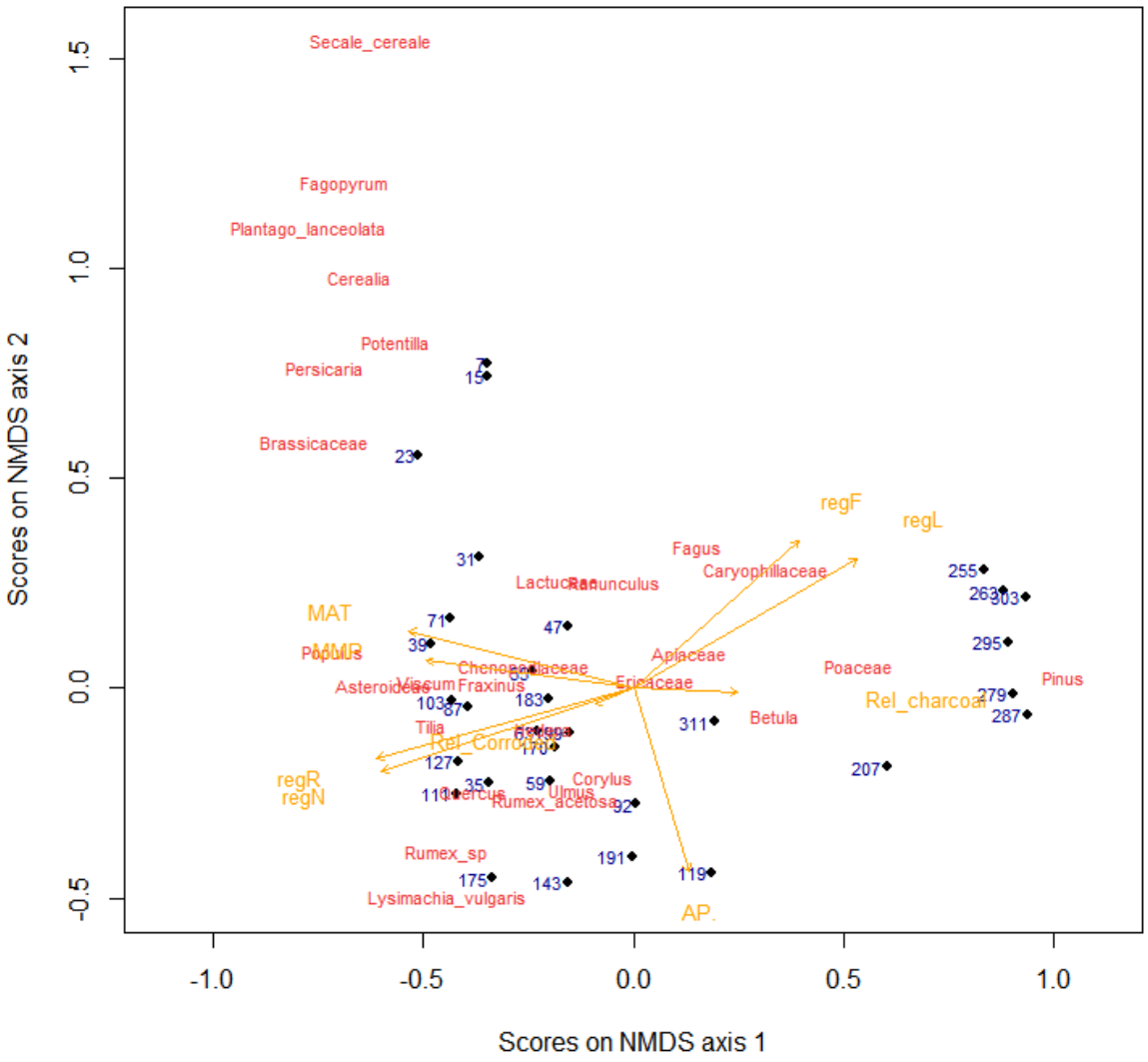

Figure 4.18: Biplot of axes 1 and 2 of the NMDS analysis of the regional pollen data, with external environmental variables plotted on top of the ordination output (orange arrows). For the meaning of the abbreviations see Table 4.2. The position on the ordination diagram of the investigated samples is indicated (blue labels showing corresponding depth) as well as the different pollen types (red labels).

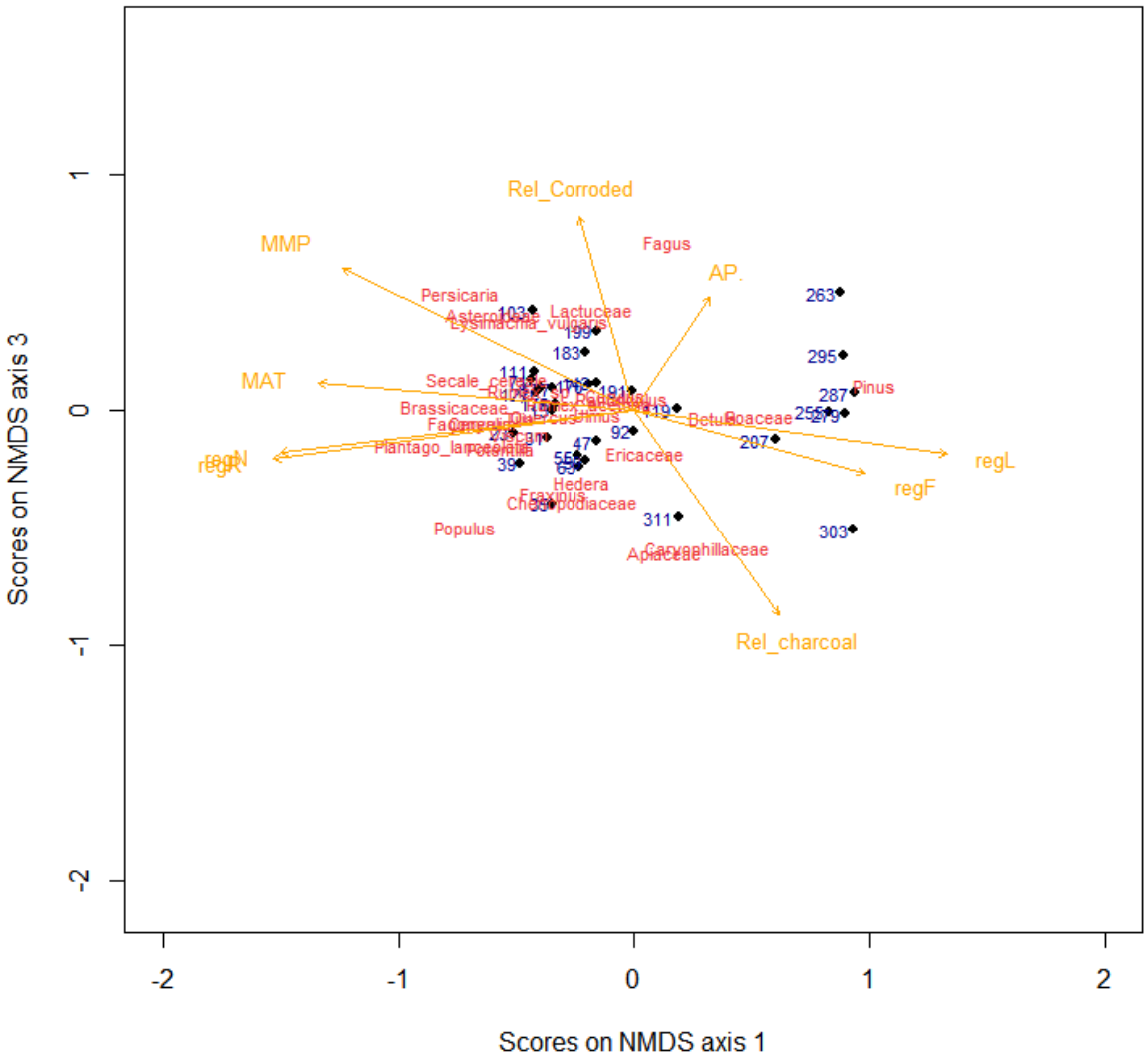

Figure 4.19: Biplot of axes 1 and 3 of the NMDS analysis of the regional pollen data, with external environmental variables plotted on top of the ordination output (orange arrows). For the meaning of the abbreviations see Table 4.2. The position of the investigated samples is indicated (blue labels) as well as the different pollen types (red labels).

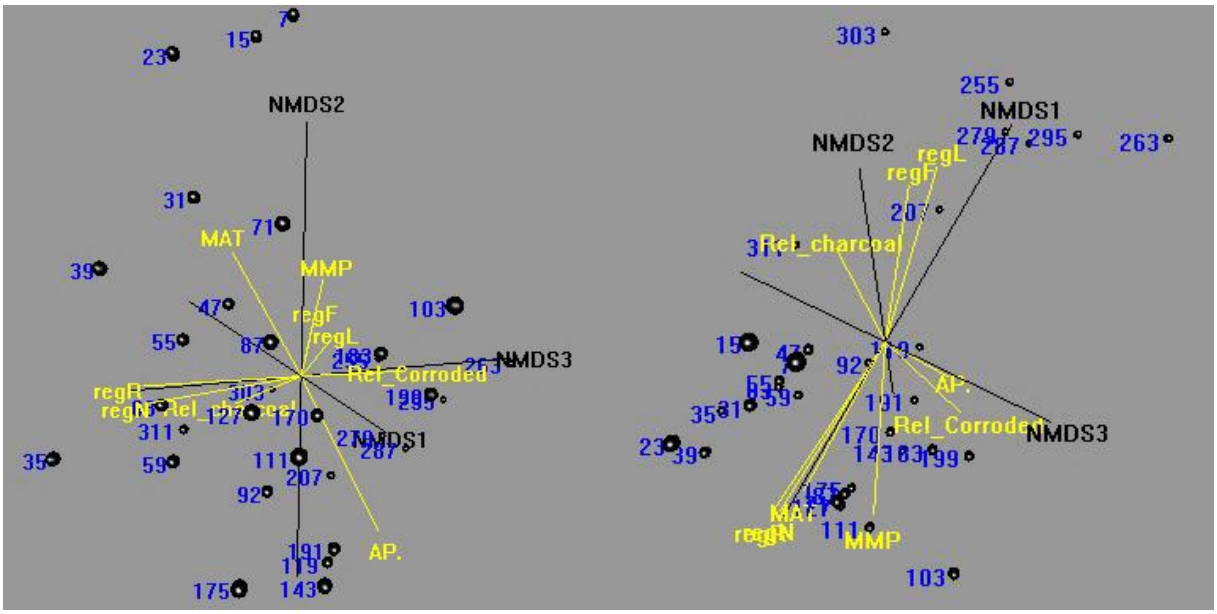

Figure 4.20: Triplots of the NMDS analysis of the regional pollen data, seen from two different angles with external environmental variables plotted on top of the ordination output (yellow arrows). For the meaning of the abbreviations see Table 4.2.. Positions of the investigated samples are displayed.

Table 4.2: Results of the R function envfit() for the fitted environmental variables in Figures 4.18, 4.19 and 4.20. Significance codes: 0 '***' 0.001 '**' 0.01 '*' 0.05

Variable	Code	NMDS1	NMDS2	NMDS3	r²	P-value
Mean annual air temperature	MAT	-0.965	0.247	0.0856	0.686	0.001 ***
Mean monthly precipitation	MMP	-0.893	0.118	0.435	0.684	0.001 ***
Charcoal abundance	Rel_Charcoal	0.580	-0.0230	-0.814	0.405	0.004 **
Corroded pollen	Rel_Corroded	-0.269	-0.104	0.958	0.265	0.030 *
Ellenberg light	regL	0.860	0.497	-0.119	0.853	0.001 ***
Ellenberg moisture	regF	0.730	0.654	-0.197	0.645	0.001 ***
Ellenberg pH	regR	-0.957	-0.260	-0.127	0.910	0.001 ***
Ellenberg nutrients	regN	-0.944	-0.311	-0.110	0.901	0.001 ***
Percentage arboreal pollen	AP.	0.264	-0.882	0.391	0.542	0.001 ***

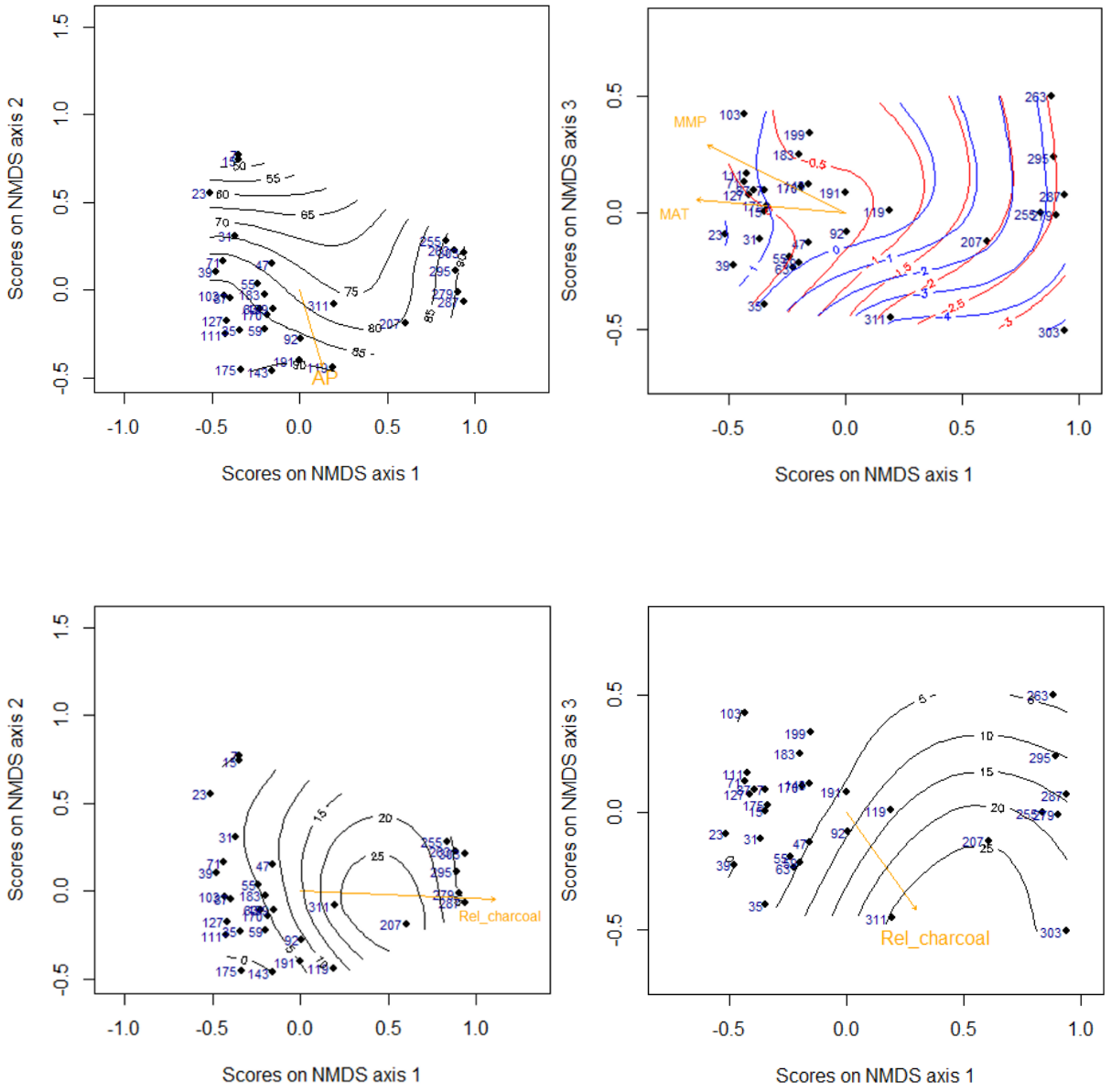

Figure 4.21: Biplot of the NMDS analysis of the regional pollen data overlain with response surfaces (black contour lines) and biplot arrows (orange) of the external variables showing a non-linear variation across the biplots: AP (top left), MAT (top right, red), MMP (top right, blue) and charcoal (bottom).

In Figures 4.22 and 4.23 the RPAZ-subdivision (Figure 4.11) is plotted on top of the ordination configurations. It shows that clusters 1, 2 and 6 have clearly distinct ordination scores while more overlap occurs between clusters 3, 4 and 5. This indicates that the position of the boundaries within this interval should be reconsidered for the final division into vegetation zones.

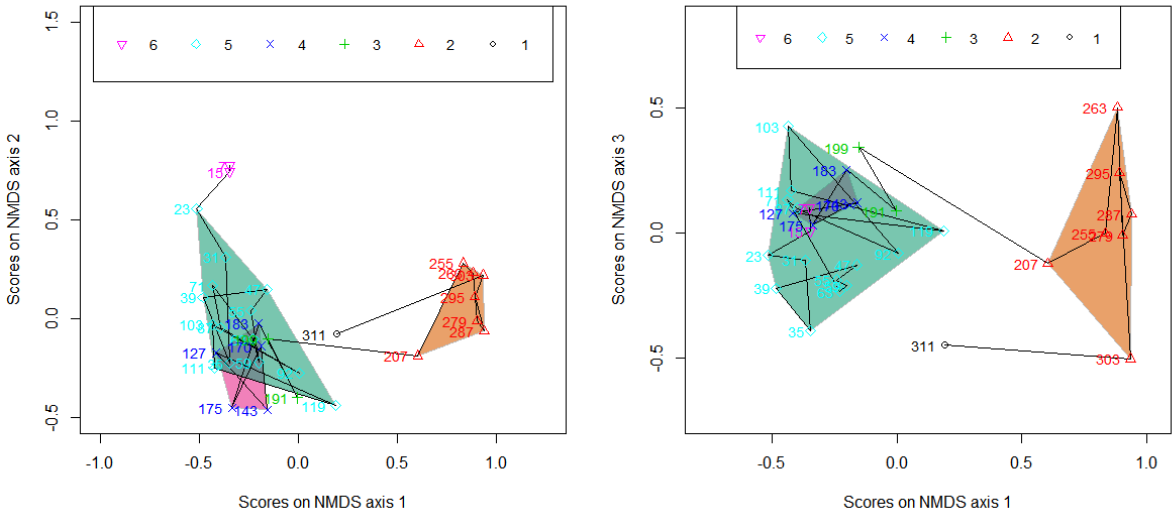

Figure 4.22: Results of the regional Coniss cluster analysis (with 6 clusters) plotted on the regional ordination biplots.

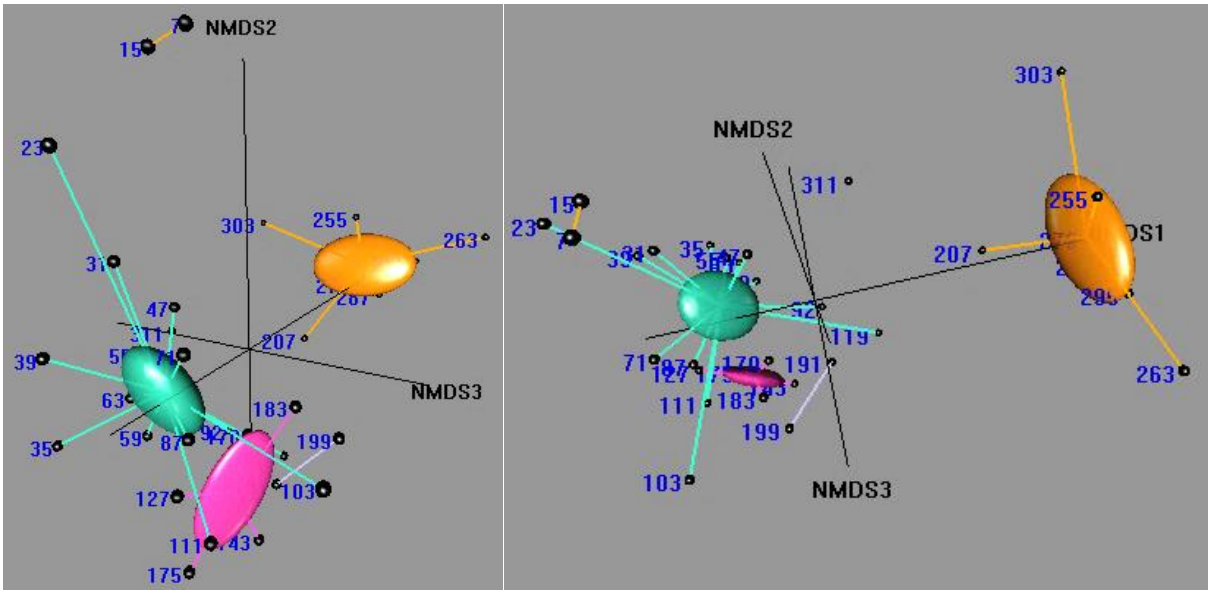

Figure 4.23: Results of the regional Coniss cluster analysis (with 6 clusters) plotted on the regional ordination triplot shown from different angles.

b. Local NMDS analysis

The scree-plot and shepherd diagram of the local NMDS analysis are shown in Figure 4.24. The NMDS biplot is shown in Figure 4.25. High scores on axis 1 are found for ferns and low scores for *Equisetum*, *Callitriche* and *Menyanthes trifoliata*. On axis 2, *Myriophyllum* has a high score while *Potamogeton* and to a lower extent *Alnus*, *Sphagnum* and *Equisetum* have low scores.

Different local vegetation types can be identified in the ordination biplot (Figure 4.25): On the right, an open herb dominated vegetation is found as indicated by the scores of Cyperaceae and ferns. On the left top of the diagrams, the presence of open water is indicated by pollen types such as *Myriophyllum*, *Menyanthes trifoliata*, *Typha* and *Nymphaea*. The lower middle to left of the diagram corresponds to an alder carr vegetation, based on the position of *Alnus*.

When we look at the evolution of the sample scores through the ordination biplot (Figure 4.25), we can see that most of the deepest samples (295-207 cm) plot on the right of the diagram corresponding to an open fern-sedge floodplain vegetation. Then the sample scores for 199 – 127 cm move to the top area of the diagram, indicating a more frequent occurrence of aquatic plant types. Afterwards a trend towards the lower left of the diagram is observed, indicating the presence of alder carr vegetation.

Figure 4.26 shows the evolution of the NMDS axes scores over time: Axis 1 has elevated values indicating a sedge-fern dominated floodplain between 11.1 and 9.9 cal. kyr BP followed by a decrease until 8.8 cal. kyr BP. Afterwards the values are intermediate except for two dips around 8.0 and 7.8 cal. kyr BP. The scores of axis 2 are low at 11.2 and from 8.2 cal. kyr BP onwards showing the establishment of the alder carr vegetation. High values are found around 11.0 and between 9.7 and 8.5 cal. kyr BP corresponding to bigger share of aquatic plants.

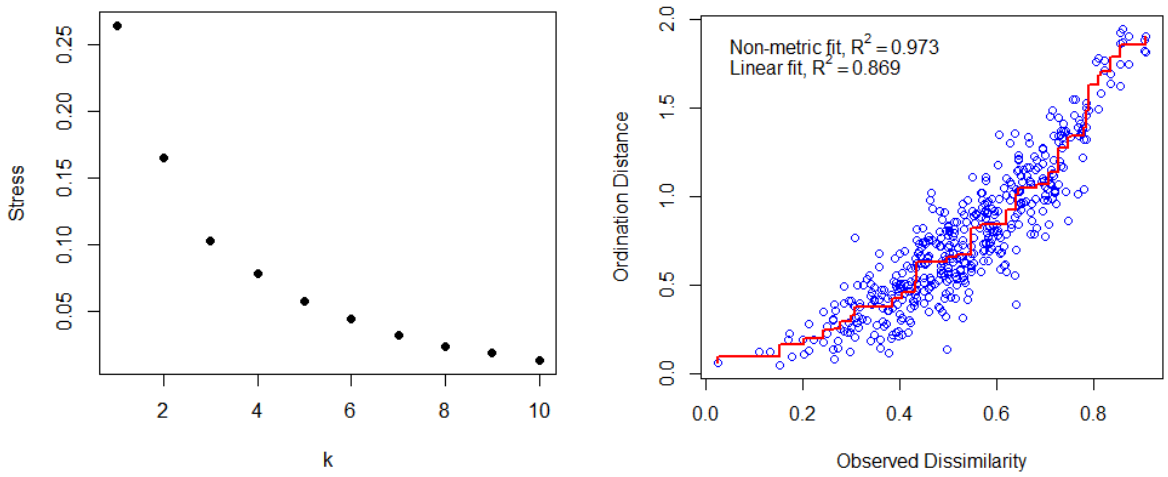

Figure 4.24: The scree-plot on the left shows the stress associated with a certain number of NMDS dimensions k for the local pollen data. The shepherd diagram on the right shows the relation between the distance on the ordination plot and the dissimilarity in the Bray-Curtis matrix for k=2.

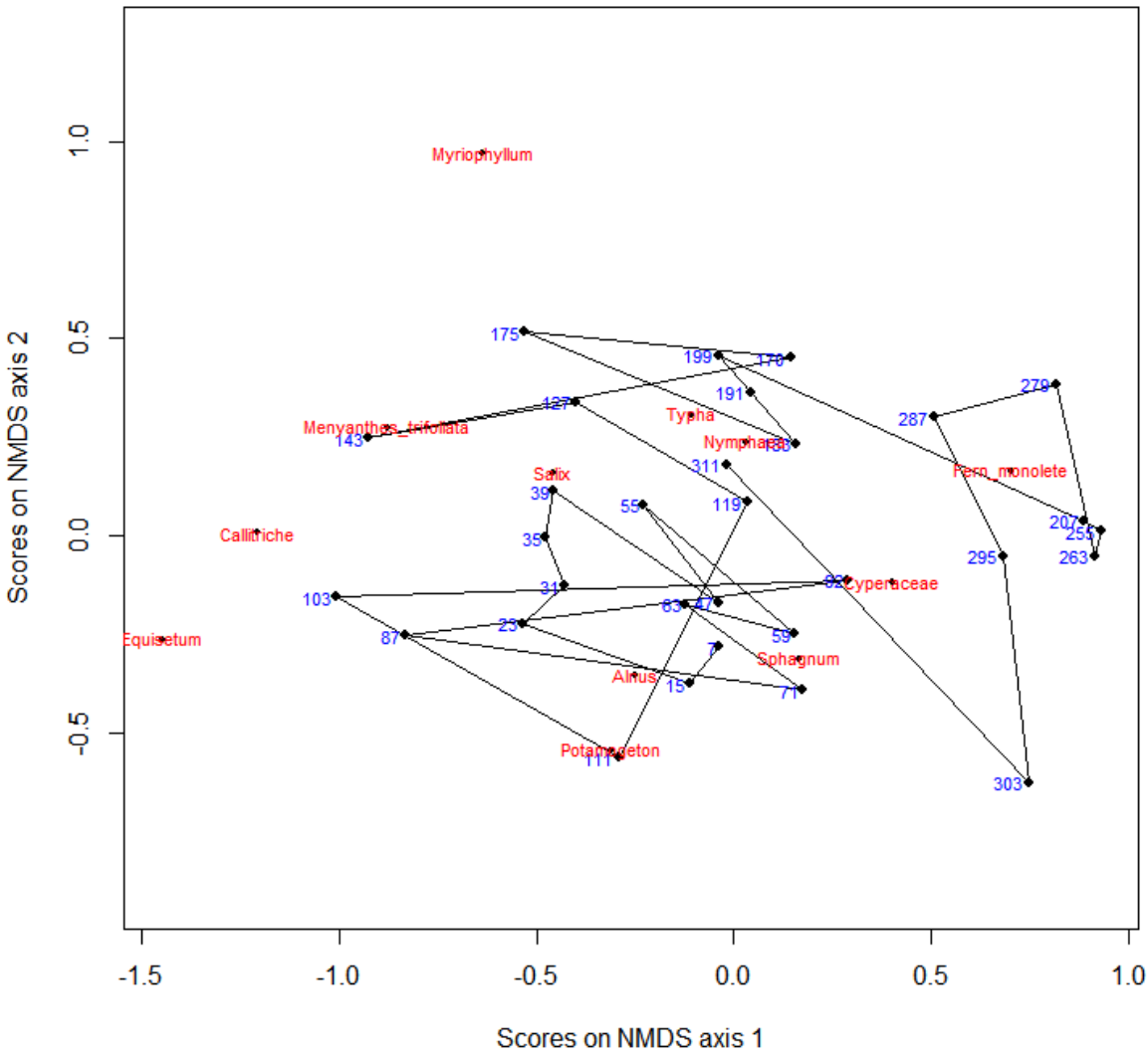

Figure 4.25: Biplot of the NMDS analysis of the local pollen data. The position of the investigated samples is indicated (blue labels) as well as the different pollen types (red labels). The black line connects the samples according to their depth.

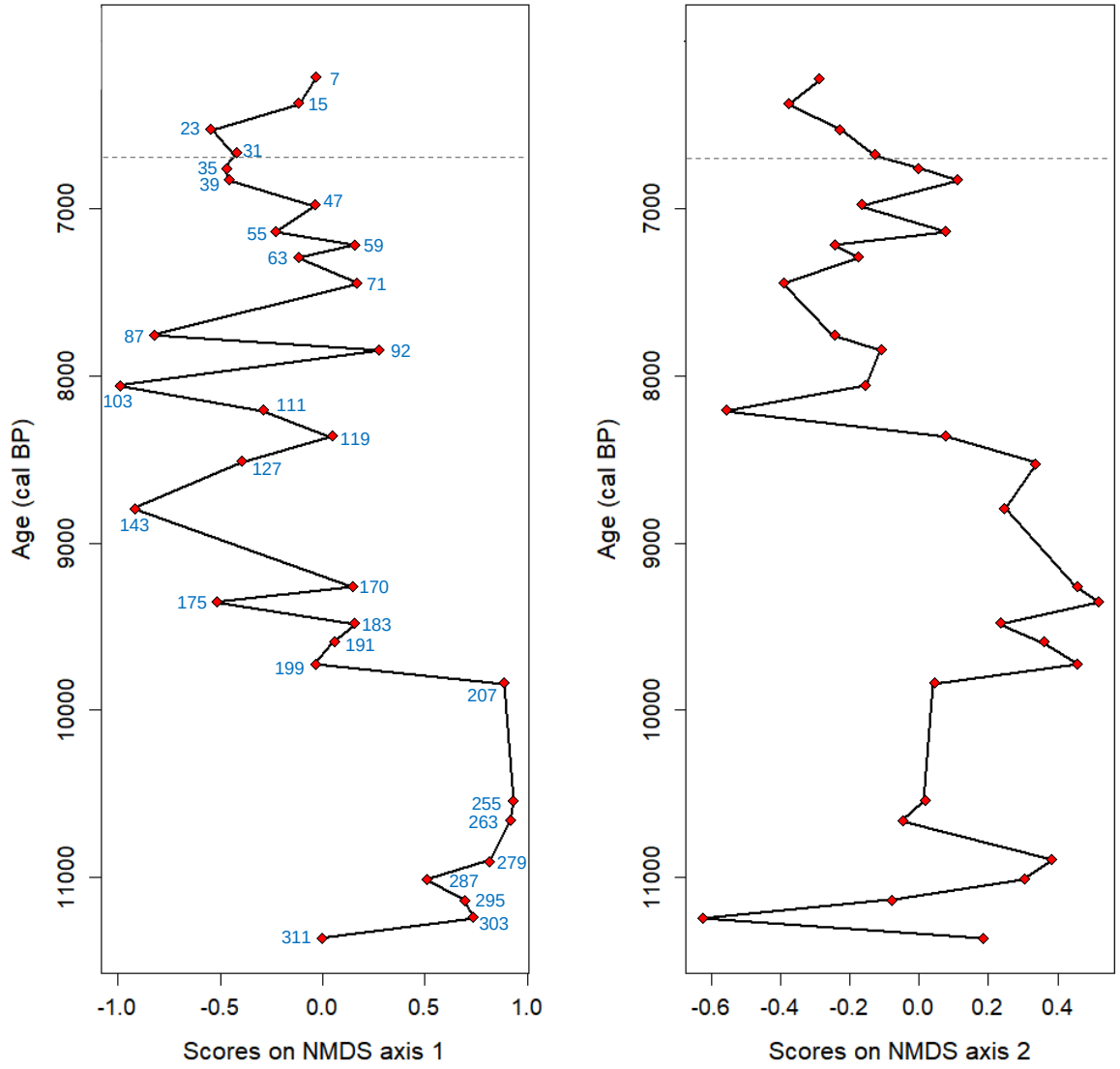

Figure 4.26: The graphs show the evolution of the axes scores of the local NMDS analysis over time. Red points indicate the position of the investigated samples and their depth in cm (blue labels). The gray dashed line indicates the position of a possible hiatus.

In Figure 4.27, a selection of environmental variables is plotted on top of the biplot. The normalized values for the positions of the arrow tips are displayed in Table 4.3 together with the squared correlation coefficients (r^2) and the p-values. The variables are shown as surfaces (Figure 4.28) when the relation of the variable with the ordination configuration is clearly not linear. From this analysis of environmental variables (Table 4.3) we learn that high values on NMDS axis 1 correspond to a high charcoal abundance, while low values indicate abundant aquatic pollen (non-linear, Figure 4.28) and a wet and warm (non-linear, Figure 4.28) climate. For NMDS axis 2 high values correspond to a high light availability (non-linear, Figure 4.28) while low values indicate abundant wetland vegetation (non-linear, Figure 4.28) and moist, basic conditions.

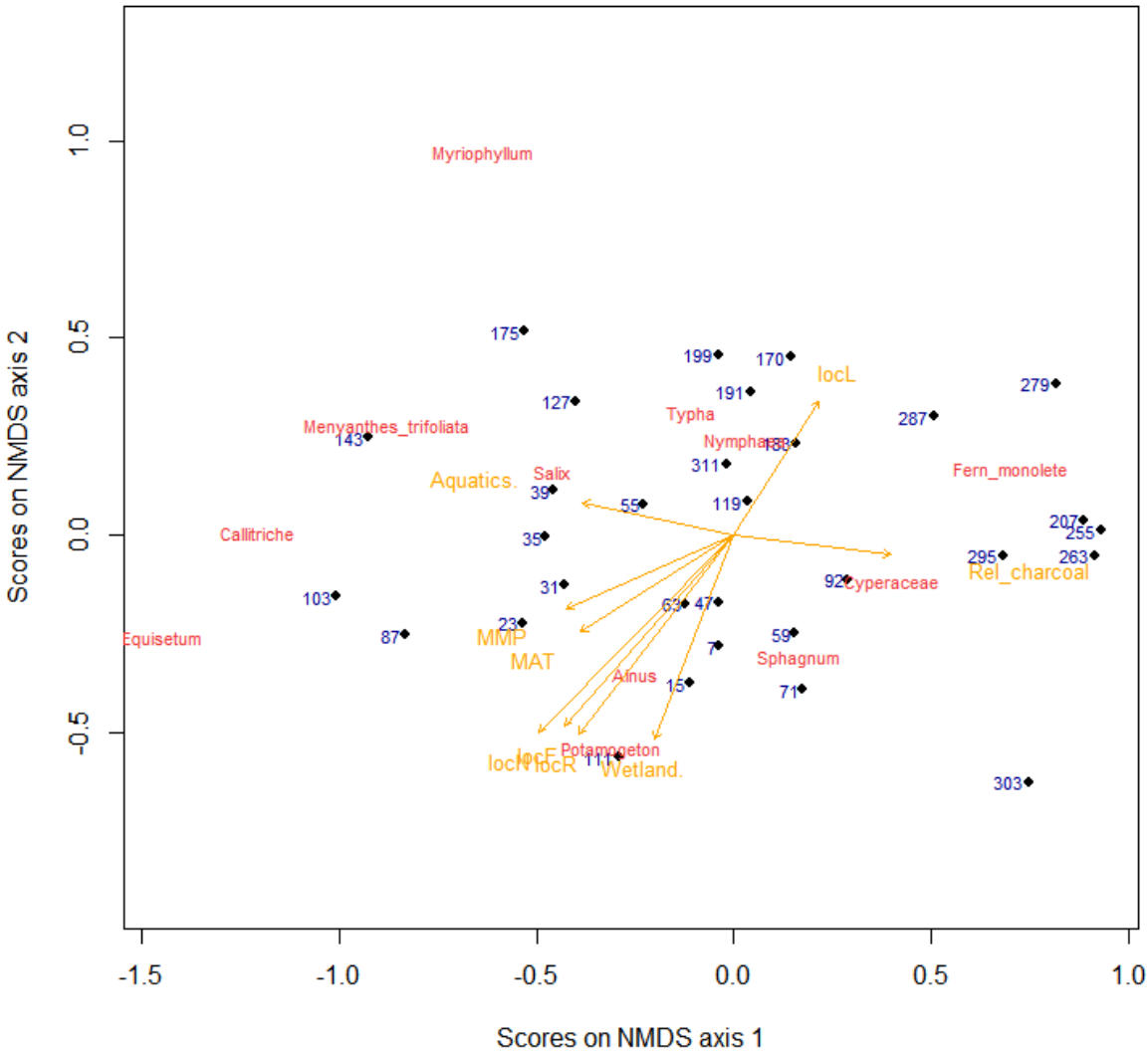

Figure 4.27: Biplot of the NMDS analysis of the local pollen data, with external environmental variables plotted on top of the ordination output (orange arrows). For the meaning of the abbreviations see Table 4.3. The position of the investigated samples is indicated (blue labels) as well as the different pollen types (red labels).

Table 4.3: Results of the R function envfit() for the fitted environmental variables in Figure 4.27. Significance codes: 0 '***' 0.001 '**' 0.01 '*' 0.05

Variable	Code	NMDS1	NMDS2	r^2	P-value
Mean annual air temperature	MAT	-0.848	-0.531	0.349	0.005**
Mean monthly precipitation	MMP	-0.917	-0.400	0.356	0.002**
Ellenberg light	locL	0.536	0.845	0.270	0.012*
Ellenberg moisture	locF	-0.665	-0.747	0.695	0.001***
Ellenberg pH	locR	-0.616	-0.788	0.679	0.001***
Ellenberg nutrients	locN	-0.705	-0.709	0.822	0.001***
Charcoal abundance	Rel_Charcoal	0.992	-0.124	0.264	0.013*
Percentage aquatic pollen	Aquatics.	-0.978	0.209	0.257	0.008**
Percentage wetland pollen	Wetland.	-0.362	-0.932	0.510	0.001***

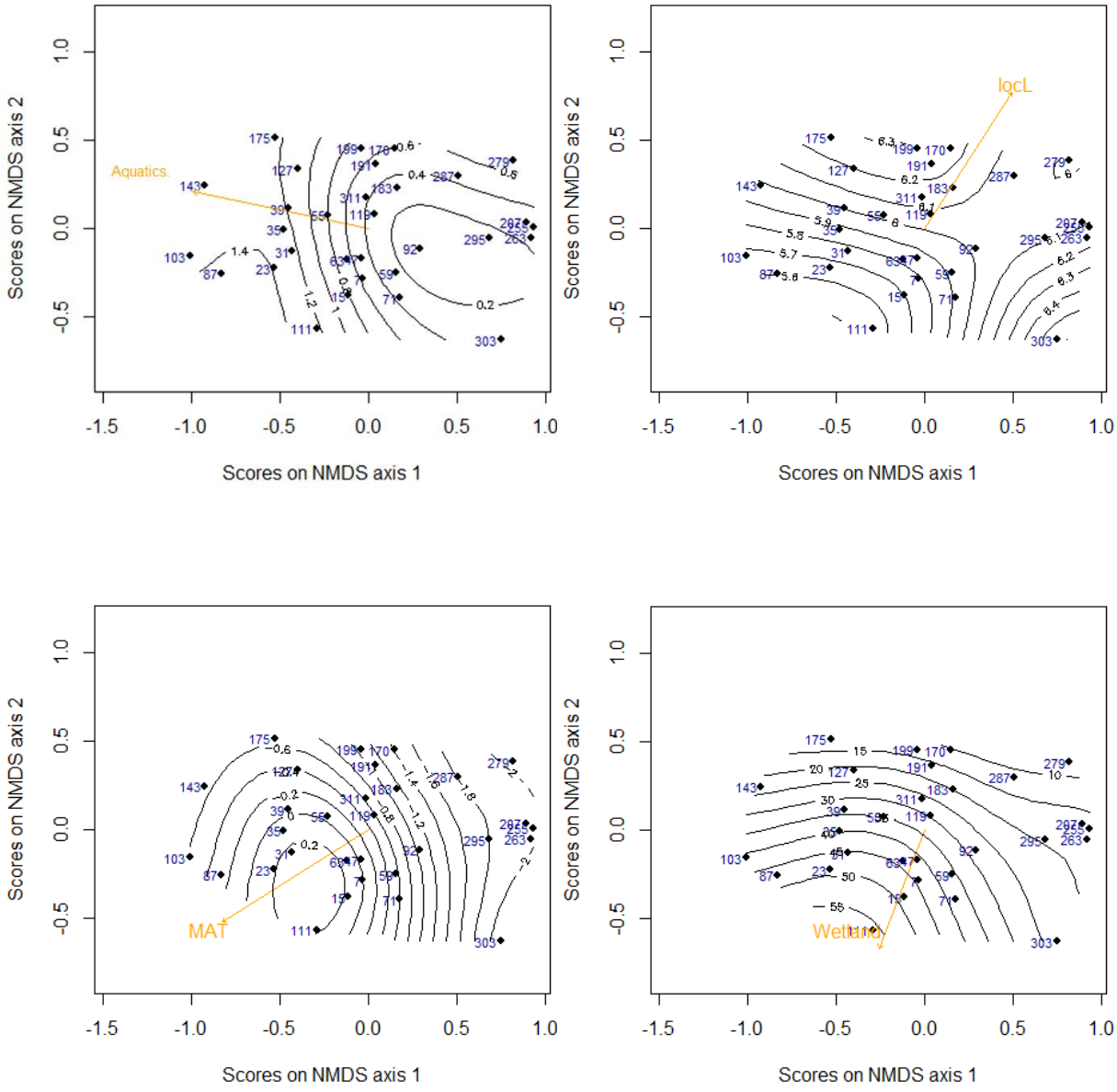

Figure 4.28: Biplot of the NMDS analysis of the local pollen data overlain with response surfaces (black contour lines) and biplot arrows (orange) of the external variables showing a non-linear variation across the biplots: Aquatics (top left), locL (top right), MAT (bottom left) and Wetland (bottom right).

In Figures 4.29 the LPAZ-subdivision (Figure 4.12) is plotted on top of the ordination configuration. It shows a good separation of clusters 1 and 2, a minor separation of zones 3 and 4 (plotting both in the upper left of the ordination space) and an overlap between clusters 5 and 6 in the left bottom region.

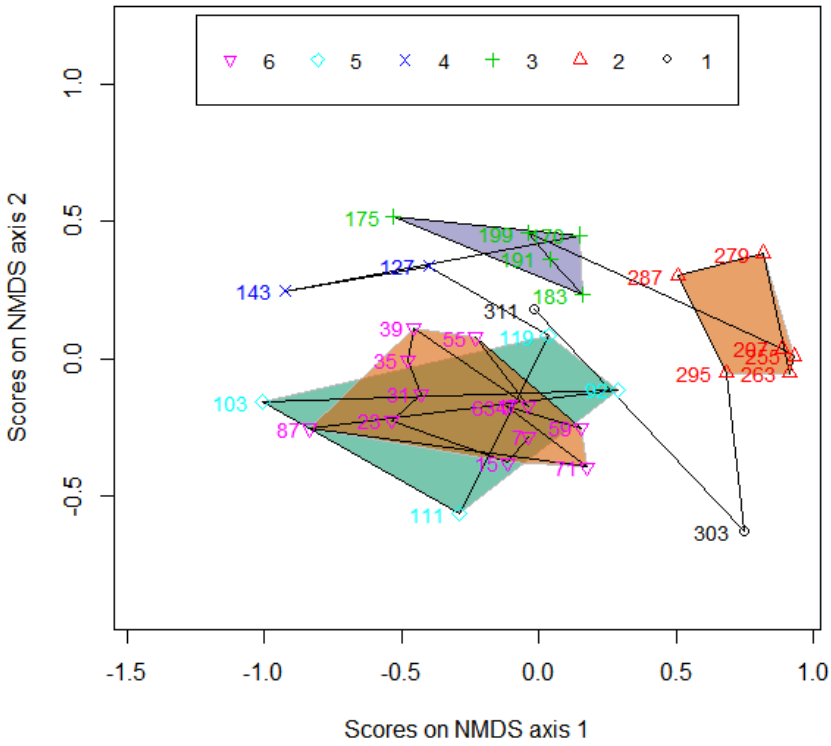

Figure 4.29: Results of the local Coniss cluster analysis (with 6 clusters) plotted on the local ordination biplot.

4.7. Additional records and final zonation

Figure 4.30 gives an overview of the encountered local plant remains from the analysed peat record: this includes both pollen (wetland and aquatic) and plant macroremains, analysed from the same samples of the Zwarte Beek peat core. The plant macroremains are dominated by *Carex*, *Sphagnum*, *Menyanthes trifoliata* and *Betula*. Figure 4.31 represents the local fire analysis, performed by counting of macro charred particles. A major peak is found at 7.2 cal. kyr BP.

The climatic data from Mauri et al. 2015 are shown in Figure 4.32 (right column) for the investigated time interval. The blue dashed line represents the mean monthly precipitation anomaly (MMP, mm/month) and the red solid line the mean annual air temperature anomaly (MAT, °C). Gradually rising values are found for both precipitation and temperature from the bottom of the record until 10.5 cal. kyr BP: here, temperature stabilizes and remains rather constant until 8.5 cal. kyr BP. The precipitation values rise further until a clear local precipitation maximum is reached at 9.5 cal. kyr BP, followed by a decrease. After 8.5 cal. kyr BP, temperature rises constantly to the top of the record and precipitation reaches a new maximum at 8.0 cal. kyr BP, followed by a minimum at 7.0 cal. kyr BP after which the values start to rise again.

Combining of the LPAZ, RPAZ (Figure 4.11 & 4.12) and additional information from the NMDS analyses and flexible beta clustering resulted in the final subdivision of the ZB-101 peat record: these zones are called ZB zones and are displayed in Figure 4.32. In Figure 4.33, these clusters are plotted on ordination diagrams to verify their validity as separate vegetation zones.

Since all clusters (vegetation zones) are clearly isolated in at least one of the ordination spaces, we can conclude that the used final zonation is statistically supported. In Figure 4.33 (T) and Figure 4.34, the results of a combined (local and regional) NMDS analysis are displayed, showing large similarities with NMDS axes 1 and 2 of the regional NMDS analysis (Figure 4.17). Therefore, axis 1 is interpreted as the forest composition with high values corresponding to a conifer forest and low values with temperate deciduous woodland. Axis 2 is flipped in comparison to the regional NMDS axis 2: here, low values indicate an open vegetation while higher values correspond to increasing canopy closure.

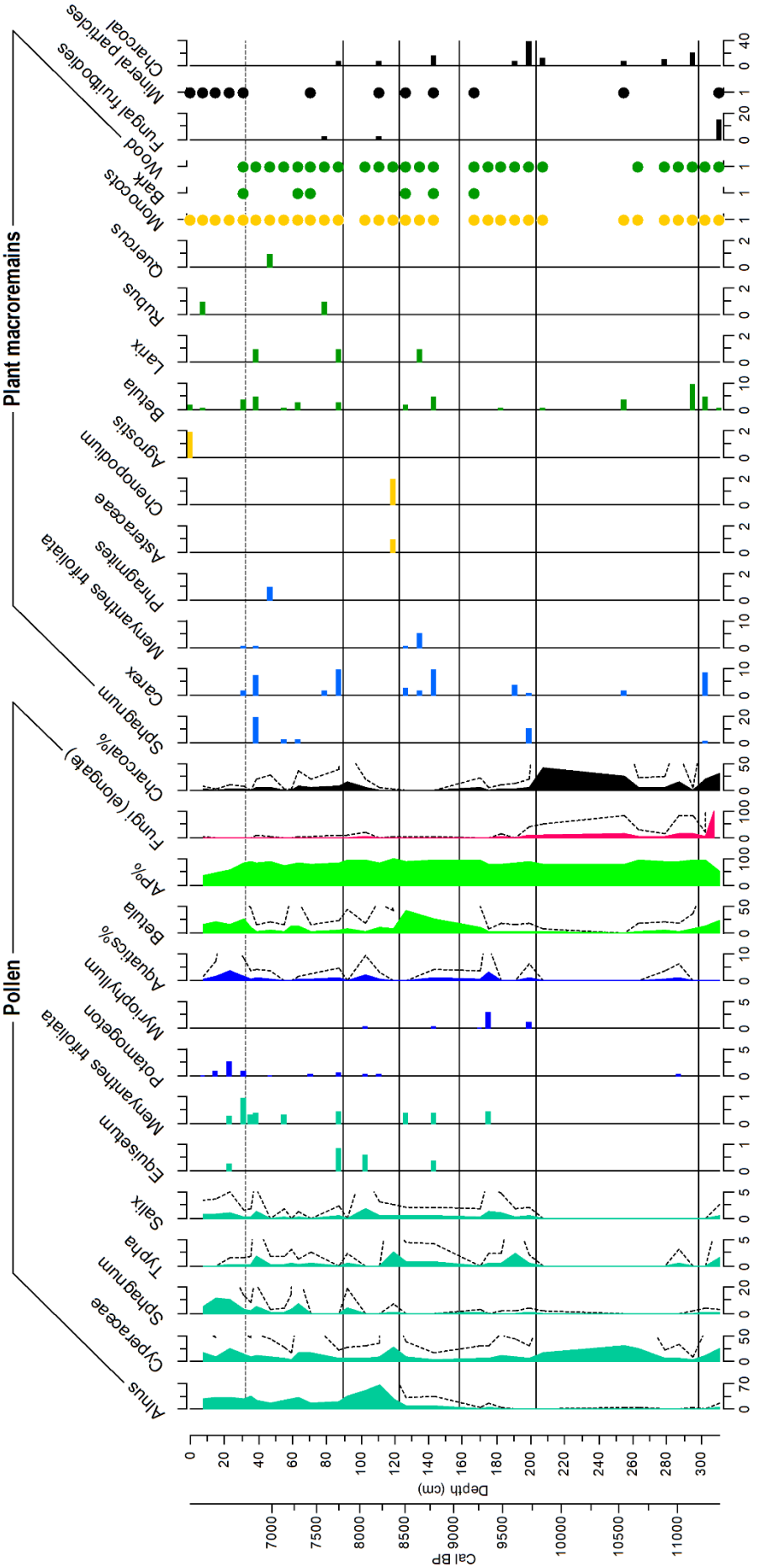

Figure 4.30: Combined diagram of pollen and plant macroremains for the valley of the Zwarte Beek. LPAZ are indicated by the black lines. The dashed line represents the position of a possible hiatus. Plant macroremain data are obtained from the Master Thesis of Laura Vervacke (Vervacke 2019).

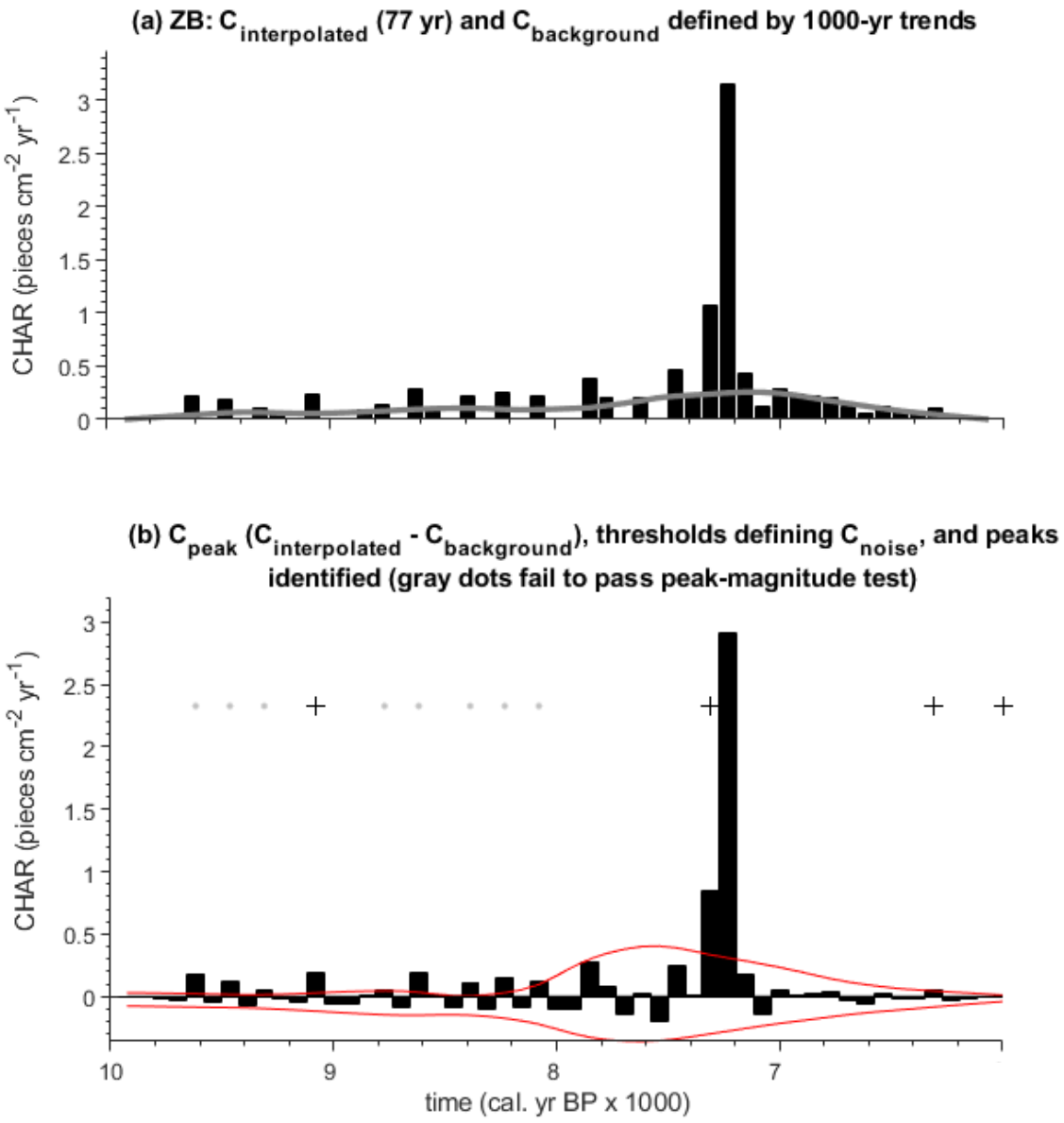

Figure 4.31: Results from the macro charred particle analysis performed on the Zwarte Beek peat core. Data are retrieved from the Bachelor Thesis of Eveline Scherps (Scherps 2019).

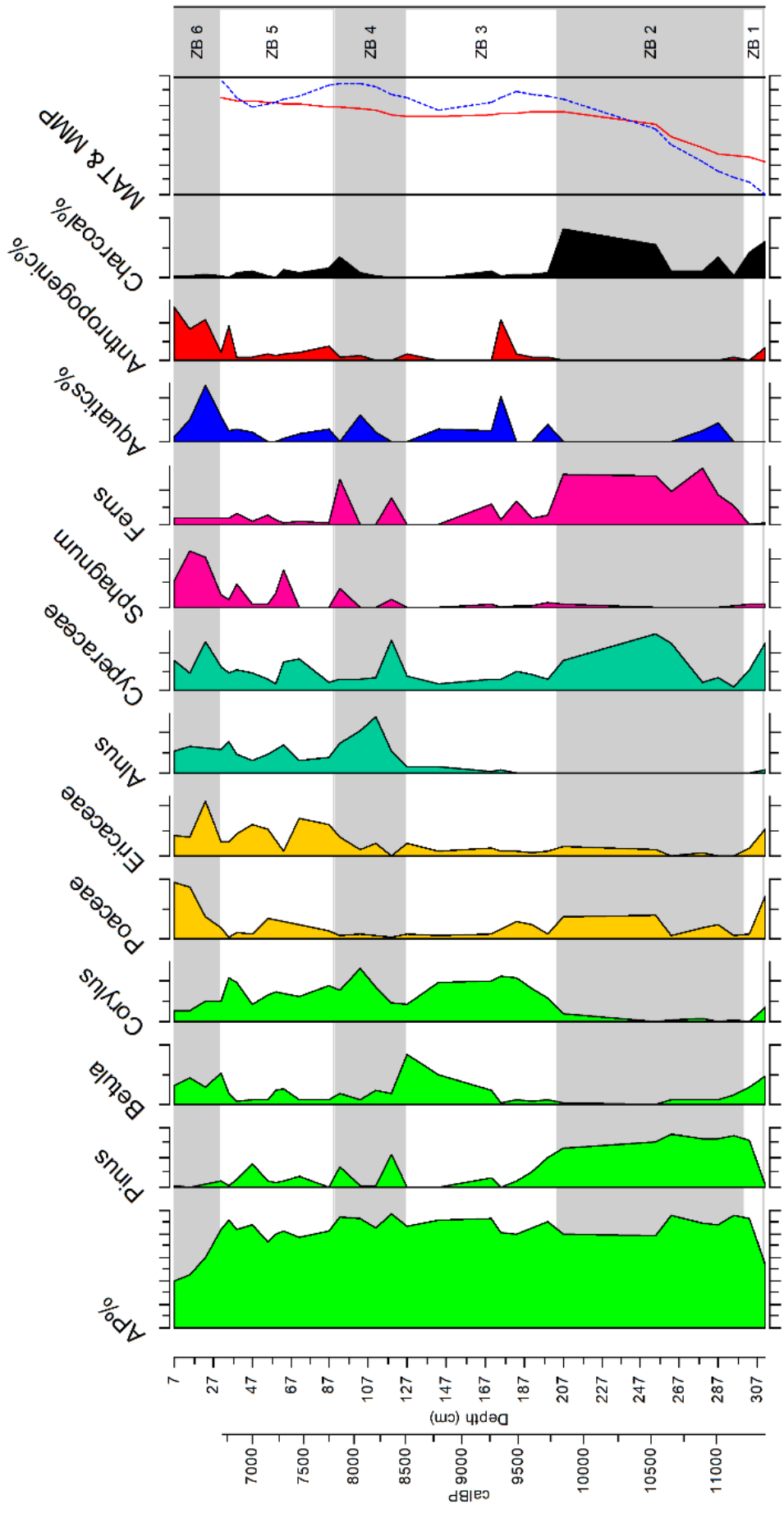

Figure 4.32: Overview diagram of the vegetation development in the Zwarte Beek area with ZB zones indicated. On the right of the diagram, the local climatic reconstructions from Mauri et al. 2015 are drawn (MAT=mean annual temperature (°C), MMP=mean monthly precipitation (mm) expressed as anomalies against 1850).

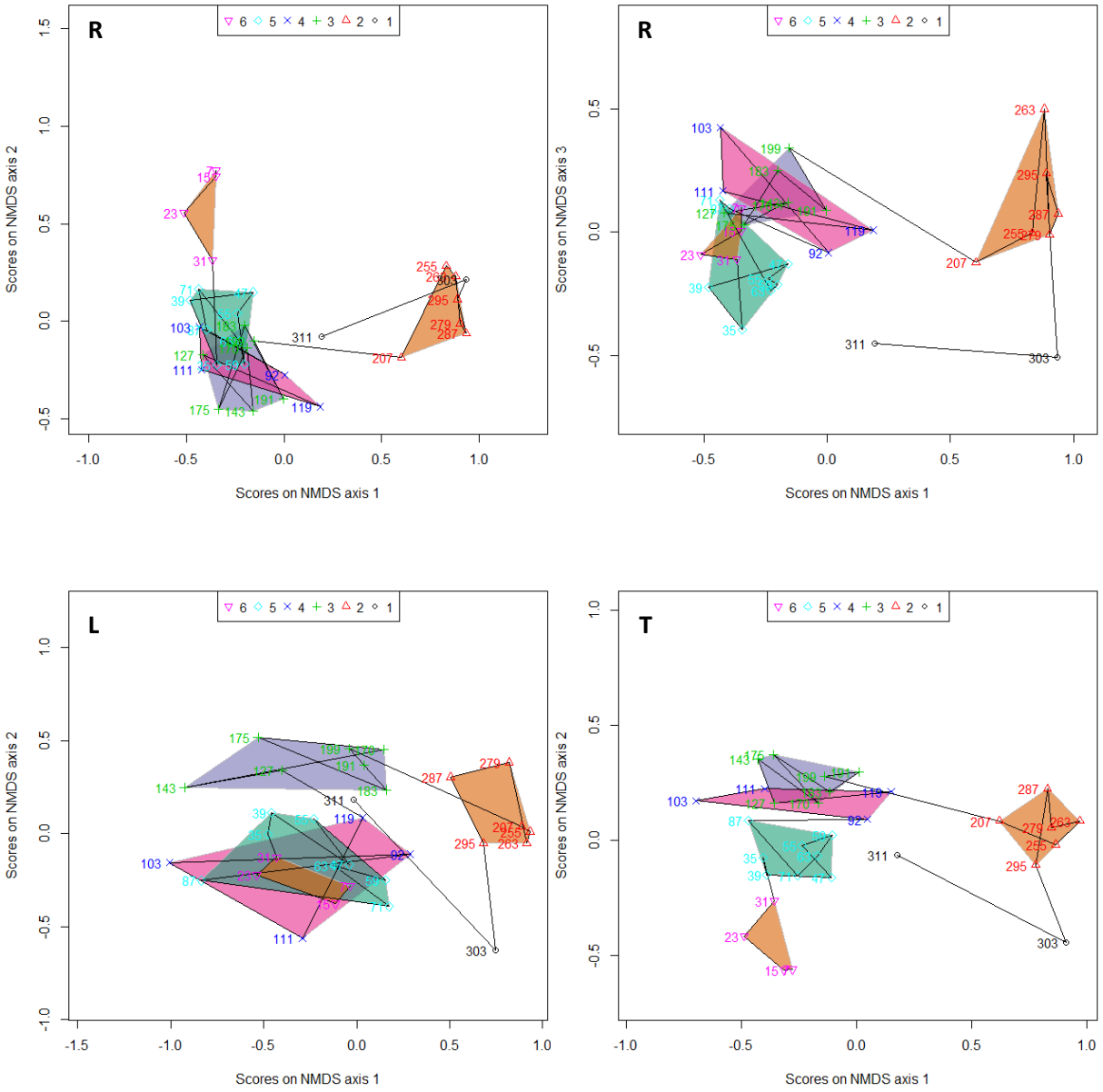

Figure 4.33: Final clusters (ZB zones) displayed on the regional (R), local (L) and combined total (T) ordination diagrams.

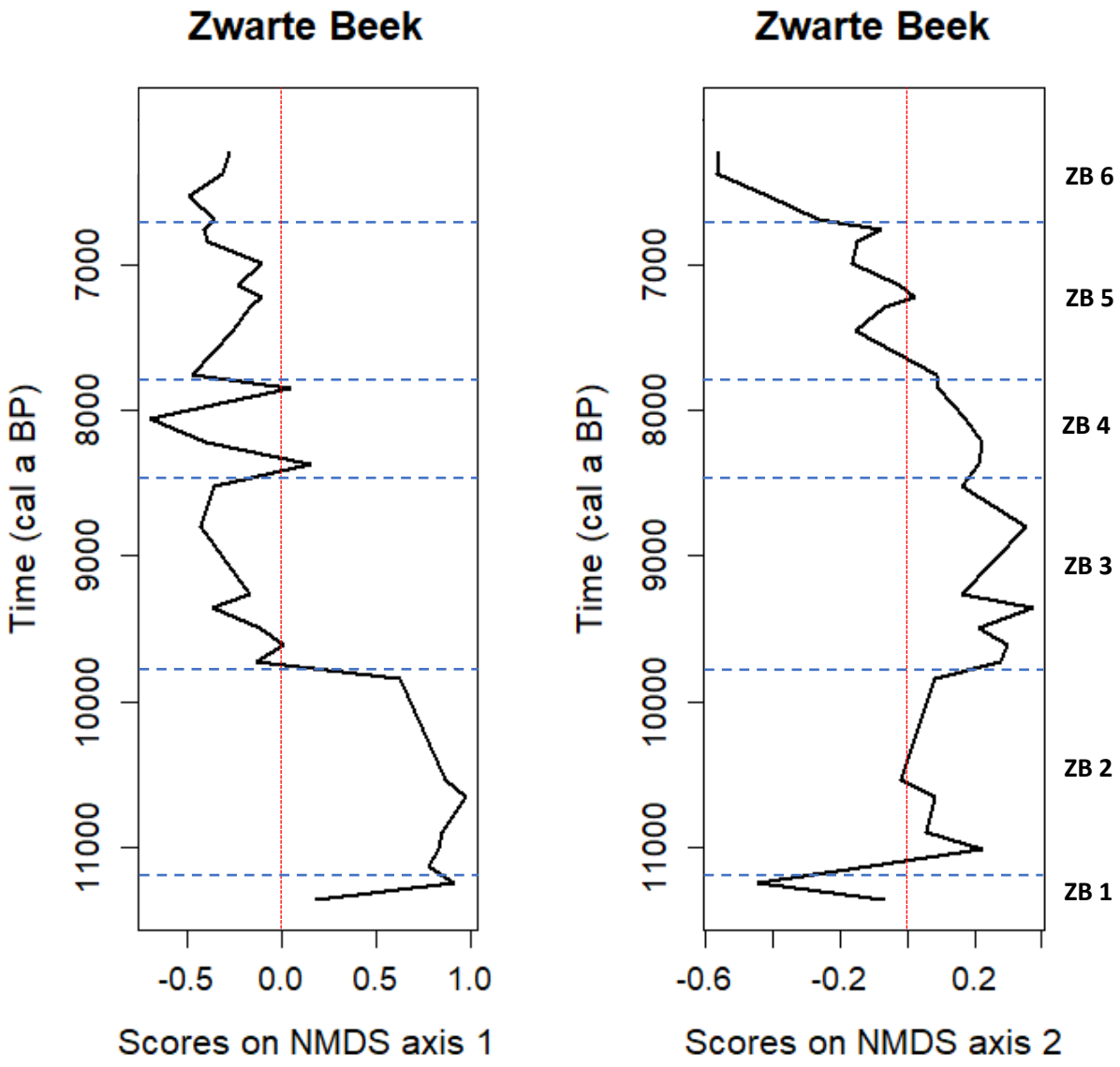

Figure 4.34: The graphs show the evolution of the axes scores of the combined total NMDS analysis over the depth of the core. The corresponding ordination diagram is displayed in Figure 4.33 (T). The subdivision into the final ZB zones is indicated.

5. Discussion

5.1. Age-depth model

In the Results section, a simple linear extrapolation without any assumptions on the age of the top of the peat sequence was used (Figure 4.4). Above 32 cm, however, all ages are uncertain: from level 31 cm, *Fagopyrum* (buckwheat) cereal pollen are encountered in the peat samples (Figure 4.11, Appendix D.1), indicating a late Medieval age or younger since this crop was only introduced from China in western Europe in the early 15th century (Campbell 1997). In addition, it is unlikely that agriculture already occurred in the region of the Zwarte Beek around 6.5 cal. kyr BP. This would predate the start of agriculture in the Loess area -which is much more suitable for these practices- with more than 2000 years (e.g. Broothaerts et al. 2014a) and the onset of agriculture in the surrounding regions with ca. 4000 years (Verbruggen et al. 2019). A sudden very strong deceleration of the peat growth from the dated level 32 cm to the top when assuming a surface age 0 is therefore impossible due to the time gap between 32 and 31 cm. It is possible that a thicker amount of peat was deposited initially before it was removed again, resulting in a hiatus. At this level in the pollen diagrams, other changes are observed as well, including a strong rise of grasses, a decrease of *Corylus* and rise of *Betula*. The position of the hiatus is thus likely between 32 (the radiocarbon dated level) and 31 (the first sample with cereal pollen) cm. The length and cause of this hiatus are, however, unknown and the presence of additional especially younger hiati cannot be excluded.

Several explanations are possible to explain the absence of peat between 6.7 cal. kyr BP (32 cm) and the middle ages: First, the peat growth can have stopped around this time, for instance by changes in hydrological condition in the valley (e.g. by local disappearing of beaver damming), and only restarted recently by a reestablishment of suitable conditions for preservation of organic matter (e.g. by introduction of a watermill such as ‘Stalse Molen’). The age of the hiatus bottom (ca. 6.7 cal. kyr BP) matches remarkably well with the reported age by Huybrechts (1999) of the transition from organic to clay deposits in valleys in central Flanders: this suggests that possibly peat growth stopped in a similar way as in these valleys. The cause of this transition can be anthropogenic in origin, with small scale deforestations leading to increased runoff and erosion in the catchments. In loamy areas, the result was increased clastic deposition in the floodplains and associated suffocation of the marsh forests. No covering with clastic deposits was recorded for the Zwarte Beek, attributed to its location in sandy Flanders where less fine grained sediments are available. However, increasing erosion of the valley slopes could have altered the valley geomorphology with for instance a transition from a diffuse channel network flowing through the peat valley being replaced by a single channel embarked by the increased sand deposits. This change could have deteriorated the conditions for peat formation in the valley. But, more recent work on the Dijle catchment showed a diachronous transition from peat to clastic deposits between 6.5 and 0.5 cal. kyr BP (Broothaerts et al. 2014c): therefore this transition and the possible transition at 6.7 cal. kyr BP in our study area, where human impact is expected to be lower and a transition expected later, are probably not related.

Alternatively, Middle and Late Holocene peat can be broken down in a later stage by drying of the climate or by local peat desiccation due to human alterations of the valley: it was reported for the Zwarte Beek that ditches were introduced in the valley as an attempt to make it more accessible for agricultural purposes (Maes et al. 2018). The peat can also be removed directly

by human intervention: both digging for iron ores and mining of peat for fuel are reported in historical documents for the investigated valley (De Becker and Huybrechts 2000). Peat mining is especially a likely cause of the missing upper peat, since it was reported that the zone where the peat core was taken (around 'Fonteintje') was almost entirely mined due to the exceptional thickness and quality of the peat as a fuel in this area (Burny 1999). According to Leenders (1989), peat bogs were once a widespread phenomenon in Flanders, but were excavated on a major scale from the Middle ages to recent times.

In Figure 5.1, two possible age-depth models including a hiatus are presented: The first model assumes an upper hiatus age of 1900 AD, representing the latest peat mining events in the 20th century. For this model, a substantial acceleration of the peat accumulation rate is required to deposit the upper 30 cm in ca. one century (from 0.52 to 2.6 mm/yr). This could indicate that peat above the hiatus is possibly not formed in situ, but a result of filling up of the peat holes after excavation, which was reported to be the common practice by Burny (1999). However, filling was usually done with sand, which was not present at the core location. Joosten (1985) showed that accumulation rates during reactivation of peat growth in excavation pits can be very high (>4 mm/yr): therefore a young hiatus age with in situ formed peat cannot be excluded. The next models represent an early peat excavation scenario, at 1420 AD: this date is chosen because it matches the onset of European *Fagopyrum* cultivation and because it results in a constant peat accumulation rate when no additional disturbances in more recent times are assumed.

Using the second model would imply that 6170 years are lacking (6.7 cal. kyr BP to 530 cal. years BP or 1420 AD), corresponding to 3.2 meter of missing peat if an accumulation rate of 0.52 mm/yr is used. When taking the slow decelerating trend in peat accumulation speed into account, this forms a good match with the depth of peat mining in the valley of the Zwarte Beek which was reported to be between 2 and 3 meter (Burny 1999). Finally, the hiatus can be the result of a combination of processes: for instance, ca. 2 meter of peat can be excavated while another meter is removed by mineralization due to the installation of drainage channels in the valley.

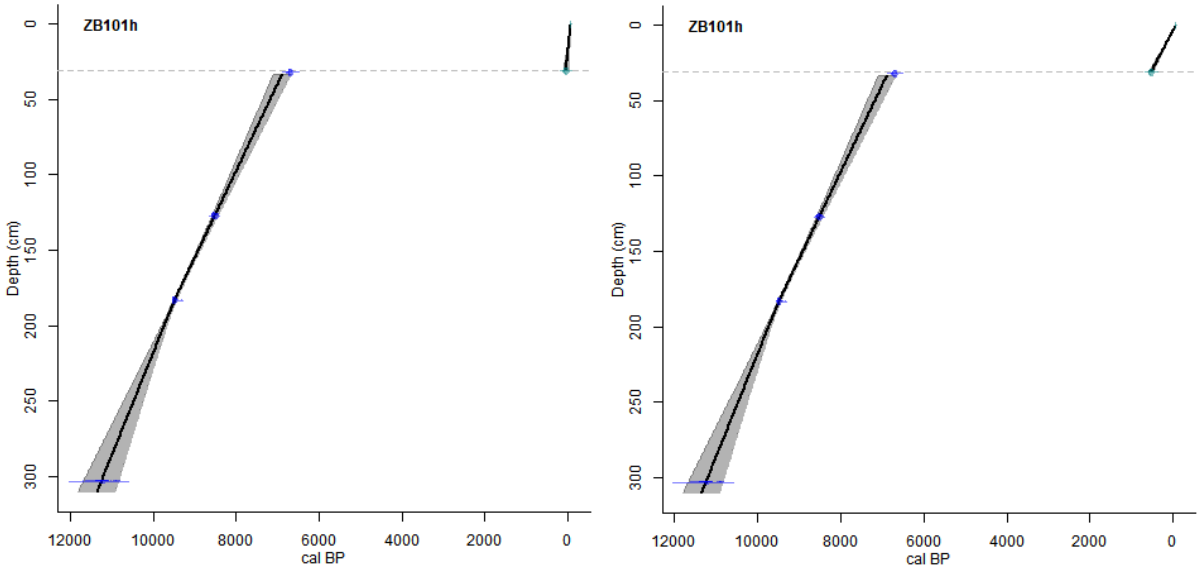

Figure 5.1: Age-depth models with hiatus at 31-32 cm, representing the two possible extremes for the upper hiatus age. On the left, the hiatus is put at 1900 AD, on the right at 1420 AD. This only affects the age-depth model of the upper 31 cm, underneath the hiatus the age-depth model is identical for both scenarios as well as the model used in Figure 4.4.

5.2. Comparison of pollen data with additional records

a. Plant macrofossils

Cyperaceae (or more specifically *Carex* in case of the plant macroremains) occur over almost the entire record as micro and macrofossils (Figure 4.30, Vervacke 2019). This confirms that sedges are an important member of the local wetland vegetation in the valley of the Zwarte Beek. According to the macroremains, the sedges are abundant at the bottom of the record and from 8.8 cal. kyr BP onwards. The elevated pollen percentages between 10.5 and 10.0 cal. kyr BP are not confirmed by the macroremains: these sedges could have been part of the boreal forest undergrowth out of the valley or the pollen can be derived from a sedge dominated valley patch situated further away from the sample site. Apart from scattered findings at the bottom of the record and at 9.7 cal. kyr BP, *Sphagnum* was mostly found as macrofossils between 7.4 and 6.8 cal. kyr BP. This forms a good match with the pollen findings of *Sphagnum*, which become more frequent from 7.4 cal. kyr BP to the top of the record. From this moment peat mosses thus become a significant part of the wetlands of the Zwarte Beek and peat bog development could be initiated. For *Menyanthes trifoliata* or bogbean, scattered observations occur from 8.8 cal. kyr BP in both the pollen and macroremain records, indicating this species belongs to the local fen flora. For *Betula* as well, the pattern observed in the pollen and macrofossil records are very similar, with peaks at the bottom of the record and frequent occurrences in the second half of the diagram. However, in the pollen analysis *Betula* was included in the regional vegetation instead of the local wetland vegetation. Seeds of *Betula* are equipped with little wings resulting in a good dispersion capacity: in this way, seeds from *Betula* growing on the valley sides and plateaus can be incorporated in the peat of the valley bottoms. A second explanation requires better knowledge of the ecology of *Betula* species: where *Betula pendula* is typical for oak (-beech) forests and can be expected in the regional vegetation, *Betula pubescens* -also called moor birch- prefers moist conditions and can be expected as a part of the wetland vegetation (Atkinson 1992). Since both species are common in Belgium, the pollen and macrofossils are probably a mixture of both *Betula* species.

Several pollen types included in the wetland vegetation group (*Alnus*, *Typha*, *Salix*) are not found as macrofossils. One explanation is that the pollen are derived from a larger distance than over which plant macroremains can travel: in this way, the differences between the micro and macroremain record indicate that patches with these vegetation types occur in the valley but not at the exact location of the investigated core. Alternative explanations include a low preservation potential of the seeds of these plants or a difficult recognisability. A remarkable plant macroremain which was not encountered in the pollen analysis is *Larix*. It is a light-demanding pioneer tree, colonizing disturbed and well-drained areas (Ronch et al. 2016).This deciduous conifer tree produces pollen lacking clear identifiable traits, explaining their absence in the pollen counts. However, the identification of the encountered needles was questionable and they could also belong to another type of conifer. Still, the findings of these needles from 8.8 cal. kyr BP onwards show that conifer trees were present in the Zwarte Beek valley or its vicinity. The macroremain data also support the position of the hiatus at the 32-31 cm transition (Figure 4.30): wood remains were found continuously in the samples below the hiatus but completely disappear above this level. At the same position, a sharp increase in the frequency of mineral particles is encountered, possibly refleceting increased erosion in the catchment associated with extensive deforestations.

b. Macro charcoal

The macro charcoal data show one clear peak between 7.4 and 7.2cal. kyr BP (Figure 4.31, Scherps 2019). Other minor but significant fire events were detected at 9.1 cal. kyr BP and at the top of the record. Since this analysis covers macro charred particles, the recorded fire events are local fires occurring in the proximity of the study site (Mooney & Tinner 2011). This contrasts with the microcharcoal signal reported in the pollen diagrams (Figure 4.5), which reflects the regional fire history and shows a different pattern with peaks at 11.4, 10.5-9.9 and 7.9 cal. kyr BP.

5.3. Vegetation development in and around the valley of the Zwarte Beek

a. Zone ZB 1 (11.4-11.2 cal. kyr BP)

The peat accumulation in the valley of the Zwarte Beek starts around 11.4 cal. kyr BP, at the onset of the Holocene epoch. During the time interval 11.4-11.2 cal. kyr BP, the slopes and uplands of the Zwarte Beek catchment are characterized by a tundra to steppe vegetation. A visualization of the vegetation zones for the Zwarte Beek area (as presented in Figure 4.32) is shown in Figure 5.2. The flexible beta clustering analysis (Figure 4.7) groups this Early Holocene vegetation with the upper samples of the peat core, reflecting the high degree of openness of the landscape. This is also confirmed by the low scores of the 2th NMDS axis (Figure 4.34, total). The open landscape was dominated by grasses and a pioneer vegetation of birch trees (Figure 4.11). A smaller proportion of the landscape was occupied with heather and hazel shrubs. However, pollen production estimates of Ericaceae (heather) as reported by Trondman et al. 2015 are relatively low: therefore the heather vegetation cover was probably significantly more than its pollen percentage (ca. 3%) suggests. During this vegetation phase conditions were cold and dry (Figure 4.32). It can be considered as a remnant of the glacial steppe-tundra vegetation of the Cryocratic vegetation phase (Iversen 1958). The dry conditions can explain the elevated regional fire frequency as reflected by the microcharcoals. Fire activities were also reported for other parts of the Campine region during this period (Verbruggen et al. 2019). The Zwarte Beek valley was dominated by sedges and must have been swampy as indicated by the peat accumulation, contrasting with the regional dry circumstances. These favourable conditions for peat formation are probably related to the hydrology of the catchment, where infiltration on the Campine plateau is directed through the sandstone layers of the Diest formation downstream in the valleys creating locally wet conditions (De Becker & Huybrechts 2000). The abundant presence of coprophilous fungi indicates the presence of large herbivores in the study area (Appendix C.2 & D.3: *Sordaria* and *Cercophora*, Van Geel 1978, Verbruggen et al. 2019). *Gelasinospora* was encountered as well and is often linked to local fire activities (Bos et al. 2013).

b. Zone ZB 2 (11.2-9.8 cal. kyr BP)

Around 11.2 cal. kyr BP, the open landscape became rapidly replaced by a pine-dominated boreal forest. This conifer forest dominated the regional vegetation in the area of the Zwarte Beek from 11.2 to 9.8 cal. kyr BP. The high values of NMDS axis 1 (Figure 4.34) reflect the dominance of the conifer forest in this zone. Axis 2 indicates an increase in vegetation closure

compared to zone ZB 1, but the values are still only around 0, indicating no full closure of the forest canopy. This zone corresponds to the Protocratic vegetation stage, in which an open pioneer forest forms in response to the early interglacial climatic ameliorations (Iversen 1958). Pine trees are shade intolerant and are a typical early successional species (Bennett 1984). They are able to survive on acidic soils including sandy substrates and peat. The abundance of grasses is relatively high, confirming the presence of an open forest with light penetrating to the forest floor. As indicated by Trondman et al. 2015, pollen production estimates of *Pinus* are exceptionally high, resulting in an overrepresentation in the pollen diagram compared to the true vegetation: the vegetation was therefore probably less closed than indicated by the high AP percentages. Precipitation values rise throughout this period (Figure 4.32), and temperature reaches a plateau at 10.5 cal. kyr BP, matching the high fire frequencies in the second half of this zone. In addition, pine wood is a good fuel source, mediating the occurrence of wildfires under warm conditions in the Early Holocene (Power et al. 2008). In the local vegetation of the valley of the Zwarte Beek, sedges are abundant and might have co-occurred with ferns. The latter are found in very high percentages during this interval, but might have been as well a part of the well-developed understory of the regional open boreal forests.

c. Zone ZB 3 (9.8-8.5 cal. kyr BP)

From 9.8 cal. kyr BP, the share of pine in the regional vegetation starts to diminish while the abundance of hazel shrubs increases sharply. In this way, a mixed open pine-hazel forest is established between 9.8 and 9.5 cal. kyr. Afterwards, when pine has almost completely disappeared from the Zwarte Beek area, a temperate deciduous woodland is established where hazel, oak and elm are the dominant trees species. A closed forest is established where light penetration is minimal, resulting in very limited undergrowth as indicated by low pollen percentages of herbs. This phase corresponds largely to the Mesocratic vegetation phase (Iversen 1958): the temperatures are constant and mild, allowing for the colonization of the study area by temperate tree species, arriving in the region from their glacial refugia in southern Europe (Deacon 1974). They formed a closed forest resulting in the displacement of the light requiring pine trees. This forest type is indicated as *Quercetum mixtum* (with possible members *Quercus, Ulmus, Tilia, Fraxinus* according to Bakels 2009), dominated in this interval by oak and elm trees and an abundant shrub layer of the very shade tolerant *Corylus* (Bakels 2009, Kull & Niinemets 1998). The gradually rising values of both temperature and precipitation throughout zones ZB 1, ZB 2 and ZB 3 correlate well with the trend of increasing closure of the forest canopy: the vegetation evolution in this interval (the Early Holocene) thus seems to be largely driven by the climatic ameliorations. Apart from increasingly suitable climatic conditions and soil development, several authors also suggested a role for fire in the transition from a boreal to a deciduous forest: in contrast to the fire sensitive pine trees, especially hazel is able to resprout quickly after fire events (Tinner et al. 1999). Prolonged periods of elevated fire activity such as the observed peak in microcharcoals at the end of zone ZB 2, could in this way have contributed to the shift in forest composition. In the macroremain data a peak in charcoal particles was observed around the ZB 2-ZB 3 transition (Figure 4.30), supporting this hypothesis. NMDS axis 1 (Figure 4.34) confirms a total reversal of the forest composition (from conifer to temperate), while axis 2 shows the formation of a maximal closed canopy. Precipitation peaks in the first half of this zone (Figure 4.32), coinciding with an elevated abundance of aquatic species: at this time the valley was probably wetter than average with the presence of small ponds and pools. This is also confirmed by the occurrence of *Typha* in this period, a wetland plant growing in shallow water at the borders of pools (Grace 1989). In

general, sedges and ferns become less important members of the wetland vegetation in this phase, while from 9.3 cal. kyr BP birches become more abundant and possibly a birch carr vegetation is formed (*Betulion pubescentis*), occurring on wet, nutrient poor fen areas (Atkinson 1992). In the second half of the zone (from ca. 9.0 cal. kyr BP), also alder trees appear: at this time they occur in low abundance in the valley of the Zwarte Beek, but they show that the local conditions are suitable for a valley forest to form (increased substrate stability, Brown 1988). At 9.1 cal. kyr BP the occurrence of a local fire event was shown by the macrocharcoal data (Figure 4.31). In the pollen data, this does not correlate to a significant shift in the local vegetation. In the macrofossils data however, after this event the occurrence of sedge and birch seeds increases. It is not clear if this is a true response of the valley vegetation to opening by fire, or that it simply reflects an improvement in preservation conditions.

d. Zone ZB 4 (8.5-7.8 cal. kyr BP)

In this zone, the regional vegetation is still dominated by temperate deciduous woodland. Apart from hazel, elm and oak, also lime trees are found in this interval and pine trees return. The latter could indicate a slight opening of the closed temperate forest, offering opportunities for the light demanding pine trees to colonize forest gaps. The pine pollen could also reflect long-distance transport of pollen grains from boreal forests in more northern regions: however, also this indicates more open conditions where strong winds could have blown in the foreign pollen (Bennett 1984). The lower values of hazel at the bottom of this zone are probably an artefact due to relatively high values of pine and birch. This phase is part of the Atlantic chronozone, characterized by the alder increase, which forms the climatic optimum of the Holocene with dominantly warm and wet climatic conditions (Rydin & Jeglum 2013). This favourable climate allowed the cold- and drought-sensitive alder trees to colonize these regions (Douda et al. 2014). Temperatures rise throughout this zone (Figure 4.32) and a peak of regional fire activity is recorded close to the end of this zone: this marks the start of a period where both heather and microcharcoal findings become more abundant, pointing to possible human fire use for the opening of the regional vegetation of the Campine area. Small scale openings could have resulted in enhanced soil erosion and depletion of the sandy soils, favouring heather which thrives on acidic poor substrates and is known for its fast recovery from fires (Blarquez & Carcaillet 2010). Mesolithic hunther-gatherers were present in the Campine area, but reliable datings of these archeological findings remain problematic (Vermeersch 2008, Derese et al. 2012). Verdumen & Tys indicated the presence of several archaeological sites with stone age artefacts in the vicinity of the Zwarte Beek valley, but again no absolute temporal framework is available. Marlon et al. 2013 reported for Europe a widescale anthropogenic use of fire for vegetation clearing from 8.0 cal. kyr BP. This forms a good match with our data, but no direct evidence of human presence is available for our study area so a natural cause for the heather spread cannot be excluded: for the period between 8 and 7 cal. kyr BP elevated fire frequencies across Europe are linked to the climatic optimum, with wetter conditions increasing the available biomass for burning and higher temperatures increasing the risk of ignition (Power et al. 2008). The statistical analyses of our data show strong fluctuations of NMDS axis 1 scores, interpreted as phases of pine reestablishment, in alignment with the decreasing axis 2 scores pointing to increasing light availability linked to small scale forest openings. In the local vegetation, after a short sedge dominated interval, the valley becomes strongly forested with the establishment of an alder carr in the valley of the Zwarte Beek. The arrival of *Alnus* is relatively early for western Europe, but not exceptional (Douda et al. 2014). A peak of aquatic

vegetation corresponds to elevated precipitation values and peat mosses are encountered more frequently in the wetland vegetation. *Sphagnum* and *Pinus* peaks correlate well, indicating that pine trees may have been part of the local fen vegetation: this is in accordance to a peat succession from a minerotrophic carr fen to a mixed carr fen with pine and later possibly to an ombrothrophic *Sphagnum* bog, by peat accumulation above the water table and acidifying conditions (Van der Valk 2012). In the macroremains (Figure 4.30) conifer needles were encountered at the top of this zone, supporting the local conifer presence in the wetland.

e. Zone ZB 5 (7.8-6.7 cal. kyr BP + hiatus)

From 7.8 cal. kyr BP, the regional vegetation becomes clearly more open, as indicated by the increased abundance of grasses, heather and shade-intolerant pine trees in the regional vegetation of the Zwarte Beek area. The composition of the temperate deciduous woodland remains unaltered but it decreases in cover. Microcharcoals and anthropogenic indicator species are found throughout this zone, indicating a role for humans in the partial opening of the landscape. The purpose of the opening can be to improve visibility for hunting or to allow grazing (e.g. Kaplan et al. 2016). Cereals are not yet encountered and are also not expected in this region during this period (e.g. Verbruggen et al. 2019). Pioneer species such as pine, birch and heather profited from the improved light availability. It is unknown if humans purposefully favoured the development of heathland to allow grazing activities, or that the latter arose in a later stage when heather became abundant by natural vegetation succession in forest openings. Significant lowering of NMDS axis 2 scores (Figure 4.34) highlights the partial vegetation opening in this zone. In the wetlands a diverse vegetation is observed: high values of both alder and sedges are found and peat mosses become more and more abundant, their local presence being confirmed by plant macrofossils. The valley was probably occupied by patches of forest, open sedge-swamps and peat bogs in a mosaic like fashion, similar as observed today (Biological Valuation Map INBO, 2018). Temperatures keep on rising (Figure 4.32), while precipitation decreases except for the upper part where they start to rise again. Between 7.4 and 7.2 cal. kyr BP a major local fire event was indicated by macro charcoal particles (Figure 4.31), adding to the evidence of fire use by local hunter-gatherers in this time period: wetland vegetation is relatively unsusceptible to fires and their burning in Mesolithic western Europe is often shown to be related to human presence (Bos et al. 2006, Verbruggen et al. 2019).

f. Zone ZB 6 (hiatus-top)

The presence of cereals in the upper part of the peat record combined with the radiocarbon dating results and historical sources (e.g. Burny 1999) indicate that a hiatus is present in the peat matrix. The peat above this hiatus is thus reflecting the valley vegetation of the last hundred(s) years, or a mixed signal by refilling the excavations holes with ground. The pollen spectra indicate an open vegetation with a strong dominance of grasses. Birch trees are also abundant and heather is widespread. A strong rise of anthropogenic indicators is recorded indicating significant disturbance of the natural vegetation in the Zwarte Beek catchment in recent times. Cereals (buckwheat, rye) are found in low abundances, indicating that agriculture is present in the region but not common. *Secale* (rye) was found, which is typical for the Campine region since it thrives well on nutrient poor sandy soils (Briggle 1959). This zone can be subdivided in two parts, where the first is characterized by buckwheat and abundant heather while grasses are still relatively sparse. The second half is characterized by both buckwheat

and rye cereals, a relative decrease of heather and strong increase of grasses. Depending on the timing of the restart of peat growth (extreme scenarios represented in Figure 5.1), this can reflect a long-term change (for medieval restart) or a quick shift (for 20th century restart) in land use from dominantly agropastorialism to increased vegetation clearing and cereal cropping. NMDS axis 2 reaches extremely low values (Figure 4.34), indicating the removal of the natural forested vegetation. Comparing the pollen signal to the contemporary vegetation indicates a relatively low proportion of pine in the peat samples: pine plants are very abundant in the Campine region since 1850 (Bosplus 2007), suggesting a probably older age of the investigated pollen samples. The local wetland vegetation is still dominated by alder carr and sedge patches, and the share of peat mosses is at its maximum in this zone, indicating the possible initiation of peat bog formation. The presence of *Rubus* shrubs is shown by the plant macrofossils. Two significant fire events are recorded locally.

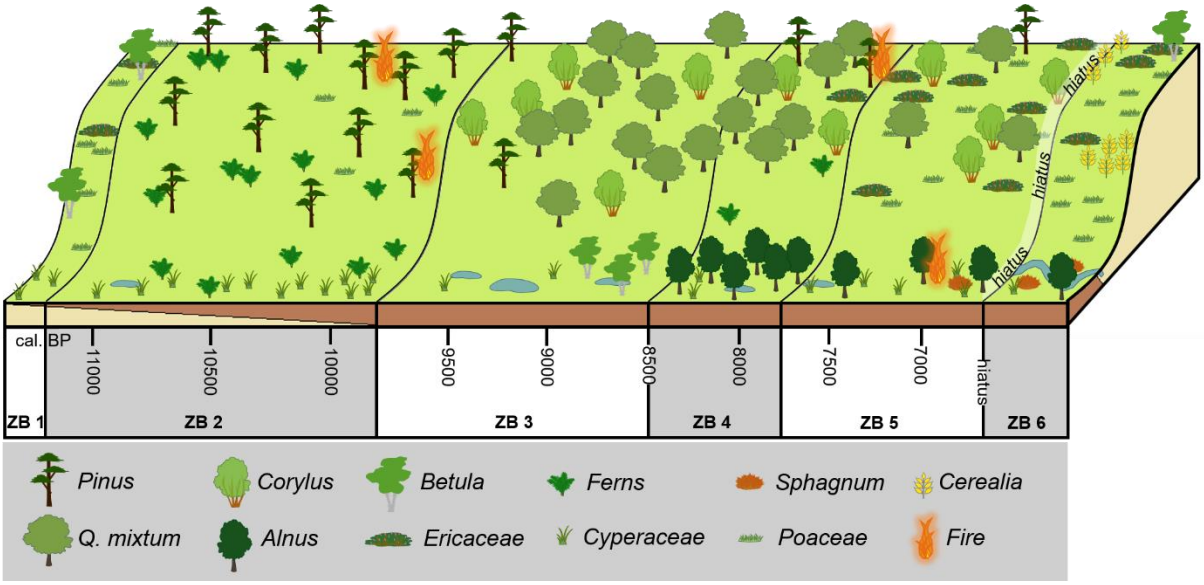

Figure 5.2: Visualization of the vegetation development in the Zwarte Beek area. The major trends are displayed, the description of the separate zones can be consulted for a more detailed vegetation evolution. The biozones are indicated at the bottom, corresponding to Figure 4.32.

5.4. Spatial comparison

a. Previous research Zwarte Beek

Our results for the vegetation development in and around the valley of the Zwarte Beek can be compared to the study of Allemeersch (2010). Since the publication of this study, additional pollen samples were counted resulting in an updated pollen diagram shown in Figure 5.4 (Storme & Deforce unpublished). In this pollen diagram, no discrimination is made between local and regional vegetation: therefore a comparison between the evolution of the openness of the vegetation (AP/NAP) is not straightforward.

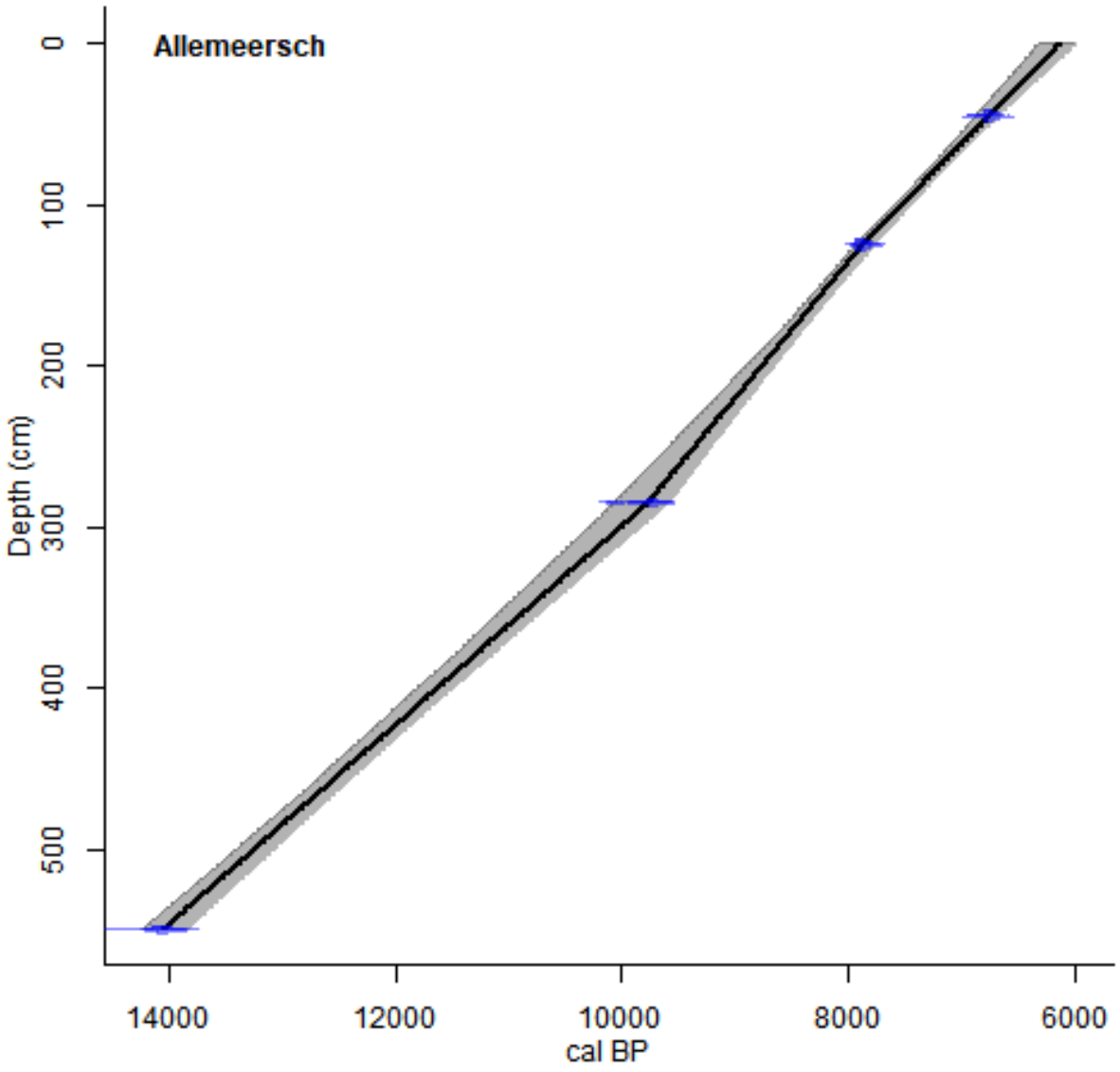

Figure 5.3: Age depth model for the radiocarbon dates as reported by Allemeersch (2010). Linear interpolation is used. The possible presence of a hiatus in the most recent part is not taken into account.

The peat sequence of this study spans a longer time interval than our peat core (Figure 5.3): its bottom age is over 14000 cal. years BP, while the top age (40 cm) is estimated at 6690 cal. years BP. The accumulation rate is 0.69 mm/yr, which is slightly higher than the 0.60 mm/yr for core ZB 101. The upper 40 cm of the sequence was strongly corroded and was a mixture of peat and sand: this part was not included in the pollen analysis. There is a remarkable synchronism of the end of the undisturbed peat sequences of this (6690 cal. years BP) and our analysis (6700 cal. years BP).

Three main vegetation zones are discriminated in the diagram (Figure 5.4): phase 1 runs from 14.0 cal. kyr BP until 10.5 cal. kyr BP. Here the vegetation is dominated by *Betula* trees and Cyperaceae (both ~40%) followed by Poaceae (20%). The vegetation is rather open (NAP upto 80%) but becomes gradually more closed to the top of this zone (AP~75%). *Pinus* appears in the diagram around 12.5 cal. kyr BP and rises to values of 40%. *Salix* forms 20% of the pollen spectrum at the bottom of the core but gradually disappears in this zone. Numerous upland herb species are present throughout the zone in low abundances. The upper 50 cm

(from 11.4 cal. kyr BP) of this zone can be correlated to zones ZB 1 and ZB 2. The boundary between both is difficult to recognize in the pollen diagram of Allemeersch (2010) due to a large overlapping zone of birch and pine trees.

In phase 2, from 10.5 to 8.8 cal. kyr BP, AP values are constantly high between 70 and 90%. Values of *Betula*, Cyperaceae and Poaceae strongly decrease (5-15%), while *Corylus* and *Pinus* become the dominant pollen types (~40%). They are accompanied by *Quercus* and *Ulmus* from the bottom of this zone. Aquatic plants are found more frequently in this interval, while upland herbs become rare. This zone correlates well with zone ZB 3, characterized by the formation of a deciduous forest. The recorded onset of this vegetation phase is ca. 700 years earlier in this core compared to ZB 101 (9.8 cal. kyr BP): possibly this is a result of the dating errors and the used age-depth models but the non-overlapping 95% confidence intervals (10399-10796 vs. 9713-9875 cal. years BP) suggest significant spatial variability of the vegetation dynamics, even over small spatial scales (ca. 1 km, Appendix B.1).

Phase 3 (8.8 to 6.7 cal. kyr BP) is characterized by the presence of *Alnus* (20-40%). In contrast to our peat sequence where *Alnus* was only found as pollen, Allemeersch (2010) also found it as macroremains in the interval 8.4-7.7 cal. kyr BP, showing that alders were indeed growing in the valley of the Zwarte Beek. *Corylus* and *Pinus* persist in this phase (20-30%) as well as *Quercus* and *Ulmus*, together resulting in continuously high AP-values. *Tilia* becomes part of the deciduous woodland in this zone, and values of *Betula* start to rise again to the top of this zone. High values of ferns are encountered and *Urtica* is present throughout the zone. Heather (*Calluna vulgaris*) and *Sphagnum* appear in the upper half of this zone. In the plant macrofossil analysis, Allemeersch (2010) was able to identify the peat mosses up to species level: this showed that the local dominant peat moss species was *Sphagnum palustre*. This is a species of wet forests and grassland habitats rather than peat bogs, contradicting the hypothesis of a trend towards bog formation in the Zwarte Beek valley. The lower half of phase 3 correlates with ZB 4, as shown by the alder carr dominance in the wetland vegetation, while the upper half correlates with zone ZB 5 as indicated by the heather and *Sphagnum* pollen and the decrease of *Alnus*. The start of ZB 4 at 8.5 cal. kyr BP matches well with this phase (8.8 cal. kyr BP), and the transition to zone ZB 5 (7.8 cal. kyr BP) also matches more or less, but this is harder to assess due to the low resolution used by Allemeersch (2010) at this level in the core.

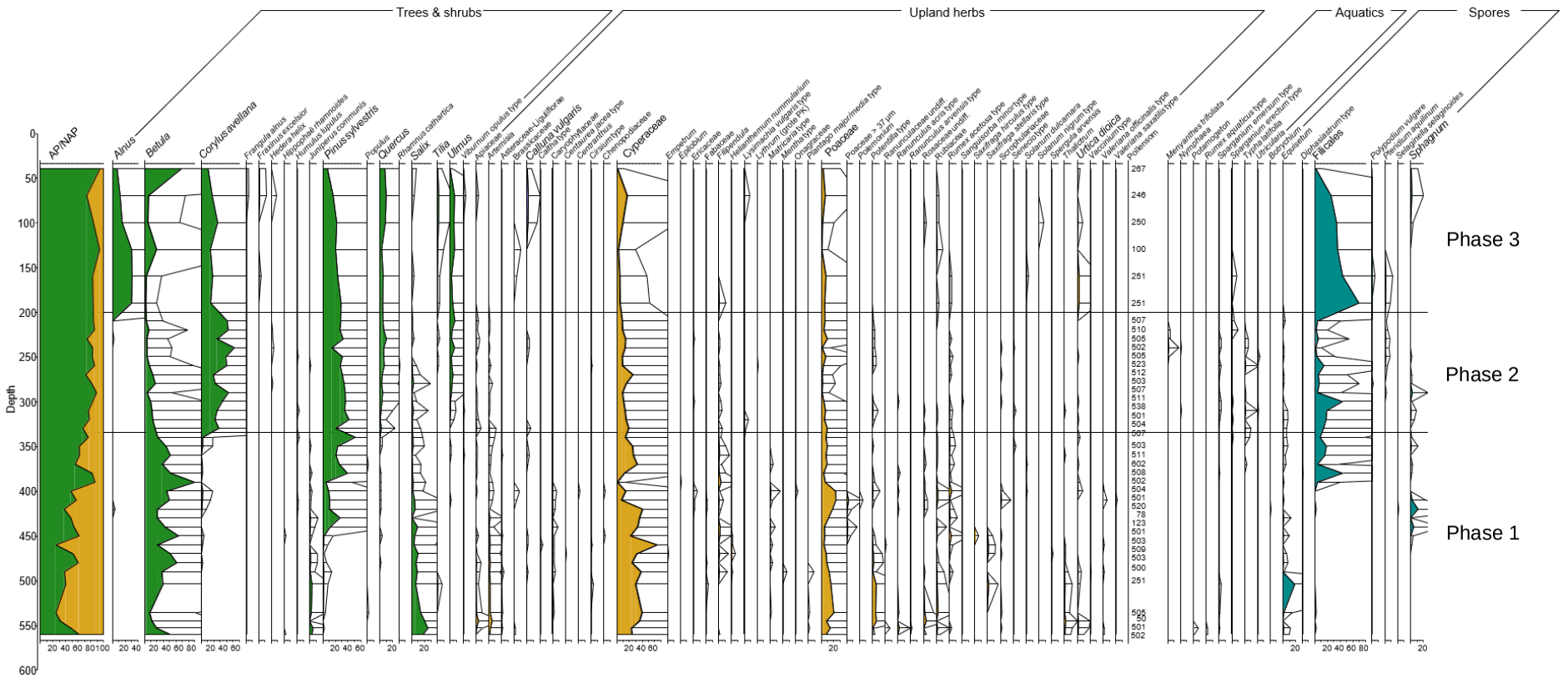

Figure 5.4: Unpublished updated diagram from Allemeersch (2010). Pollen countings are performed by Koen Deforce and Annelies Storme. For the timing of the vegetation changes, see Figure 5.3.

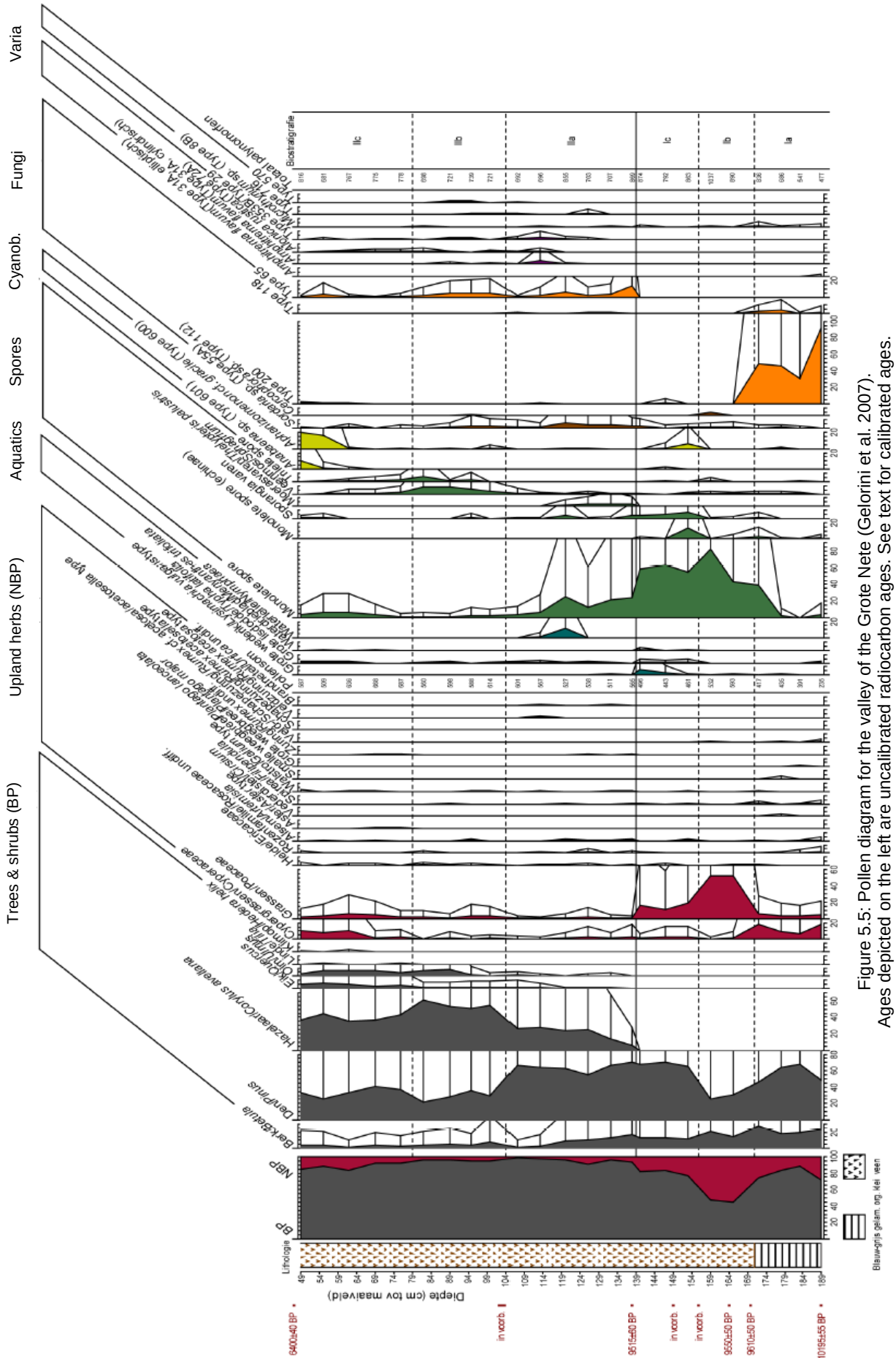

Figure 5.5: Pollen diagram for the valley of the Grote Nete (Gelorini et al. 2007).
Ages depicted on the left are uncalibrated radiocarbon ages. See text for calibrated ages.

b. Sandy region

In the Campine area, the most nearby high resolution peat record is the Grote Nete sequence studied by Gelorini et al. 2007. This record from the Campine Plateau starts 11.9 cal. kyr BP with a phase (Ia) dominated by pine, birch and sedges and frequent observations of fungi (Figure 5.5). The upper part thus correlates with zone ZB 1 (Figure 5.7), with the only difference being the higher abundance of pine in the Grote Nete area. The peat accumulation starts around 11.0 cal. kyr BP, a few hundred years after the Zwarte Beek. Zones Ib and Ic correlate well with ZB 2, with a clear dominance of pine trees and high abundances of ferns and grasses. The strong peak in grasses in Ib is not recorded in the Zwarte Beek and could reflect a local forest opening possibly associated with increased fire activity. Zone IIa, starting at 10.9 cal. kyr BP, is still dominated by *Pinus* (ZB 2) but also hazel becomes now relatively abundant in the pollen diagram: *Corylus* was also present at this time in the Zwarte Beek, but only at very low abundances. From IIb, pine starts to decline and hazel becomes dominant, indicating the start of zone ZB 3. However, this level is not yet dated for the Grote Nete core. Peat mosses expand in this zone in the Grote Nete, which is not the case for the Zwarte Beek. Where in the Zwarte Beek record, the rise of the temperate trees oak, elm and hazel was simultaneously, here a time lag is observed before elm and eventually oak increase. The top of the record is dated at 7.4 cal. kyr BP, roughly corresponding to the transition ZB 4-ZB 5: however, the zone ZB 4 was not detected in the Grote Nete sequence since no *Alnus* pollen were found here. Apparently, an alder carr was only formed later in this area, or maybe not at all.

Also for the Campine area, the general pattern found in the Zwarte Beek area correspond to the vegetation succession reported for the Molse Nete (Gelorini et al. 2008). However, they only used two carbon dates and obtained very young ages (e.g. a typical Late Glacial open birch forest landscape with *Artemisia* and *Thalictrum* dated around 4.7 cal. kyr BP) indicating possible erroneous dating. For the northern Campine area, recently a peat sequence starting from 11.5 cal. kyr BP was investigated (Verbruggen et al. 2019). Here, the transition from an open birch to pine forest (ZB 1 to ZB 2) is more gradual than in the Zwarte Beek area and dated at ca. 11.0 cal. kyr BP. The pine forest persists until 10.2 cal. kyr BP (9.85 cal. kyr BP for ZB 3), but hazel appears already earlier (ca. 10.8 cal. kyr BP) similar the Grote Nete. This could indicate that on the Campine plateau, pine forests are even more open than in the Zwarte Beek region, allowing hazel shrubs to grow in the understory. In the investigated peat sequence of Verbruggen et al. 2019, the establishment of a temperate deciduous woodland (ZB 3) apparently coincides with the formation of an alder carr (ZB 4): the authors highlight that at this level probably a hiatus is situated, related to dry conditions. Therefore the ages of the deciduous woodland and alder carr formation for the Campine plateau remain uncertain.

Verbruggen et al. (unpublished) studied two additional cores from the north of the Campine plateau, showing the co-occurrence of pine and alder around 9.5 cal. kyr BP: in this area a large wet depression was present during the early Holocene, creating suitable conditions for alder carr formation, while pine dominated the dry elevated cover sand ridges for a prolonged period. The differences in timing of *Pinus* and *Alnus* dominance within the Campine region therefore possibly reflects the vicinity of dry and wet grounds respectively rather than the true regional vegetation patterns. Short-term pine peaks can also reflect hydrological changes, since pine pollen float well on water and can be transported into the peat sequence by a close by channel. *Sphagnum* was present in the sequence of Verbruggen et al. (2019) from ca. 10.0 cal. kyr BP and increased from 5.0 cal. kyr BP, confirming the evolution towards increased

importance of peat mosses from the Middle Holocene in the Campine region. At 5.0 cal. kyr BP also the first evidence of grazing activities appeared, which intensified around 2.6 cal. kyr BP when also crop cultivation became important in the Campine area (Verbruggen et al. 2019).

In the Scheldt basin, peat deposition starts later than in the Zwarte Beek valley: for the Scheldt estuary, deposition occurred between 7.0 and 2.0 cal. kyr BP (Deforce 2011). Storme et al. 2017 studied several sequences from the Scheldt basin: here peat deposits occurred from 11.0-4.0 cal. kyr BP. The start of peat formation in the Zwarte Beek valley (11.4 cal. kyr BP) thus predates the onset in the Scheldt basin. In the study of Storme et al. 2017, a pollen zonation for the Scheldt basin was established. An open birch woodland zone was found during the interval 11.7-11.0 cal. kyr BP (SB 2, correlating to ZB 1, Figure 5.7), followed by pine forest zone until 10.6 cal. kyr BP (SB 3). The establishment of the pine forest is well correlated with the Zwarte Beek sequence (11.2 cal. kyr BP, ZB 2), but the replacement by a temperate deciduous woodland occurs earlier in the Scheldt basin (10.6 cal. kyr BP, SB 4) compared to the Zwarte Beek (9.9 cal. kyr BP, ZB 3). The arrival of lime trees in the deciduous woodland and alder in the wetlands was dated at 8.6 cal. kyr BP in the Scheldt basin (SB 5), almost simultaneously to the Zwarte Beek (8.5 cal. kyr BP, ZB 4). In the Scheldt estuary, an alder carr was only established from 7.7 cal. kyr BP (Deforce 2011). Though the regional start of human impact as indicated by opening of the vegetation and cereals only starts at 4.0 cal. kyr BP in the Scheldt region, locally earlier indications of anthropogenic disturbances were reported. At the site of Aard (located within the Scheldt basin) for example this was observed between 7.5 and 7.0 cal. kyr BP, and in combination with elevated fire frequencies it was interpreted as a period with local presence of hunter-gatheres using fire as a strategy when hunting for large herbivores (Crombé 2016). This matches with the elevated fire activities and partial vegetation openings of zone ZB 5. In the cores investigated by Storme et al. 2017, *Secale* and *Fagopyrum* cereals are found starting from the Middle Ages. These pollen types are also found at the top of the Zwarte Beek peat sequence (ZB 6). In the Scheldt basin, peat bog initiated as indicated by *Sphagnum* was reported for the estuary region: here, *Sphagnum* started to increase from 4.2 cal. kyr BP. and was associated with *Calluna* (Ericaceae) and *Myrica gale:* these plants are considered to be possible members of the bog vegetation and the renewed rise of *Corylus*-type pollen (simultaneously with heather and *Sphagnum*) from ZB 4 in the Zwarte Beek could thus represent an elevated signal due to rising values of *Myrica* (due to the identical pollen morphology).

Zuidhoff & Bos 2017 studied the Meuse catchments in the south-eastern Netherlands. They recorded the transition from a birch to a pine forest at 11.2 cal. kyr BP, similar to the ZB 1-ZB 2 transition in Zwarte Beek catchment. The establishment of a temperate deciduous woodland was observed from 8.9 cal. kyr BP, and the alder carr from 7.9 cal. kyr BP, both substantially later than in the Zwarte Beek (ZB 3 at 9.9 and ZB 4 at 8.5 cal. kyr BP respectively). The start of peat growth in this region only started around 8.0 cal. kyr BP, possibly linked to the alder carr vegetation in the wetlands, and stopped around 3.2 cal. kyr BP. Human impact as indicated by cereals became significant from Roman times and no bog development with *Sphagnum* was recorded.

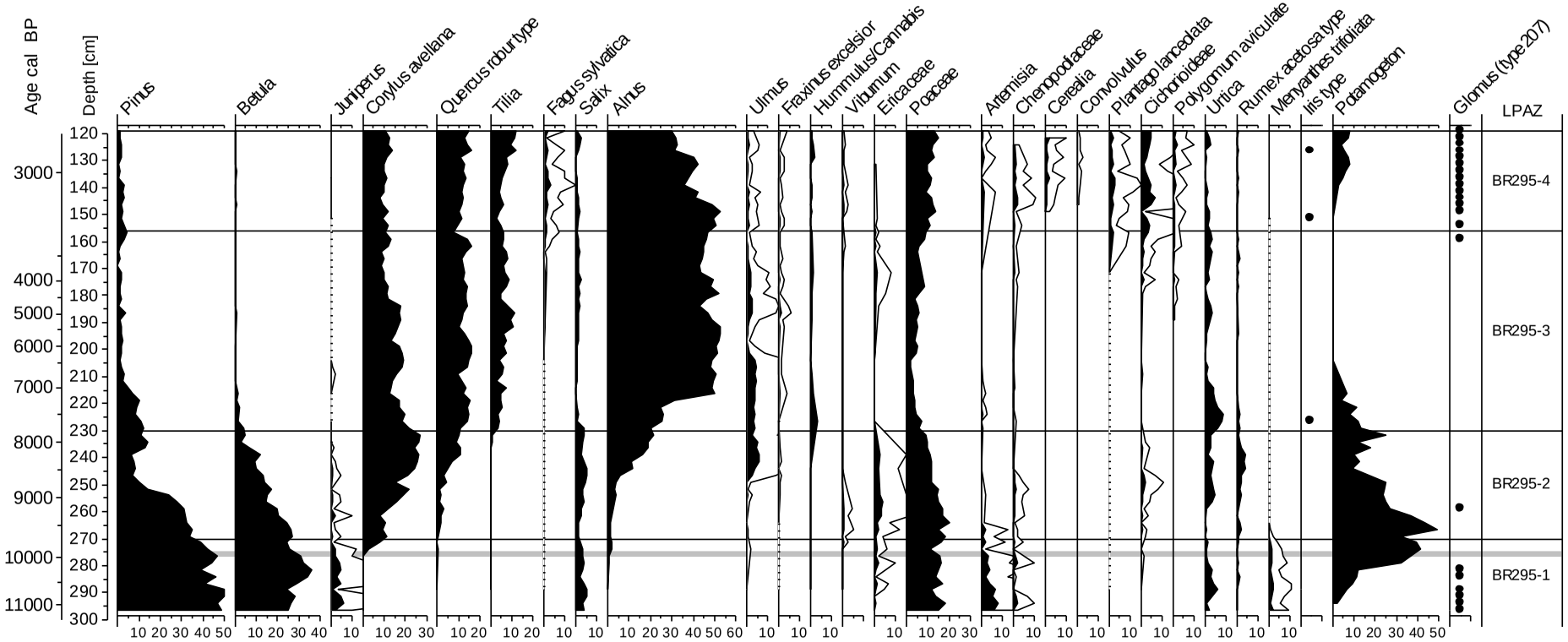

Figure 5.6: Unpublished pollen diagram for the Senne valley (Marinova et al. 2018).

c. Loamy region

Comparison of the vegetation development of the Zwarte Beek with the floodplain reconstructions for the Dijle catchment is impeded due to the absence of a continuous peat record for the last 6500 years, which is the period for which pollen analysis are performed in the Dijle sediments (e.g. Broothaerts 2014b). The reconstructed middle Holocene vegetation largely corresponds to the Zwarte Beek region, being dominated by a deciduous forest (with *Corylus*, *Quercus* and *Tilia*) and with alder carrs occurring in the valleys. For the Senne river, also situated in loamy Flanders, longer pollen records reaching into the Early Holocene are available from excavations in Brussels (Figure 5.6). Here, the first zone (BR 1, 11.0-9.7 cal. kyr BP) is dominated by the pioneer species *Pinus* and *Betula*, and *Juniperus* and *Salix* in lower abundances. Together with high values of Poaceae, this indicates the presence of an Early Holocene open forest, correlating to zone ZB 2 (Figure 5.7). *Betula* was here recorded in the macroremains and interpreted as being part of the wetland vegetation, in contrast to the Zwarte Beek where this was not the case during this time interval. Zone BR 2 (9.7-7.8 cal. kyr BP) represents the establishment of a temperate forest (correlating with ZB 3) and the start of the alder carr from 8.7 cal. kyr BP (correlating with ZB 4). The timing of these transitions is very synchronous for both regions. The following zone BR 3 differs from zone ZB 5: Instead of an *Alnus* decline, the alder carr becomes even more abundant in this zone, and no indications of vegetation opening are recorded, while heather disappears. Also, no peat mosses are observed in the valley of the Senne.

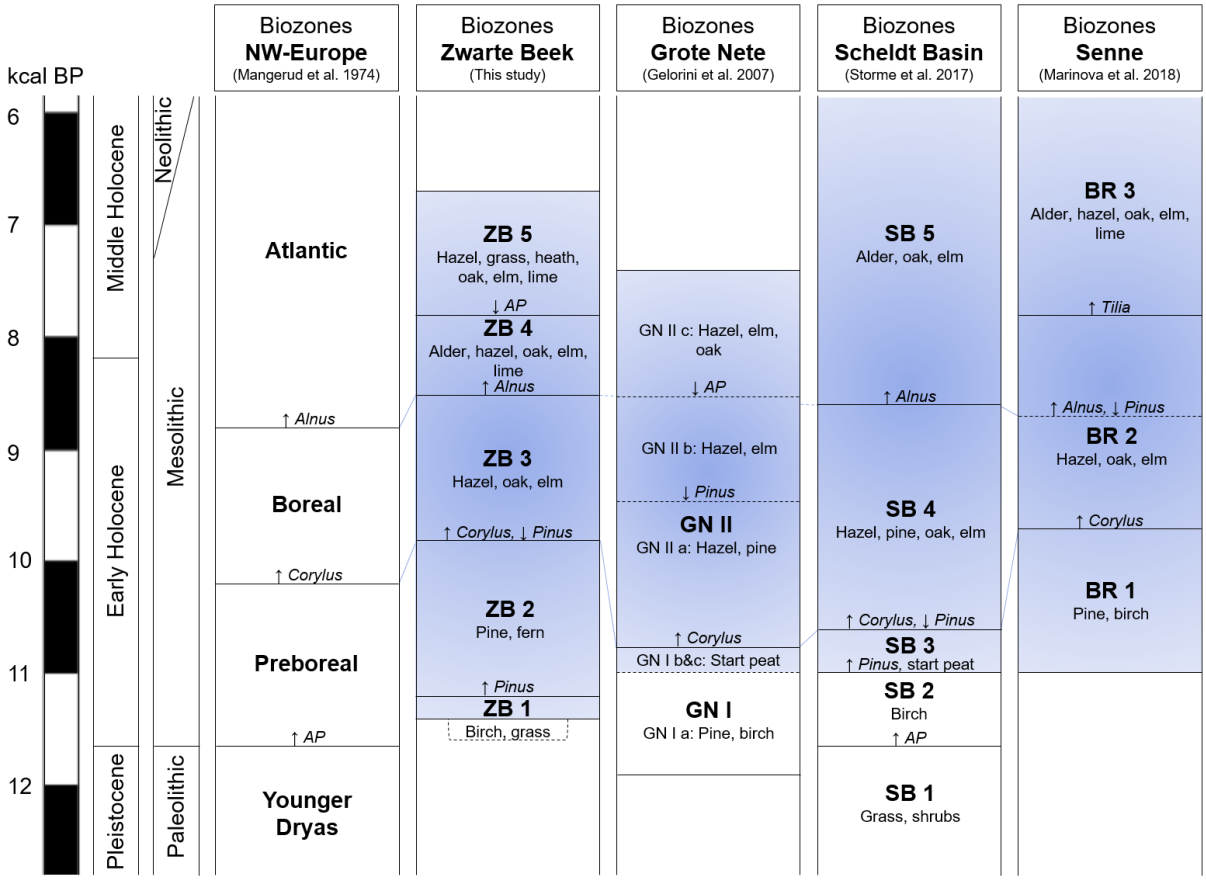

Figure 5.7: Correlation diagram of Early to Middle Holocene vegetation development in Flanders. In blue the time interval with peat deposits is indicated. Arrows indicate increasing/decreasing pollen abundances at biozone boundaries. Light blue lines between the collumns connect the levels where *Corylus* and *Alnus* start to rise.

5.5. Temporal comparison: The Eemian

Unfortunately, no continuous Eemian pollen records are available for Belgium. Therefore, it should be kept in mind that differences between the Eemian and Holocene patterns can be caused both by the temporal and spatial discrepancy. For instance, the records for Germany studied by Aalbersberg & Litt (1998) show in general a strong resemblance to the Zwarte Beek pollen diagram between zones II an IVb (Figure 5.8). However, some differences are observed including an earlier rise of *Quercus* and *Ulmus* and the presence of additional species such as *Taxus* and *Fraxinus*. Comparison of this record to Holocene peat sequences from this region is required to distinguish between temporal and spatial effects.

For the Massif Central, pollen records from several crater lakes were analysed spanning the five last interglacials (Reille et al. 2000). The observed vegetation pattern can be generalized as follows: the interglacial starts with a peak of *Pinus* (correlating to ZB 2), followed by the appearance of *Betula*, *Quercus* and *Corylus* in the mentioned order. The expansion of these trees preludes the arrival of mesophilous trees with the amelioration of the climate, similar as for the Holocene in ZB 3. Next, *Carpinus*, *Abies* and *Fagus* expand (absent in the Zwarte Beek due to peat truncation) and in a last stage *Picea* and *Pinus* are found at the return of cold conditions which has not yet occurred in the Holocene. For northwestern Europe, the hazel expansion is often the earliest of the mesophileous taxa in the current and previous interglacials. This could indicate that this tree could arrive quickly by the dispersion from central European refugia, limiting the travel distance compared to the refugia in southern Europe for most mesophileous trees. The recorded order of temperate tree arrival in this Eemian record is thus rather the consequence of a spatial than a temporal effect.

In the Grande Pile peat bog in the Vosges in France, a continuous peat sequence was analysed for the last 140 kyr (Woillard 1978). For the Eemian interglacial, seven vegetation phases were discriminated: 1) A tundra vegetation with herbs and shrubs of *Betula*, *Salix* and *Juniperus*. This composition corresponds to zone ZB 1. 2) A boreal *Betula-Pinus* forest with presence of *Juniperus* and later *Ulmus*. This phase mostly resembles zone ZB 2, though *Betula* and *Ulmus* were less important during the Holocene in comparison with the Eemian record. 3) The formation of a *Quercetum mixtum* forest. The composition varies from *Quercus-Pinus-Betula-Ulmus-Fraxinus* over *Quercus-Ulmus-Fraxinus* to *Quercus-Ulmus-Fraxinus-Corylus*. This phase corresponds to zone ZB 3, with first a mix of conifers and deciduous trees and later a dominance of oak, elm and hazel. During the Eemian, *Fraxinus* seems to be more abundant and the rise of hazel occurred relatively late. 4) A *Corylus* dominated forest forms, complemented by first a *Quercetum mixtum* vegetation followed by *Quercus* and *Taxus-Quercus-Alnus*. The first half still belongs to zone ZB 3 when comparing it to the Holocene, while the appearance of *Alnus* indicates the start of zone ZB 4. During the Eemian, *Taxus* also became more important in this zone. The following phases in the Grande Pile peat bog are not recorded in the Holocene peats of the Zwarte Beek and consist of a *Carpinus* forest followed by a cold temperate *Abies-Picea* forest and the return of a boreal (*Pinus-Picea-Betula*) forest.

Analysis of sediments from the Lys plain in Northern France revealed the following patterns (Sommé et al. 1996): the bottom of the sequence is dominated by *Corylus* and *Quercus*, while *Alnus* and *Pinus* occur frequently. *Ulmus*, *Hedera* and *Fraxinus* are found in lower abundances. At the top of this zone, pine decreases while *Corylus* remains dominant accompagnied by *Quercus*. This stage is correlated to zone ZB 4, representing the Eemian and Holocene climatic

optimum. It is very similar in both periods, except for *Fraxinus* which is more rare in this zone during the Holocene.

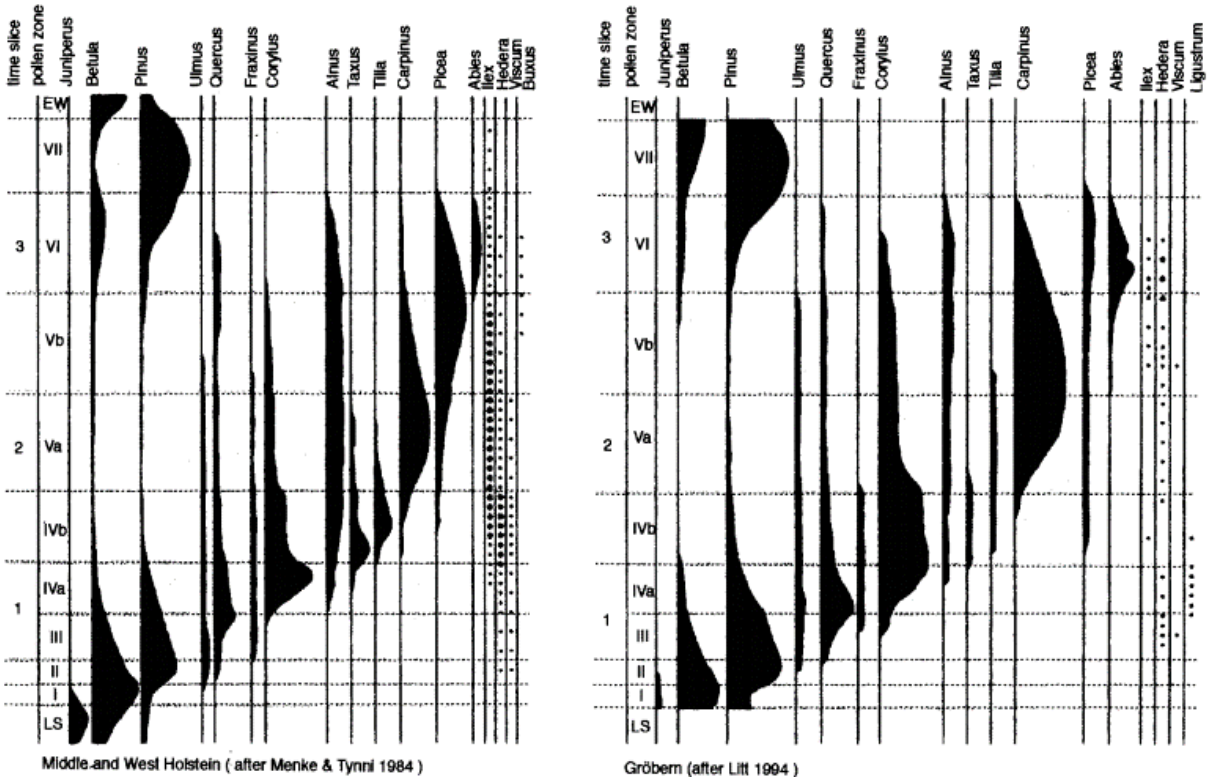

Figure 5.8: Northwest European Eemian vegetation evolution based on continuous pollen sequences from Germany (Aalbersberg & Litt 1998).

The limited temporal resolution and scarcity of detailed Eemian records (containing in most cases tree species only, lacking e.g. heather, *Sphagnum* and charcoal countings) on the one hand and the truncated Zwarte Beek record on the other hand impede the detection of Holocene anthropogenic vegetation disturbances based on their Eemian analogues. Due to the low temporal resolution of the available Eemian records, the occurrence of short term events such as fires is also harder to detect. As mentioned, this analogue approach is only possible when accounting for spatial effects within the natural vegetation development. The persistence of tree taxa is another important factor to be assessed when using previous interglacials as analogues for the current interglacial (Magri 2010) . Especially the last glacial period was reported to be severe with extinction of several tree species as a consequence. The long-term survival of trees can be investigated by long-core records spanning several (inter)glacials. However, these are mostly preserved for southern Europe, where the vegetation composition is markedly different compared to western Europe.

5.6. Final remarks

During the lab procedure, *Lycopodium* tablets were added to the peat samples to allow an absolute quantification of the pollen accumulation values over time. However, in samples ZB 207-ZB 311, no *Lycopodium* grains were observed. In the other samples their observations varied strongly, resulting in unrealistic fluctuations of pollen accumulation rates spanning

several orders of magnitude (Appendix E.1). The first time this lab procedure was performed (bottom samples), the work was stopped before the density separation and water was added to prevent drying of the samples. However, when the lab work was retaken, this water was not removed resulting in lowering of the density of the sodiumpolytungstate. Therefore this step was repeated (addition of heavy liquid & centrifugation), to increase the density of the heavy liquid. Some heavy pollen could have been lost due to this adapted procedure, especially when the tablets were not well dissolved resulting in *Lycopodium* aggregates, possibly explaining the absence of *Lycopodium* in the pollen slides.

The pollen analysis performed in this study confirmed the value of pollen as a proxy to reconstruct ancient vegetation types. The abundant presence of pollen allowed high pollen counts on which statistical analysis could be performed, used to support the visual analyses of the pollen diagrams. The records of pollen taxa were continuous, enabling the assessment of the presence or absence of pollen types, in contrast to the scattered macrofossil data were preservation conditions and coincidence are more important factors. However, also some weaknesses of pollen analysis as a paleo-ecological method were encountered: it is for instance not possible to unambiguously separate pollen taxa reflecting the regional and local vegetation. This was especially problematic for birches, pines, sedges and ferns. The interpretation of the local vegetation was aided by the macroremain data, but this was not able to solve everything due to the incomplete overlap of plant taxa. Though the recorded amount of taxa in the pollen analysis was substantially higher than in the macroremains, the observed diversity remains clearly an underrepresentation of the true plant communities of the past: several factors are responsible for this, including the small paleo-surface which was sampled, low pollen production rates or preservation potential of multiple taxa or the lack of identifiable traits of certain pollen grains.

The reported pollen percentages are an example of 'closed sum' data, reflecting the relative abundances of pollen grains against the total amount of pollen counted. Therefore, especially since the outcome of the *Lycopodium* analysis was not reliable, it is difficult to interpret the observed changes as changes of vegetation cover. For instance, if a pollen type first occurred at low percentages and then rises to higher values, we tend to say that the taxon rises in abundances while it can also reflect a decrease in vegetation cover of the remainder of the vegetation. In addition, in the reported vegetation reconstructions no compensation was applied for differences in production rates, transport capacity and preservation potential since these values also change over time and obtaining reliable factors is therefore very hard. A specific problem which was encountered for the investigated peat core was the discrimination between pine pollen reflecting true nearby pine stands from incoming pine pollen known for their high transport capacity, as a result of wind transport into openings of the vegetation cover. Therefore the focus for the analysis of the pollen diagrams should be on the general trends, since other oscillations might reflect other processes than true changes in the vegetation cover and composition.

The exceptionally thick peat deposits of the Zwarte Beek have proven to be valuable, high resolution archives of the vegetation changes of the Early and Middle Holocene in sandy Flanders. To protect them and secure the ecosystem services that they deliver (e.g. carbon storage), specific measures are required (Maes et al. 2018): especially filling up of the anthropogenic channels and ditches for drainage purposes is crucial to protect the peat deposits from desiccation and maintain further peat accumulations in the future. In addition,

classifying the re-meandering of the Zwarte Beek as a measure to reinstall the natural hydrological situation can be questioned. The geomorphological reconstructions in this study suggest that this is a rather recent phenomenon in this valley, probably linked to severe forest clearings, with a more diffuse channel pattern being the dominant Holocene hydrological situation. The vegetation reconstructions in this study showed a Middle Holocene wetland vegetation composited by patches of alder carr, sedge swamps and peat mosses. This corresponds relatively well with the current situation of the valley (Figure 2.14) except for the current presence of pine plants and cultivated grasslands. The designation by the potential vegetation map (Figure 2.13) of the entire valley as alder carr is too simplistic, since this study showed that the natural vegetation composition of the wetlands is more diverse. For the regional vegetation, the pollen diagrams showed that the contemporary vegetation cover is strongly more opened in comparison to the Middle Holocene situation. The potential vegetation map (Figure 2.13) indicates the entire area as oak forests: this was indeed the dominant vegetation type in the Zwarte Beek area, but also heather and pine are part of the natural Zwarte Beek area vegetation. For nature conservation these findings would imply that the diverse vegetation of the Zwarte Beek valley should be retained while limiting human activities and reinstalling an optimal hydrology for peat accumulation. For the wider region, which is currently dominated by heathland and pine plants (Figure 2.14), a reforestation of major areas with deciduous woodland would be recommended.

6. Conclusion

The investigated peat core from the Zwarte Beek valley had a bottom age of ca.11.4 cal. kyr BP (311 cm) and an age of ca. 6.7 cal. kyr BP at 32 cm. The accumulation rate decreased slowly from bottom to top, with 0.6 mm/year being the average speed. A hiatus was found at the 31-32 cm transition as indicated by the Middle Holocene age underneath the hiatus and the presence of cereals suggesting a Medieval age or younger above the hiatus. We cannot conclude about the exact cause of this missing time interval: both halting of the peat growth at 6.7 cal. kyr BP (32 cm) and removing of the deposited peats in a later stage are possible. For the latter especially peat excavation and break down linked to desiccation are likely contributors.

Based on pollen spectra of the 31 analysed peat samples, combined with a statistical analysis of them using ordination and clustering techniques, a zonation of the vegetation development was proposed: from 11.4 to 11.2 cal. kyr BP (ZB 1) an open landscape dominated by grasses, shrubs and birch trees was reconstructed and interpreted as a remnant of the Late Glacial steppe-tundra vegetation. The local environment was dominated by sedges. Peat growth started early in comparison to other Flemish valley systems, indicating suitable local conditions for peat build-up. Between 11.2 and 9.8 cal. kyr BP (ZB 2) the regional vegetation was dominated by an open conifer forest with pine as main tree type. In the second half of this zone a high fire frequency was observed. In the local vegetation sedges and ferns were encountered. From 9.8 cal. kyr BP (ZB 3) hazel starts to increase rapidly resulting in a pine-hazel forest followed by the formation of a closed temperate deciduous woodland. Hazel, oak and elm become the dominant tree species. In this interval evidence for open water conditions in the valley are found and *Typha* becomes more abundant in the wetland vegetation as well as birches. At 9.8 cal. kyr BP (ZB 4) a strong increase of alder trees is observed, resulting in a local vegetation strongly dominated by alder carrs. In the regional vegetation the temperate forest persists with lime trees as a new member. Pine pollen return in this interval and an increased fire frequency is observed towards the top of this zone. For the interval 7.8-6.7 cal. kyr BP (ZB 5), a partial opening of the temperate forest is observed with increasing values of grasses, heather and pine. Elevated fire frequencies suggest a role for fire in the vegetation opening, possibly anthropogenic in origin as indicated by human indicator pollen types. In the local vegetation several vegetation types co-occur including alder carrs, sedges and peat mosses. Above the hiatus (ZB 6) the regional vegetation becomes really open now, with abundant grasses, heather and birches. Human impact peaks, as indicated by cereal and other human indicator pollen. In the local vegetation, alder carrs and sedges are still important and peat mosses become more abundant.

Additional information about the local Zwarte Beek vegetation was provided by plant macrofossils: this showed the local presence of sedges, peat mosses, birches as well as conifers. Alder was not encountered in this study but was found in the macrofossils studied by Allemeersch (2010) showing that it was growing at some localities in the valley. The analysis of macrocharred particles revealed the occurrence of a major local fire event at 7.3 cal. kyr BP. This could have been linked to the local presence of hunter-gatherers explaining the partial vegetation opening during ZB 5.

Spatial comparison for Flanders showed a large spatial variability in the rise of *Corylus* pollen while the *Alnus* increase was more synchronic. The temporal comparison with the Eemian interglacial showed the need for high detail pollen analyses of Eemian records to allow their use as analogues. This also highlighted the spatial effects of vegetation dynamics.

To further clarify the Holocene vegetation and human impact history of the Zwarte Beek area, additional research will be required: a better temporal framework for nearby archaeological sites could increase the insight in the possible alteration of the Campine vegetation by Mesolithic hunter-gatherers. Dating of additional peat samples from the ZB-101 core could shed light on the age of the peat encountered above the hiatus. Further investigations of the Zwarte Beek peat will also be required to conclude about the cause of the missing Late Holocene peat: if this sequence is derived from the location of a former peat excavation pit, it is expected that on other locations in the valley non-excavated sequences spanning the entire Holocene should be available. If these cannot be found, a disappearing by desiccation or stopping of the peat formation at 6.7 kyr BP is probably more likely. If Late Holocene deposits are encountered, it might be very interesting to study their pollen content, enabling the reconstruction of the entire Holocene vegetation and especially human impact history of the Zwarte Beek area. In this way the spatial comparison of pollen records across Flanders could be completed and the timing of landscape alterations in sandy Flanders could be further clarified.

References

Aalbersberg, G., & Litt, T. (1998). Multiproxy climate reconstructions for the Eemian and Early Weichselian. *Journal of Quaternary Science: Published for the Quaternary Research Association*, *13*(5), 367-390.

Aho, K., Roberts, D. W., & Weaver, T. (2008). Using geometric and non-geometric internal evaluators to compare eight vegetation classification methods. *Journal of Vegetation Science*, *19*(4), 549-562.

Allemeersch, L. (2010). Archeologische en paleo-ecologische evaluatie en waardering van de vallei van de Zwarte Beek (Beringen, provincie Limburg). *Instituut voor Natuur- en Bosonderzoek.*

Anderson, D. E., Anderson, D., Goudie, A., & Parker, A. (2013). *Global environments through the quaternary: exploring evironmental change*. Oxford University Press, USA.

Armstrong, H., & Brasier, M. (2013). *Microfossils*. John Wiley & Sons.

Atkinson, M. D. (1992). Betula pendula Roth (B. verrucosa Ehrh.) and B. pubescens Ehrh. *Journal of Ecology*, *80*(4), 837-870.

Bakels, C. C. (2009). *The Western European loess belt: agrarian history, 5300 BC-AD 1000*. Springer Science & Business Media.

Beerten, K., De Craen, M., & Leterme, B. (2014a). Long-term evolution of the surface environment of the Campine area, northeastern Belgium: first assessment. *Geological Society, London, Special Publications*, *400*, SP400-23.

Beerten, K., Heyvaert, V., Vandenberghe, D., Van nieuland, J., & Bogemans, F. (2017). Revising the Gent Formation: a new lithostratigraphy for Quaternary wind-dominated sand deposits in Belgium. *Geologica Belgica*, *20*(1-2), 95-102.

Beerten, K., Vandersmissen, N., Deforce, K., & Vandenberghe, N. (2014b). Late Quaternary (15 ka to present) development of a sandy landscape in the Mol area, Campine region, north-east Belgium. *Journal of Quaternary Science*, *29*(5), 433-444.

Behre, K. E. (1981). The interpretation of anthropogenic indicators in pollen diagrams. *Pollen et spores*, *23*(2), 225-245.

Bell, M. & J.C. Walker (2005). *Late Quaternary Environmental Change – Physical and Human Perspectives.* Routledge, New York.

Bennett, K. D. (1984). The post-glacial history of Pinus sylvestris in the British Isles. *Quaternary Science Reviews*, *3*(2-3), 133-155.

Beug, H. J. (2004). Leitfaden der Pollenbestimmung für Mitteleuropa und angrenzende Gebiete.Faegri, K., & Iversen, J. (1993). *Bestimmungsschlüssel für die nordwesteuropäische Pollenflora*. Fischer.

Bio, A. M., De Becker, P., De Bie, E., Huybrechts, W., & Wassen, M. (2002). Prediction of plant species distribution in lowland river valleys in Belgium: modelling species response to site conditions. *Biodiversity & Conservation*, *11*(12), 2189-2216.

Blaauw, M. (2010). Methods and code for 'classical'age-modelling of radiocarbon sequences. *quaternary geochronology*, *5*(5), 512-518.

Blarquez, O., & Carcaillet, C. (2010). Fire, fuel composition and resilience threshold in subalpine ecosystem. *PLoS One*, *5*(8), e12480.

Bos, J. A., van Geel, B., Groenewoudt, B. J., & Lauwerier, R. C. M. (2006). Early Holocene environmental change, the presence and disappearance of early Mesolithic habitation near Zutphen (The Netherlands). *Vegetation History and Archaeobotany*, *15*(1), 27-43.

Bos, J. A., Verbruggen, F., Engels, S., & Crombé, P. (2013). The influence of environmental changes on local and regional vegetation patterns at Rieme (NW Belgium): implications for Final Palaeolithic habitation. *Vegetation history and archaeobotany*, *22*(1), 17-38.

Bosplus. (2007). Duurzaam beheer van Kempense naaldbossen. *Beheersfiches, duurzaam beheer van naaldbossen.*

Bragg, O., & Lindsay, R. (2003). *Strategy and action plan for mire and peatland conservation in Central Europe*. Wetlands International.

Briggle, L. W. (1959). *Growing rye* (No. 2145). US Department of Agriculture.

Broothaerts, N., Verstraeten, G., Kasse, C., Bohncke, S., Notebaert, B., & Vandenberghe, J. (2014a). Reconstruction and semi-quantification of human impact in the Dijle catchment, central Belgium: a palynological and statistical approach. *Quaternary Science Reviews*, *102*, 96-110.

Broothaerts, N., Verstraeten, G., Kasse, C., Bohncke, S., Notebaert, B., & Vandenberghe, J. (2014b). From natural to human-dominated floodplain geoecology–a Holocene perspective for the Dijle catchment, Belgium. *Anthropocene*, *8*, 46-58.

Broothaerts, N., Notebaert, B., Verstraeten, G., Kasse, C., Bohncke, S., & Vandenberghe, J. (2014c). Non-uniform and diachronous Holocene floodplain evolution: a case study from the Dijle catchment, Belgium. *Journal of Quaternary Science*, *29*(4), 351-360.

Broothaerts, N., Verstraeten, G., Notebaert, B., Assendelft, R., Kasse, C., Bohncke, S., & Vandenberghe, J. (2013). Sensitivity of floodplain geoecology to human impact: a Holocene perspective for the headwaters of the Dijle catchment, central Belgium. *The Holocene*, *23*(10), 1403-1414.

Brown, A. G. (1988). The palaeoecology of Alnus (alder) and the Postglacial history of floodplain vegetation. Pollen percentage and influx data from the West Midlands, United Kingdom. *New Phytologist*, *110*(3), 425-436.

Burke, K. D., Williams, J. W., Chandler, M. A., Haywood, A. M., Lunt, D. J., & Otto-Bliesner, B. L. (2018). Pliocene and Eocene provide best analogs for near-future climates. *Proceedings of the National Academy of Sciences*, 201809600.

Burny, J. (1999). *Bijdrage tot de historische ecologie van de Limburgse Kempen (1910-1950): tweehonderd gesprekken samengevat*. Roermond: Natuurhistorisch Genootschap in Limburg.

Campbell, C. G. (1997). *Buckwheat: Fagopyrum esculentum Moench* (Vol. 19). Bioversity International.

Cohen, K. M., Finney, S. C., Gibbard, P. L., & Fan, J. X. (2013). The ICS international chronostratigraphic chart. *Episodes*, *36*(3), 199-204.

Crombé, P. (2016). Forest fire dynamics during the early and middle Holocene along the southern North Sea basin as shown by charcoal evidence from burnt ant nests. *Vegetation History and Archaeobotany*, *25*(4), 311-321.

Crombé, P., Sergant, J., & Perdaen, Y. (2009). The neolithisation of the Belgian lowlands: new evidence from the Scheldt Valley. In *Mesolithic Horizons. Papers presented at the Seventh International Conference on the Mesolithic in Europe, Belfast 2005* (pp. 564-569). Oxbow Books.

De Becker, P. (2009). Natuurinrichtingsproject Vallei van de Zwarte Beek (Koersel-Beringen Limburg). Streefbeeldendiscussie, advies INBO.A.2099.4

De Becker, P., & Huybrechts, W. (2000). Vallei van de Zwarte Beek–Ecohydrologische Atlas. *Institute of Nature Conservation, Brussels, Belgium*.

Deacon, J. (1974). The location of refugia of Corylus avellana L. during the Weichselian glaciation. *New Phytologist*, *73*(5), 1055-1063.

Deforce, K. (2008). Pollen en sporen. *Onderzoeksbalans Onroerend Erfgoed Vlaanderen*.

Deforce, K. (2011). Middle and late Holocene vegetation and landscape evolution of the Scheldt estuary: a palynological study of a peat deposit from Doel (Belgium). *Geologica Belgica*, *14*(3-4), 277-288.

Derese, C., Vandenberghe, D. A. G., Van Gils, M., Mees, F., & Paulissen, E. (2012). Final Palaeolithic settlements of the Campine region (NE Belgium) in their environmental context: optical age constraints. *Quaternary international*, *251*, 7-21.

Dixon, P. (2003). VEGAN, a package of R functions for community ecology. *Journal of Vegetation Science*, *14*(6), 927-930.

Douda, J., Doudová, J., Drašnarová, A., Kuneš, P., Hadincová, V., Krak, K., & Mandák, B. (2014). Migration patterns of subgenus Alnus in Europe since the Last Glacial Maximum: a systematic review. *PLoS One*, *9*(2), e88709.

DOV. (2018). DOV Verkenner. Retrieved from www.dov.vlaanderen.be

Dusar, M. & Lagrou, D., (2007). Cretaceous flooding of the Brabant Massif and the lithostratigraphic characteristics of its chalk cover in northern Belgium. Geologica Belgica, 10/1-2: 27-38.

Faegri, K., & Iversen, J. (1989). *Textbook of pollen analysis*. Blackburn press.

Gelorini, V., Meersschaert, L., Bats, M., Caljon, L., Boudin, M., Van Strydonck, M., & Crombé, P. (2008). Laatneolithische landschappelijke ontwikkeling van de vallei van de Molse Nete (Lommel, Limburg, B). *NOTAE PRAEHISTORICAE*, *28*, 113-124.

Gelorini, V., Meersschaert, L., Boudin, M., Van Strydonck, M., Thoen, E., & Crombé, P. (2007). Vroeg-en middenholocene vegetatie-ontwikkeling en preboreale klimatologische oscillatie in de vallei van de Grote Nete (Hechtel-Eksel, Limburg). *Notae Praehistoricae*, *27*, 5-17.

Gelorini, V., Meersschaert, L., Verleyen, E., & Verbruggen, C. (2006). Paleo-ecologisch onderzoek van een Holocene sequentie uit het Deurganckdok te Doel (Wase Scheldepolders, Noord-België). *Belgeo. Revue belge de géographie*, (3), 243-264.

Gibling, M. (2018). River Systems and the Anthropocene: A Late Pleistocene and Holocene Timeline for Human Influence. *Quaternary*, *1*(3), 21.

Goudie, A. S. (2018). *Human impact on the natural environment*. John Wiley & Sons.

Grace, J. B. (1989). Effects of water depth on Typha latifolia and Typha domingensis. *American Journal of Botany*, *76*(5), 762-768.

Grimm, E. C. (1987). CONISS: a FORTRAN 77 program for stratigraphically constrained cluster analysis by the method of incremental sum of squares. *Computers & geosciences*, *13*(1), 13-35.

Guiot, J., Pons, A., de Beaulieu, J. L., & Reille, M. (1989). A 140,000-year continental climate reconstruction from two European pollen records. *Nature*, *338*(6213), 309.

Gullentops, F., Bogemans, F., De Moor, G. (2001). Quaternary lithostratigraphic units (Belgium). *Geologica Belgica 4: 153–164.*

Hill, M. O., Mountford, J. O., Roy, D. B., & Bunce, R. G. H. (1999). *Ellenberg's indicator values for British plants. ECOFACT Volume 2 Technical Annex* (Vol. 2). Institute of Terrestrial Ecology.

Holden, J. (Ed.). (2017). *An introduction to physical geography and the environment*. Pearson Education.

Houben, P., Schmidt, M., Mauz, B., Stobbe, A., & Lang, A. (2013). Asynchronous Holocene colluvial and alluvial aggradation: A matter of hydrosedimentary connectivity. *The Holocene*, *23*(4), 544-555.

Hudson, P. F., Middelkoop, H., & Stouthamer, E. (2008). Flood management along the Lower Mississippi and Rhine Rivers (The Netherlands) and the continuum of geomorphic adjustment. *Geomorphology*, *101*(1-2), 209-236.

Huybrechts, W. (1999). Post-pleniglacial floodplain sediments in Central Belgium. *Geologica Belgica (Belgium)*.

INBO. (2015). Vallei- en brongebied van de Zwarte Beek, Bolisserbeek en Dommel met heide en vengebieden. Retrieved from http://natura2000.eea.europa.eu/Natura2000/SDF.aspx?site=BE2200029

IUSS Working Group Wrb. (2015). World Reference Base for Soil Resources 2014, update 2015 International soil classification system for naming soils and creating legends for soil maps. *World Soil Resources Reports No. 106*, 192.

Iversen, J. (1958). The bearing of glacial and interglacial epochs on the formation and extinction of plant taxa. Uppsala Universiteit Arsskrift, 6, 210-215.

Janssens, W., & Ferguson, D. K. (1985). The palaeoecology of the Holocene sediments at Kallo, Northern Belgium. *Review of Palaeobotany and Palynology*, *46*(1-2), 81-95.Joosten, J. H. J. (1985). A 130 year micro-and macrofossil record from regeneration peat in former peasant peat pits in the Peel, The Netherlands: a palaeoecological study with agricultural and climatological implications. *Palaeogeography, palaeoclimatology, palaeoecology*, *49*(3-4), 277-312.

Joosten, H., & Clarke, D. (2002). Wise use of mires and peatlands. *International Mire Conservation Group and International Peat Society*, *304*.

Juggins, S. (2007). C2: Software for ecological and palaeoecological data analysis and visualisation (user guide version 1.5). *Newcastle upon Tyne: Newcastle University*, *77*.

Kaplan, J. O., Pfeiffer, M., Kolen, J. C., & Davis, B. A. (2016). Large scale anthropogenic reduction of forest cover in Last Glacial Maximum Europe. *PLoS One*, *11*(11), e0166726.

Kondolf, G. M. (1997). PROFILE: hungry water: effects of dams and gravel mining on river channels. *Environmental management*, *21*(4), 533-551.

Kull, O., & Niinemets, Ü. (1998). Distribution of leaf photosynthetic properties in tree canopies: comparison of species with different shade tolerance. *Functional Ecology*, *12*(3), 472-479.

Leenders, K. (1989). *Verdwenen venen : Een onderzoek naar de ligging en exploitatie van thans verdwenen venen in het gebied tussen Antwerpen, Turnhout, Geertruidenberg en Willemstad 1250-1750* (Pro Civitate. Historische uitgaven. Reeks in-8° 78). Brussel: Gemeentekrediet van België.

Maes D., De Becker P., Denys L., Packet J. & De Keersmaeker L. (2018). PAS-Gebiedsanalyse in het kader van herstelmaatregelen voor BE2200029 Vallei- en brongebieden van de Zwarte Beek, Bolisserbeek en Dommel met heide en vengebieden. Rapporten van het Instituut voor Natuur- en Bosonderzoek 2018 (17). Instituut voor Natuur- en Bosonderzoek, Brussel.

Magri, D. (2010). Persistence of tree taxa in Europe and Quaternary climate changes. *Quaternary International*, *219*(1-2), 145-151.

Mangerud, J. A. N., Andersen, S. T., Berglund, B. E., & Donner, J. J. (1974). Quaternary stratigraphy of Norden, a proposal for terminology and classification. *Boreas*, *3*(3), 109-126.

Marinova, E., Devos, Y., Speleers, L., Augustijns, F., Hautekiet, S., Vrydaghs, L., & Modrie, S. (2018). Multi-proxy analysis of a peat deposit from Brussels (Belgium): a case study for the Holocene evolution of the landscape in the Senne valley.

Mauri, A., Davis, B. A. S., Collins, P. M., & Kaplan, J. O. (2015). The climate of Europe during the Holocene: a gridded pollen-based reconstruction and its multi-proxy evaluation. *Quaternary Science Reviews*, *112*, 109-127.

Meylemans, E., Bastiaens, J., Boudin, M., Deforce, K., Ervynck, A., Perdaen, Y. & Crombé, P. (2018). The oldest cereals in the coversand area along the North Sea coast of NW Europe, between ca. 4800 and 3500 cal BC, at the wetland site of 'Bazel-Sluis'(Belgium). *Journal of Anthropological Archaeology*, *49*, 1-7.

Mooney, S. D., & Tinner, W. (2011). The analysis of charcoal in peat and organic sediments. *Mires and Peat*, *7*(9), 1-18.

Moore, P. D., Webb, J. A., & Collison, M. E. (1991). *Pollen analysis*. Blackwell scientific publications.

Notebaert, B., Houbrechts, G., Verstraeten, G., Broothaerts, N., Haeckx, J., Reynders, M., & Poesen, J. (2011a). Fluvial architecture of Belgian river systems in contrasting environments: implications for reconstructing the sedimentation history. *Netherlands Journal of Geosciences*, *90*(1), 31-50.

Notebaert, B., Verstraeten, G., Vandenberghe, D., Marinova, E., Poesen, J., & Govers, G. (2011b). Changing hillslope and fluvial Holocene sediment dynamics in a Belgian loess catchment. *Journal of Quaternary Science*, *26*(1), 44-58.

Oldfield, F., & Dearing, J. A. (2003). The role of human activities in past environmental change. In *Paleoclimate, global change and the future* (pp. 143-162). Springer, Berlin, Heidelberg.

Parducci, L., Väliranta, M., Salonen, J. S., Ronkainen, T., Matetovici, I., Fontana, S. L., & Suyama, Y. (2015). Proxy comparison in ancient peat sediments: pollen, macrofossil and plant DNA. *Phil. Trans. R. Soc. B*, *370*(1660), 20130382.

Philben, M., Kaiser, K., & Benner, R. (2014). Does oxygen exposure time control the extent of organic matter decomposition in peatlands?. *Journal of Geophysical Research: Biogeosciences*, *119*(5), 897-909.

Power, M. J., Marlon, J., Ortiz, N., Bartlein, P. J., Harrison, S. P., Mayle, F. E., & Mooney, S. (2008). Changes in fire regimes since the Last Glacial Maximum: an assessment based on a global synthesis and analysis of charcoal data. *Climate dynamics*, *30*(7-8), 887-907.

Punt, W., Blackmore, S., Hoen, P. P., & Stafford, P. J. (Eds.). (2003). *The northwest European pollen flora* (Vol. 121). Elsevier.

Reille, M., Beaulieu, J. L. D., Svobodova, H., Andrieu-Ponel, V., & Goeury, C. (2000). Pollen analytical biostratigraphy of the last five climatic cycles from a long continental sequence from the Velay region (Massif Central, France). *Journal of Quaternary Science: Published for the Quaternary Research Association*, *15*(7), 665-685.

Rogiers, B., Lermytte, J., Els, D. E., & Batelaan, O. (2011). Evaluating the impact of river restoration on the local groundwater and ecological system: a case study in NE Flanders. *Geologica Belgica*.

Ronch, F., Caudullo, G., Tinner, W., & de Rigo, D. (2016). Larix decidua and other larches in Europe: distribution, habitat, usage and threats.

Rydin, H., & Jeglum, J. (2013). *The Biology of Peatlands. Second Edition.* Oxford University Press, Oxford.

Scherps, E. (2019). Reconstrueren van Holocene Branden in de Vallei van de Zwarte Beek (Vlaanderen).Seppä, H. (2013). Pollen analysis, principles. *Encyclopedia of Quaternary Science. Edited by SA Elias and CJ Mock. Elsevier, Edinburgh, UK*, 794-804.

Seppä, H., Alenius, T., Muukkonen, P., Giesecke, T., Miller, P. A., & Ojala, A. E. (2009). Calibrated pollen accumulation rates as a basis for quantitative tree biomass reconstructions. *The Holocene*, *19*(2), 209-220.

Sergant, J., Crombé, P., & Perdaen, Y. (2009). Mesolithic territories and land-use systems in north-western Belgium. In *Mesolithic Horizons. Papers presented at the Seventh International Conference on the Mesolithic in Europe, Belfast 2005* (pp. 277-281). Oxbow Books.

Slechten, K. (2004). Namen noemen: het CAI-thesaurusproject. *CAI-rapport I, IAP-Rapporten*, *14*, 49-54.

Sleutel, S., Moeskops, B., Huybrechts, W., Vandenbossche, A., Salomez, J., De Bolle, S., & De Neve, S. (2008). Modeling soil moisture effects on net nitrogen mineralization in loamy wetland soils. *Wetlands*, *28*(3), 724-734.

Sommé, J., Munaut, A. V., Puisségur, J. J., Cunat-Bogé, N., Heyvaert, F., & Leplat, J. (1996). L'Eemien sous les formations fluvatiles Weichseliennes et holocènes du sondage d'Erquinghem (Nord de la France) dans la plaine de la Lys. *Quaternaire*, *7*(1), 15-28.

Storme, A., Louwye, S., Crombé, P., & Deforce, K. (2017). Postglacial evolution of vegetation and environment in the Scheldt Basin (northern Belgium). *Vegetation History and Archaeobotany*, *26*(3), 293-311.

Strack, M. (Ed.). (2008). *Peatlands and climate change*. IPS, International Peat Society.

Sugita, S. (2007a). Theory of quantitative reconstruction of vegetation I: pollen from large sites REVEALS regional vegetation composition. *The Holocene*, *17*(2), 229-241.

Sugita, S. (2007b). Theory of quantitative reconstruction of vegetation II: all you need is LOVE. *The Holocene*, *17*(2), 243-257.

Tinner, W., Hubschmid, P., Wehrli, M., Ammann, B., & Conedera, M. (1999). Long-term forest fire ecology and dynamics in southern Switzerland. *Journal of Ecology*, *87*(2), 273-289.

Trondman, A. K., Gaillard, M. J., Mazier, F., Sugita, S., Fyfe, R., Nielsen, A. B., & Björkman, L. (2015). Pollen-based quantitative reconstructions of Holocene regional vegetation cover (plant-functional types and land-cover types) in Europe suitable for climate modelling. *Global change biology*, *21*(2), 676-697.

Tschudy, R.H., & Scott, R.A. (Ed). (1969). *Aspects of Palynology*. Wiley-Interscience, New York.

Van der Meijden, R. (2005). *Heukels flora van nederland 23e druk*. Wolters-Noordhoff.

Van der Valk, A. (2012). *The biology of freshwater wetlands*. Oxford University Press.

Van Geel, B. (1978). A palaeoecological study of Holocene peat bog sections in Germany and the Netherlands, based on the analysis of pollen, spores and macro-and microscopic remains of fungi, algae, cormophytes and animals. *Review of Palaeobotany and Palynology*, *25*(1), 1-120.

Vanacker, V., Bellin, N., Molina, A., & Kubik, P. W. (2014). Erosion regulation as a function of human disturbances to vegetation cover: a conceptual model. *Landscape ecology*, *29*(2), 293-309.

Vanacker, V., Govers, G., Van Peer, P., Verbeek, C., Desmet Jr, J., & Reyniers, J. (2001). Using Monte Carlo simulation for the environmental analysis of small archaeologic datasets, with the Mesolithic in Northeast Belgium as a case study. *Journal of Archaeological Science*, *28*(6), 661-669.

Vandenberghe, N. (1978). *Sedimentology of the Boom Clay (Rupelian) in Belgium* (Verhandelingen van de Koninklijke academie voor wetenschappen, letteren en schone kunsten van België. Klasse der wetenschappen 147). Brussel: Koninklijke academie voor wetenschappen, letteren en schone kunsten van België.

Vandenberghe, N., Laga, P., Steurbaut, E., Hardenbol, J., & Vail, P. R. (1998). Tertiary Sequence Stratigraphy at the Souther Border of the North Sea Basin in Belgium.

Vanmontfort, B. (2008). Forager–farmer connections in an 'unoccupied'land: First contact on the western edge of LBK territory. *Journal of Anthropological Archaeology*, *27*(2), 149-160.

Verbruggen, F., Bourgeois, I., Cruz, F., Boudin, M., & Crombé, P. (2019). Holocene vegetation dynamics in the Campine coversand area (Liereman, N Belgium) in relation to its human occupation. *Review of Palaeobotany and Palynology*, *260*, 27-37.

Verdurmen, I. & Tys, D. (2007). Centrale Archeologische Inventaris (CAI) III De archeologische waarde van militaire domeinen. VIOE-rapporten 03.

Vermeersch, P. M. (2008). La transition Ahrensbourgien-Mésolithique ancien en Campine belge et dans le sud sableux des Pays-Bas. *P. Fagnart, A. Thévenin, T. Ducrocq, B. Souffi, P.*

Coudrec (red.), Le début du Mésolithique en Europe du Nord-Ouest, Mémorie XLV de la Societé préhistorique française, 11-29.

Vermeersch, P. M. (2011). The human occupation of the Benelux during the Younger Dryas. *Quaternary international*, *242*(2), 267-276.

Verstraeten, G., Broothaerts, N., Van Loo, M., Notebaert, B., D'Haen, K., Dusar, B., & De Brue, H. (2017). Variability in fluvial geomorphic response to anthropogenic disturbance. *Geomorphology*, *294*, 20-39.

Vervacke, L. (2019). Reconstructing Holocene changes in floodplain ecology based on plant macrofossils - a case study of the Zwarte Beek Valley, Belgium.

Wildi, O. (2017). *Data analysis in vegetation ecology*. CABI.

Woillard, G. M. (1978). Grande Pile peat bog: a continuous pollen record for the last 140,000 years. *Quaternary Research*, *9*(1), 1-21.

Zuidhoff, F. S., & Bos, J. A. (2017). Sedimentation and vegetation history of a buried Meuse terrace during the Holocene in relation to the human occupation history (Limburg, the Netherlands). *Netherlands Journal of Geosciences*, *96*(2), 131-163.

Zuur, A., Ieno, E. N., & Smith, G. M. (2007). *Analyzing ecological data*. Springer Science & Business Media.

Appendix

Appendix A

Table A.1: Drillings ZB1 1-8-2018: Transect 1. Numbers refer to the order of drilling, ranking in the table is according to the order along the transect. Adm=admixture, (+)+=(very)abundant, +/-=medium, -=limited.

Dril-ling	Depth (cm)	Texture	Colour	Organic material
1	0-8	Peat, crumbly, adm. sand	Dark brown	+/- Roots
	8-85	Peat	Black	+ Roots/wood/sedges
	85-105	Sand: medium	Gray	- Roots
	105	White gravel (sample)	White	/
2	0-9	Peat, crumbly, adm. sand	Dark brown	+/- Roots
	9-208	Peat	Black	++ Roots / wood
	208-215	Transition peat-sand	Brown price	- Roots
	215-238	Sand	Bluish	- Roots
11	0-15	Peat, crumbly, adm. sand	Dark brown	+/- Roots
	15-270	Peat	Black	++ Roots / wood
	270-277	Sand	Bluish	- Roots
3	0-6	Peat, crumbly, adm. sand	Dark brown	+/- Roots
	6-295	Peat (sharp border to sand)	Black	++ Roots / wood
	295-326	Sand	Bluish	- Roots
4	0-9	Peat, crumbly, adm. sand	Dark brown	+/- Roots
	9-34	Peat, dryer	Dark brown	+ Roots
	34-328	Peat	Black	++ Roots / wood
	328-343	Sand	Bluish	- Roots
10	0-20	Peat, crumbly, adm. sand	Dark brown	+/- Roots
	20-44	Peat	Black	+/- Roots
	44-258	Peat	Black	++ Wood / other pl.
	258-270	Sand	Gray	-Roots
9	0-14	Peat, crumbly, adm. sand	Dark brown	+/- Roots
	14-50	Peat	Black	+/- Roots
	50-241	Peat	Black	++ Wood / other pl.
	241-256	Sand	Bluish	-Roots
5	0-4	Peat, crumbly, adm. sand	Dark brown	+/- Roots
	4-49	Peat	Black	+/- Roots
	49-225	Peat	Black	++ Wood / other pl.
	225-231	Transition: sandy loam	Brown price	-Roots
	231-238	Sand	Bluish	-Roots
6	0-27	Peat, crumbly, adm. sand	Dark brown	+/- Roots
	27-53	Peat	Black	+/- Roots
	53-156	Peat	Black	++ Wood / other pl.
	156-159	Loamy sand	Brown-gray	-Roots
	159-161	Peat	Black	++ Wood / other pl.
	161-167	Loamy sand	Brown-gray	-Roots
	167-179	Peat	Black	++ Wood / other pl.
	179-191	Loamy sand	Brown price	-Roots

	191-200	Sand	Blue	-Roots
7	0-20	Peat, crumbly, adm. sand	Dark brown	+/- Roots
	20-32	Peaty, adm. sand	Light Black	+/- Roots / wood
	32-62	Peaty	Dark black	+/- Roots / wood
	62-80	Sand: medium	Gray	-Roots
8	0-7	OM and fine sand	Dark brown	+/-Roots
	7-14	Very fine sand	Gray	/
	14-20	Very fine sand	Light brown	/
	20-42	Very fine sand	Gray brown	/
	42-83	Very fine sand	Light brown	/
	83-134	Fine sand	Yellow green	/
	134-136	Gravel (sample)	White grey	/
	136-156	Sand, clumped together	Bluish to blue	/

Table A.2: Drillings ZB 2 2-8-2018: Transect 2. Adm=admixture, (+)+=(very)abundant, +/-=medium, -=limited.

Dril-ling	**Depth (cm)**	**Texture**	**Colour**	**Organic material**
9	0-26	Loamy org. rich, adm. sand	Brown	+/-OM
	26-35	Peat	Black	+OM
	35-47	Sand	Yellow-white	-OM
8	0-12	Loamy org. rich, adm. sand	Brown	+/-OM
	12-53	Peat	Black	+OM
	53-57	Unknown	Red	-OM
	57-68	Alternation peat/sand	Variable	+/-OM
	68-80	Medium sand	Gray	-OM
7	0-10	Loamy org. rich, adm. sand	Brown	+/-OM
	10-72	Peat	Black	+/- Roots/wood
	72-83	Medium sand	Gray	-OM
6	0-13	Loamy org. rich, adm. sand	Brown	+/-OM
	13-117	Peat	Black	+OM
	117-130	Transition	Gray-brown	+/-OM
	130-141	Coarse sand	Bluish	-OM
5	0-130	Peat	Black	+ wood
	130-144	Transition	Gray	+/-OM
	144-167	Fine sand	Blue-gray	-OM
1	0-44	Loamy org. rich, adm. sand	Brown rusty	+/- OM
	44-60	Transition to peat	Dark brown	+ OM
	60-129	Peat	Black	++OM +/- Roots/wood
	129-144	(Sandy) loam, transition	Gray-yellow	-OM
	144-156	Very fine sand	Bluish	-OM
2	0-63	Loamy org. rich, adm. sand	Brown	+/- OM
	63-77	Transition to peat	Dark brown	+OM
	77-103	Peat	Black	+OM
	103-160	Peat-gyttja, lime-beds	Variable	+OM
	160-190	Peat	Black	+OM
	190-202	Fine sand	Gray	-OM

	202-210	Gyttja	Variable	+OM
	210-224	Coarse sand	Bluish	-OM
3	0-190	Peat (gyttja at 150)	Black	+/- Roots
	190-227	Gyttja with hard concretions	Variable	+OM
	227-239	Peat	Black	+OM
	239-249	Coarse sand	Blue-gray	-OM
4	0-214	Peat	Black	+OM
	214-233	Coarse sand	Bluish	-OM
12	0-53	Peat	Black	+OM
11	0-24	Peat	Black	+/- Roots/wood
	24-44	Medium sand	Gray	-OM
10	0-37	Peat	Black	+OM
	37-51	Medium sand	Blue	-OM

Table A.3: Collected core ZB-100 at Transect 1 (3-8-2018).

Part	Depth (cm)	Sub-parts	Remarks
1	0-100	0-28/28-77/77-100	
2	100-196	100-106/109-155/155-172/172-196	106-109 lost, 172-196 disturbed
3	196-296	196-270/270-296	
4	296-335	296-335	Sand from 323

Table A.4: Collected core ZB-101 (selected sequence) at Transect 1 (3-8-2018).

Part	Depth (cm)	Sub-parts	Remarks
1	0-100	0-28/28-74/74-100	70-75 wood, 74-84 disturbed
2	100-211	100-148/160-211	148-160 lost, 160-170 disturbed
3	211-314	211-251/251-314	211-251 disturbed

Table A.5: Overview of the laboratory analyses during the first semester.

Date	Samples	Remarks
22-25 Oct.	**311, 303, 295, 287, 279, 263, 255, 207, 199**	Adapted heavy liquid density
13-15 Nov.	**191, 183, 175, 143, 127, 111, 103, 87, 71**	71, 127: woody
5-7 Dec.	**170, 119, 92, 63, 59, 55, 47, 39, 35, 31, 23, 15, 7**	7, 15, 23: sandy

Appendix B

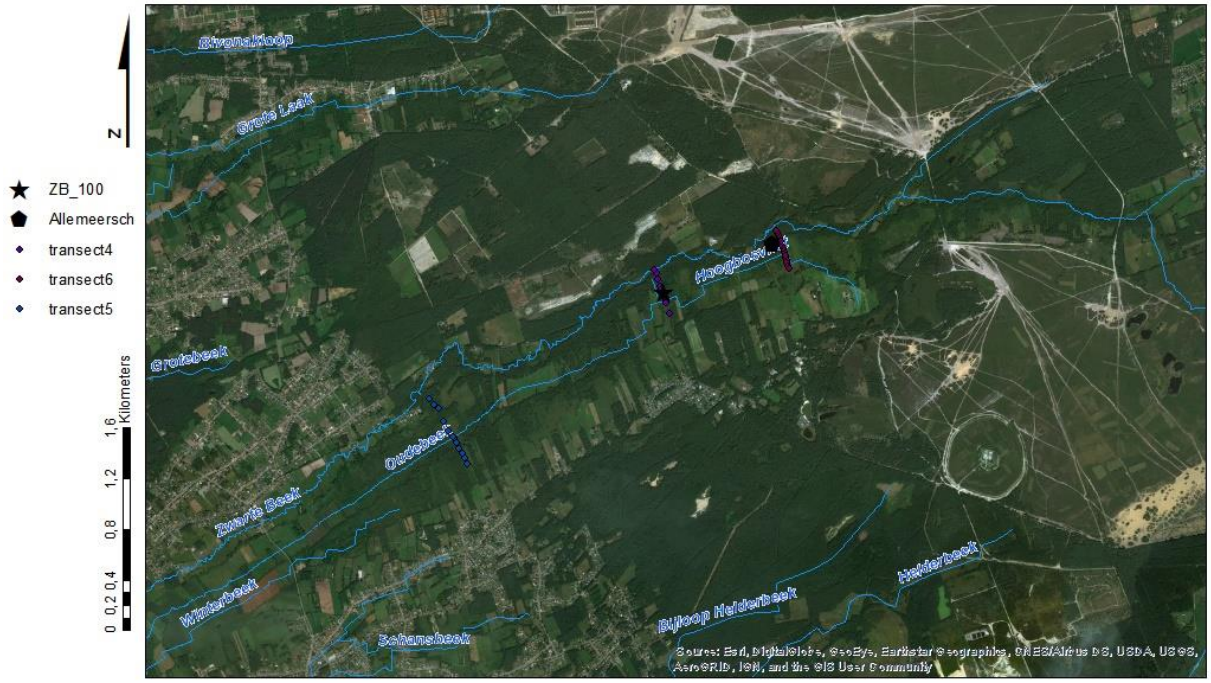

Figure B.1: Satellite imagery map of the upper Zwarte Beek valley with indication of the two transects made in this study and the location of the core studied by Allemeersch (2010).

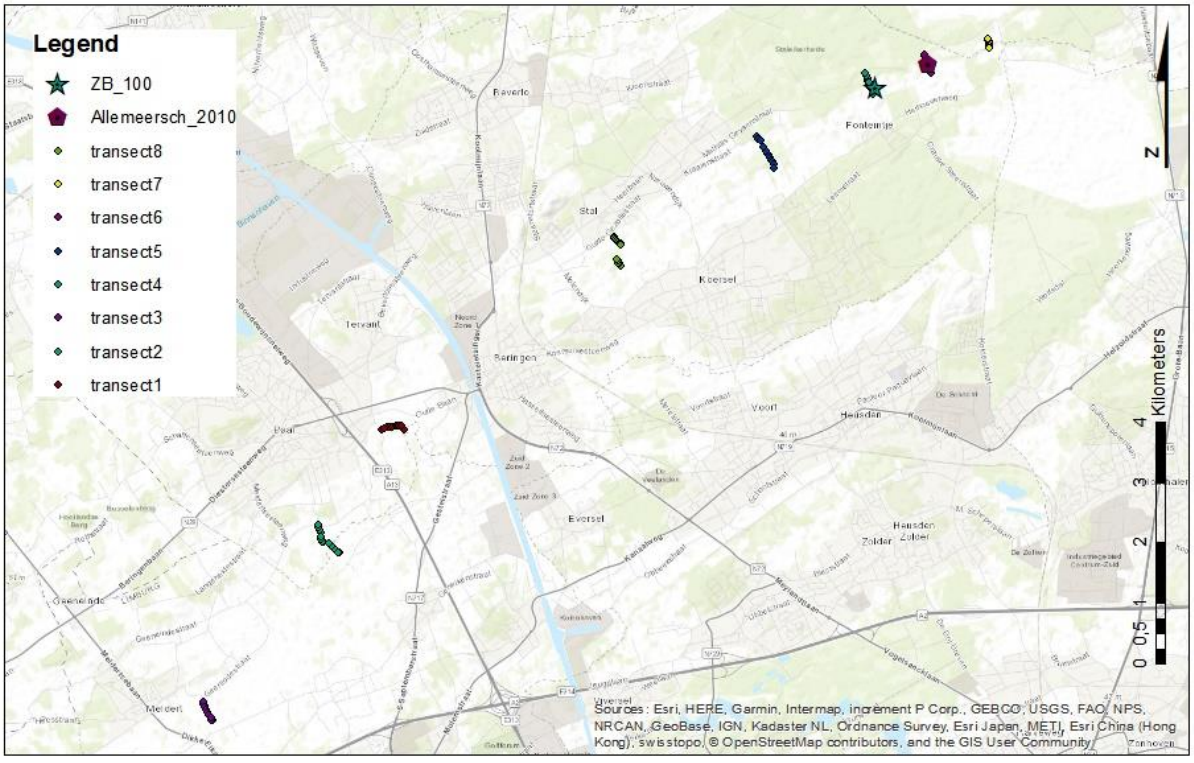

Figure B.2: Overview map of all the transects made in the Zwarte Beek valley for the Future Floodplains project.

Appendix C

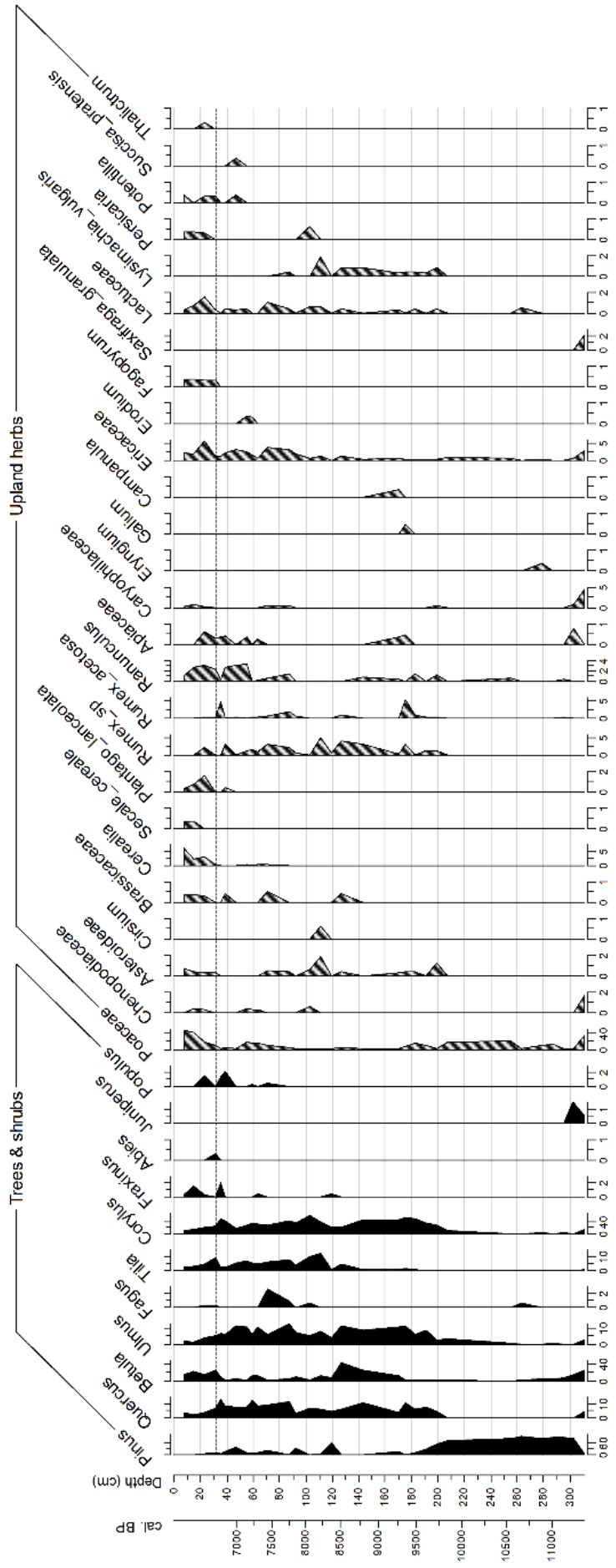

Figure C.1: Complete pollen diagram of core ZB-101 (Part 1).

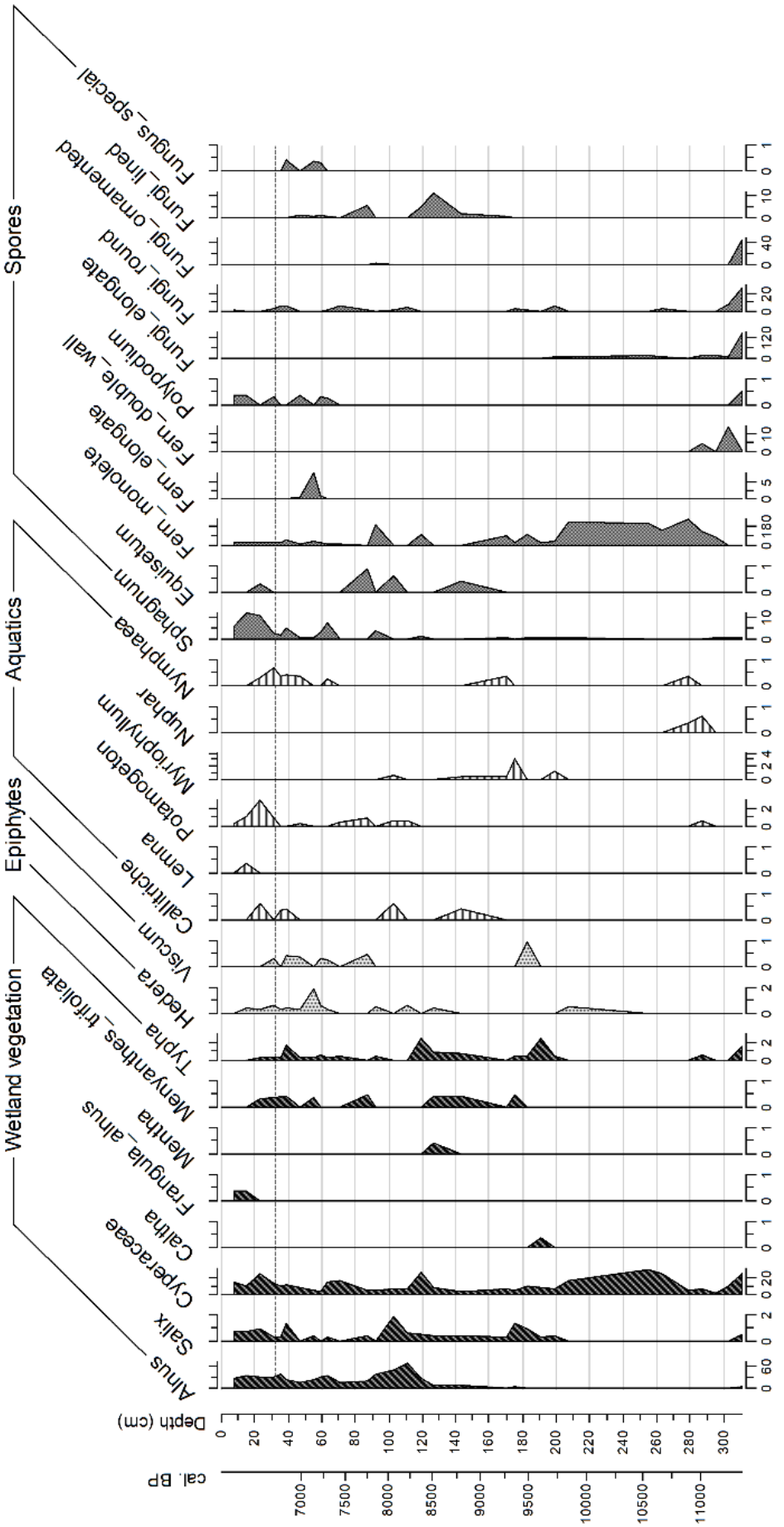

Figure C.2: Complete pollen diagram of core ZB-101 (Part 2).

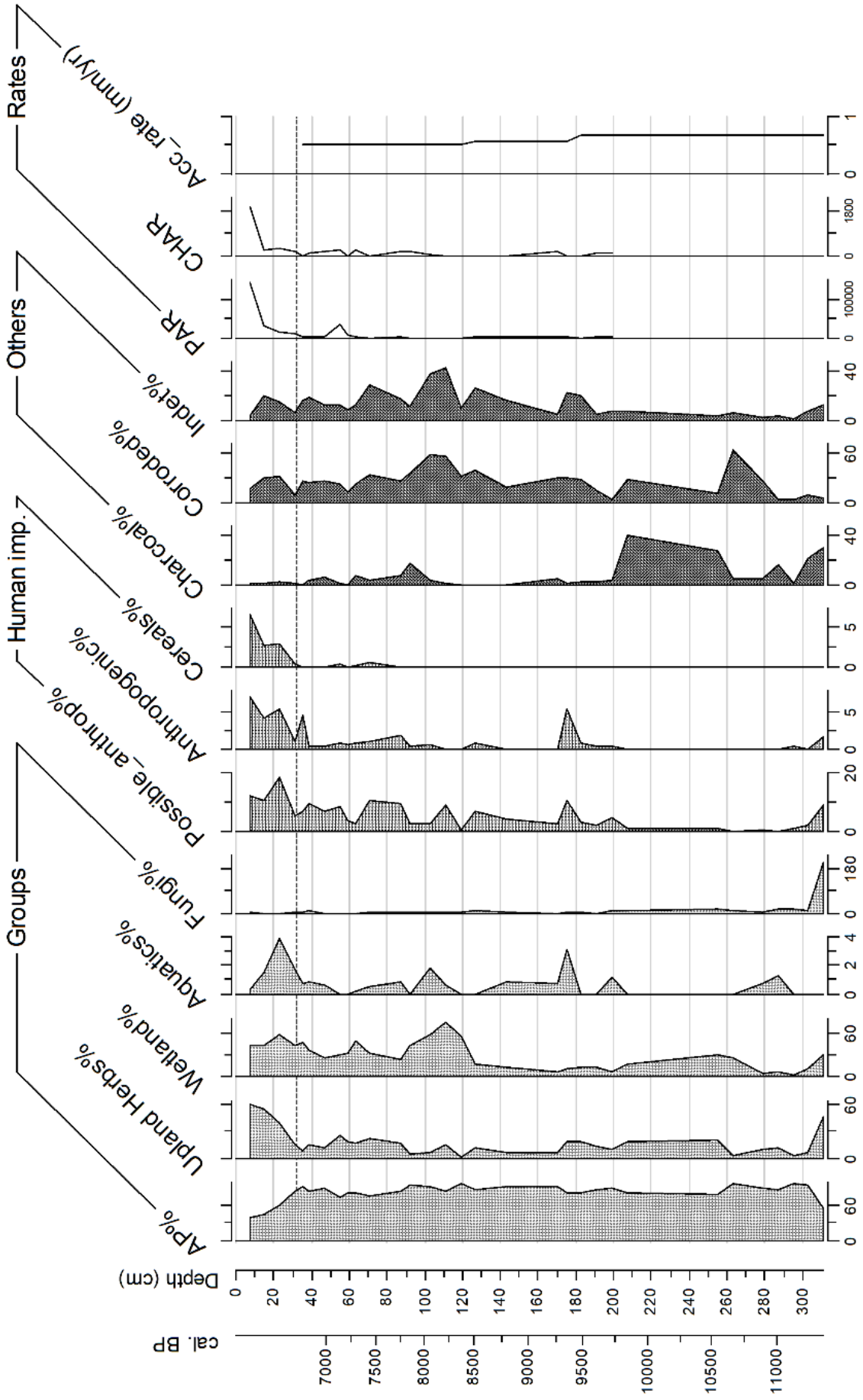

Figure C.3: Complete pollen diagram of core ZB-101 (Part 3).

Appendix D

Figure D.1: *Secale cereale* (7 cm, left), *Sphagnum* (7 cm, middle) and *Fagopyrum* (23 cm, right).

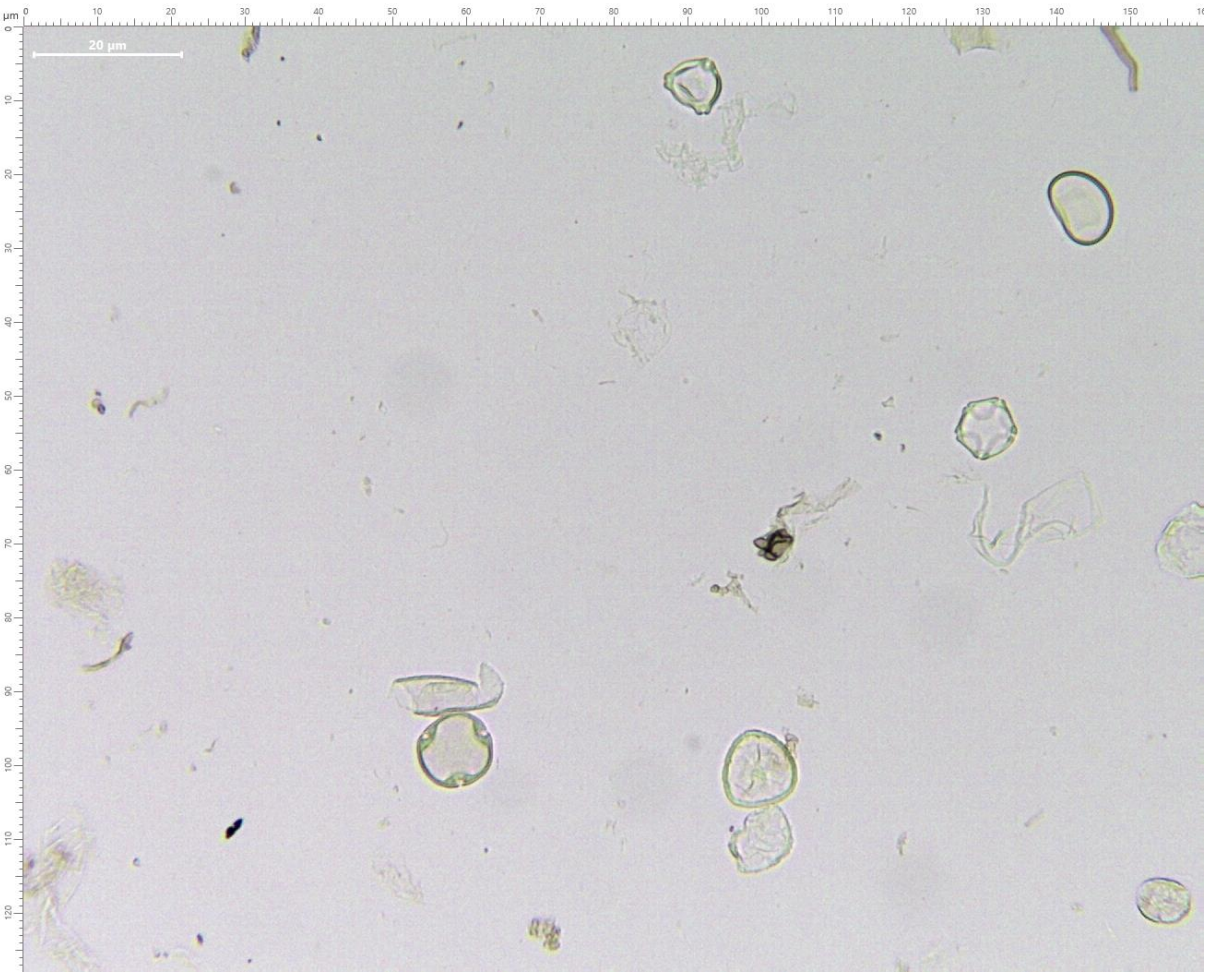

Figure D.2: Microscopic image of a view on a pollen slide. The picture shows level 59 cm: *Tilia, Betula, Alnus, Sphagnum* and a monolete fern are recognizable.

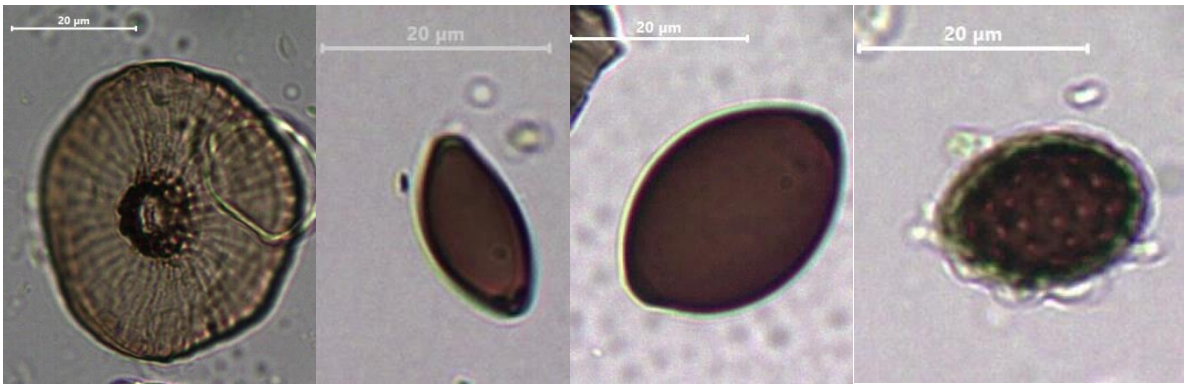

Figure D.3: 'Special' fungus (Type 8 as described by Van Geel 1978, 55 cm, left), 'elongated' fungus (Type 112 *Cercophora*, 311 cm, middle left), 'round' fungus (Type 55 *Sordaria*, 311 cm, middle right) and 'ornamented' fungus (Type 1 *Gelasinospora*, 311 cm, right).

Appendix E

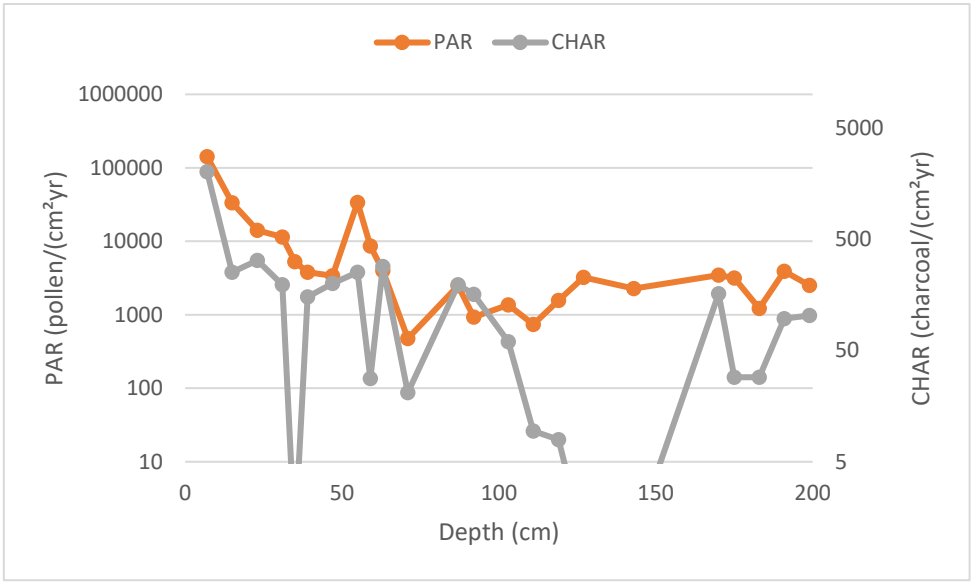

Figure E.1: Calculated values of (absolute) pollen and charcoal accumulation rates. For levels 35, 127 and 143 no charcoal particles were encountered. Samples deeper than 2 meter could not be calculated due to absence of *Lycopodium*. Note the logarithmic scale for both PAR and CHAR values.

AFDELING GEOLOGIE
Celestijnenlaan 200E bus 2408
3000 LEUVEN, BELGIË
tel. + 32 16 32 64 60
fax + 32 16 32 29 80
www.kuleuven.be